RICE UNIVERSITY

Assessing Coastal Vulnerability: Advanced Modeling Methods and Dynamic Hydraulic Characteristics of Gulf Coastal Systems

by

Jason Keigh Christian

A THESIS SUBMITTED
IN PARTIAL FULFILLMENT OF THE
REQUIREMENTS FOR THE DEGREE

Doctor of Philosophy

APPROVED, THESIS COMMITTEE:

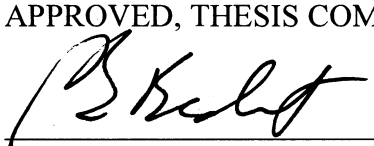

Philip Bedient,
Herman and George R. Brown
Professor of Civil Engineering
Civil and Environmental Engineering

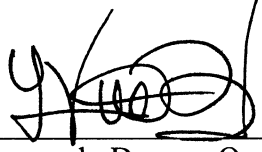

Leonardo Duenas-Osorio,
Assistant Professor
Civil and Environmental Engineering

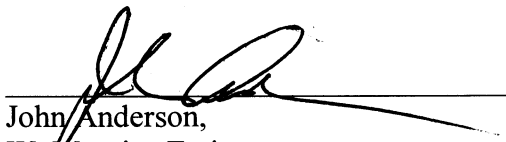

John Anderson,
W. Maurice Ewing
Professor in Oceanography
Earth Sciences

HOUSTON, TEXAS

April 2012

ABSTRACT

Assessing Coastal Vulnerability: Advanced Modeling Methods and Dynamic Hydraulic Characteristics of Gulf Coastal Systems

Jason Keigh Christian

The United States coastline contain some of the most valued ecological resources, the most populated urban areas, the most complex infrastructure systems, the most prolific economic engines, and the busiest ports of trade. However important the coastline may be to our nation, the history of our coastal communities suggests that they are extremely vulnerable to natural disasters, including hurricane landfall. There are many potential reasons for this vulnerability, and several of them are considered in this work. The common goal of research presented here is to better understand the hydrodynamic forces developed as hurricanes impact the coast so that the resulting effects on coastal resources can be better understood and managed, and vulnerability can be significantly minimized.

This work begins with consideration of the hydraulic domain at the interface between inland riverine and coastal environments. Regulators, and therefore those being regulated, generally prefer to separate riverine systems from coastal systems in the design and analysis of coastal infrastructure. Although analysis is greatly simplified, important synergistic hydrodynamic effects are not considered which can have dramatic negative effects on the ability of infrastructure to withstand hurricane impact.

Research continues by evaluating how society delineates the coastal flood hazard. Current methods apply a deterministic, steady-state approach to defining this highly dynamic feature influenced by multiple uncertain and variable parameters. By ignoring

the variability inherent in the coastal floodplain, society is not able to correctly define the flood hazard, and therefore cannot fully asses the risk to which it is exposed. A methodology is presented to more realistically quantify the coastal flood hazard and to calculate an appropriate flood risk metric.

Finally, this research considers the reliability of a coastal community's water distribution system under hurricane impact. By understanding system vulnerability and system interdependence, community leaders can provide more reliable infrastructure systems, thereby reducing the magnitude of disaster and shortening the recovery time. A methodology is presented to quantify the reliability of a water system under several hurricane impact scenarios.

ACKNOWLEDGMENT

I would like to sincerely thank my advisor, Philip Bedient, for his insightful comments, constructive suggestions, and motivating guidance. I cannot imagine a better role model to imitate as I embark into the rest of my professional career. Thank you also to the other members of my advisory committee, Leonardo Duenas-Osorio and John Anderson, and my colleague, Zheng Fang, who unselfishly provided their time, talents, suggestions and ideas in the completion of this work.

Most importantly, I would like to thank my family, Christi, MacKinsey, Madison and Macy, who motivated me with patient and loving support. Finally, I dedicate this work to my father, Quentin Christian, who continues to teach me by example how to be a man, a scholar, and a loving father for my children.

TABLE OF CONTENTS

List of Tables

List of Figures

Chapter 1

Introduction

Vulnerability is defined in this work as the incapability of a system or entity to withstand the effects of an antagonistic environment. The history of our coastal communities suggests that they are vulnerable to natural disasters, most notably to hurricane landfall. According to a NOAA weather related disaster summary for the United States covering the years 1980 to 2011, there have been twenty-four hurricane landfall events on the Gulf and Atlantic coasts that have resulted in more than one billion dollars of damage each with a total cost (in 2011 dollars) in excess of $390 billion (NOAA, 2011). These events are not just coastal problems, and no segment of our society is exempt from impact because much of the burden is carried by local, regional and federal governments which then redistribute the losses over their tax base (Pompe and Rinehart, 2008). Similarly, the losses covered by insurance companies are recovered through increased premium rates over all policy holders. Any perturbation in one segment of our highly interconnected economic network will ripple to all reaches of the nation. For example the Greater Houston Partnership estimates that a hurricane disruption of the Houston Ship Channel would cost the national economy approximately $60 billion monthly (GHP, 2009).

1.1 Social Vulnerability

Potential reasons for our continued social vulnerability to hurricanes may be that engineers, planners, and developers do not fully understand the physical characteristics of these natural events and therefore are not able to design coastal infrastructure systems to withstand these impact events. Reasons may include a lack of historical information (i.e., a short observed weather record) to properly characterize extreme events, a lack of accurate physics-based predictive models for use in risk assessment and sustainable design of infrastructure systems, or a general lack of understanding of the physical processes at play. In these cases, a more directed research approach to studying the processes and effects could result in a significant decrease in vulnerability.

An alternate reason could be that the regulatory framework guiding coastal infrastructure development is not geared to adequately address such high risk, low frequency natural phenomena. Decision makers tend to discount very low probability events, which distorts their understanding of true risk (Kousky et al., 2006). An example is the National Flood Insurance Program (NFIP) which implements flood insurance premium rates that are not actuarially sound (i.e., they are not based upon actual risk being insured) on approximately 25% of their policies sold (Pompe and Rinehart, 2008). Under these circumstances engineers and developers may fully understand the coastal risks, but the regulatory policies do not recognize or seek to protect against this level of hazard.

Finally, it could be that the political will or opportunity to enact and enforce sustainable land development practices is lacking. Fragmented governance of coastal areas can create perverse incentives that encourage unsustainable development and

increases social vulnerability (Dolan and Wallace, 2012). An all too common example of this along the Texas coast is local governmental support of risky development in hazardous areas in an attempt to increase the local tax base. Availability of government backed flood and wind hazard insurance transfers much of the risk to the state or federal government, so the local government is not held to account for their land development policies. This situation creates a moral hazard as the entity that ultimately ends up bearing the economic impact of disaster (i.e., the federal or state government) is not the entity that encourages or facilitates this risk taking (Dolan and Wallace, 2012; Pompe and Rinehart, 2008). In this case, local politicians and decision makers who lack long-term vision may not support sustainable development efforts because of the potential loss of tax base or the retarding effects sustainable practices could have on local economic growth, even though the natural hazards are well known.

1.2 Hurricane Disasters

This research represents an effort to better understand the natural processes at play as hurricanes approach and impact the coast. In pursuit of this goal, Chapter 2 contains summaries from the peer-reviewed literature on a number of topics related to hurricane development, growth, movement and coastal impact. Topics range from global warming, coastal geomorphology, sea-level rise, salinity intrusion, hydrodynamic processes, and several other subjects relating to hurricane impacts. This review is important to provide a big-picture view of natural and anthropogenic processes at play, so that cause-and-effect patterns can be identified, negative impacts of coastal development can be minimized, and social vulnerability can be reduced.

The research presented here considers coastal hydrologic and hydraulic topics for detailed consideration with the intent of better understanding the fundamental physical processes at play, identifying how these processes interact with our coastal infrastructure, and suggesting opportunities to reduce social vulnerability. Specific topics of research include studying the complex hydraulics at the coastline to better understand how coastal and riverine systems interact at their interface, studying coastal floodplains with the intent of quantifying uncertainty and identifying true flood risk, and studying a water infrastructure system and how it is vulnerable to hurricane impact. Figure 1.1 shows the relationship between disasters, hazards, the proposed research, and the associated social vulnerability.

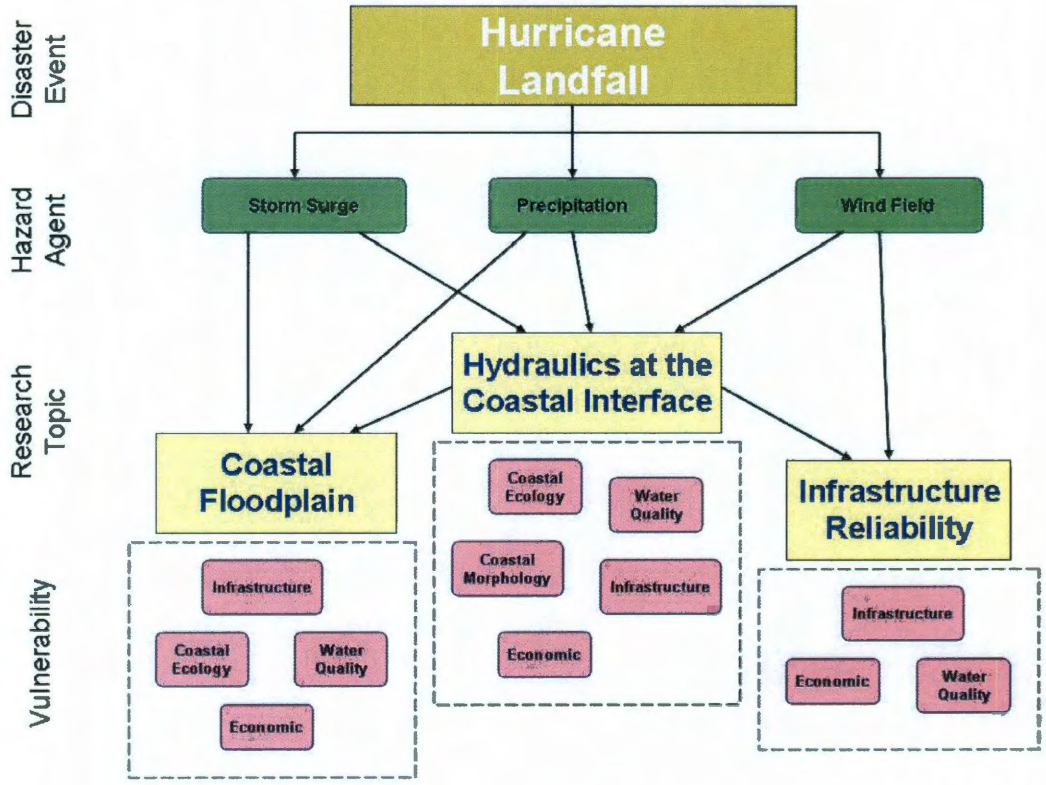

Figure 1.1. Research Logic Flow

Chapter 2

Climate, Hurricanes and Vulnerability (Literature Review)

In 2008, Hurricane Ike charted a direct course through Galveston Bay, Texas and heavily impacted local communities, industries and infrastructure systems in its path. Total estimated economic impact due to Hurricane Ike was about $27 billion (NOAA, 2011). Although Hurricane Ike landfall was a media sensation, the problem of coastal vulnerability to hurricanes is not new, and certainly not unique to Texas. Other memorable Gulf Coast events include the Great Hurricane of 1900 and its impact on Galveston Island; Hurricane Camille's assault on the Mississippi coast in 1969; Hurricane Andrew's rampage across Florida and Louisiana in 1992; and Hurricane Katrina and Rita's devastation of the Texas, Louisiana, Mississippi and Alabama coasts in 2005 (Keim and Muller, 2009). After each of these events, there was much public discussion regarding the vulnerability of our coastal communities. Also, there was dialog about how best to protect our coastal infrastructure networks, industries, communities and economies so that such devastating losses are not repeated. Occasionally, the public response to hurricane impact results in implementation of significant protective measures with notable examples including construction of the Galveston Seawall built after the 1900 hurricane; implementation of much improved building codes and inspections in Florida following Hurricane Andrew in 1992; and the drafting of comprehensive coastal

protection and management plans in response to Hurricane Katrina in 2005 (Hansen, 2007; Sirkin, 1995; Evans-Cowley and Gough, 2008).

The cumulative economic and social consequences of these natural disasters demonstrates that our coastal communities are highly vulnerable. The engineering standards we have historically applied to the design and construction of coastal infrastructure systems have proven to be inadequate to withstand these disasters, leaving the social systems dependent upon them at significant, but at least partially avoidable risk. Whatever the reasons for our failing social systems, understanding the hydraulic processes present at the coastal-riverine interface and understanding the vulnerability of our infrastructure systems to these hydraulic processes are of paramount importance to the analysis and design of flood protection levees, seawalls and gates, the design of sea ports and terminals, coastal infrastructure systems and any number of other constructed improvements residing along the natural coastline.

The research presented here considers the hydraulic environments generated by extreme events that are driven by regional and global climatic phenomena, which may be changing. While this research does not attempt to delve into the arguments of climate change – whether it is actually occurring, and what prime motivating forces might be responsible – a summary explanation of scientific discussions taking place seems in order.

2.1 Global Climate

According to the Intergovernmental Panel on Climate Change (IPCC), warming of the atmosphere is "unequivocal." This statement being justified through observations of rising mean air temperatures, rising mean ocean temperatures, rising sea levels, an

acceleration in receding of glacier and ice cap formations, and a reduction in the aerial extent of permafrost regions (IPCC, 2007). These observations have been logged and collaborated within atmospheric, terrestrial and oceanic domains using environmental data from the last 150 years. There appears little doubt that human activities have resulted in the discharge and accumulation of greenhouse gases (GHGs) at rates far in excess of naturally occurring emissions, with atmospheric concentrations of the most predominant greenhouse gas (CO_2) increasing 35% (from 280 ppm to 379 ppm) in the industrial time period between 1750 and 2005. The "radiative forcing" effect – the measure of the GHG's ability to affect the balance of energy gains and losses in the atmosphere – has increased as the atmospheric concentrations of anthropogenic CO_2, CH_4, and N_2O increased. The resulting effect is an atmosphere that is less able to radiate as much solar energy back into space, which leads to gradual energy accumulation and temperature increase in the atmosphere. The IPCC states with "very high confidence" that anthropogenic activity occurring in the industrial period has caused the current accelerated climate warming (IPCC, 2007).

The IPCC "Special Report on Emissions Scenarios" projects that global emissions of GHGs will continue to grow in the future (IPCC, 2007). Even with current emission mitigation policies and sustainable growth directives, the report estimates a 40 to 119% increase in CO_2 emissions in the next thirty years, which will lead to an estimated continued 0.2°C temperature increase per decade for the near future. Therefore, more immediate mitigations and globally radical adaptations would be required to respond to the currently accelerating climate changes.

For the continental United States, there is an excellent atmospheric weather record covering the last 100 years, which has recorded observations of temperature, barometric pressure, precipitation, and other climate parameters over the industrial time period, and a generally complete historic weather dataset for the globe is available for the last 30 years (Groisman et al., 2004; Pryor et al., 2009; Liu et al., 2009). Scientists have been able to determine atmospheric levels of anthropogenic greenhouse gases over this same time period, and recent scientific study has focused on identification of possible causal relationships between increases in GHGs and observed changes in climate parameters (Groisman et al., 2004; Liu et al., 2009). This on-going research is difficult due to the complexity of global climate and the interaction of large scale characteristics (i.e., Hadley cell circulations and jet streams) with regional or local scale phenomena (including land use and land cover changes), and on the shear number of interrelated chemical and physical processes continually occurring in the atmosphere. Observations of the frequency and magnitude of tropical storms suggests an upward trend attributable to warmer ocean temperatures, but the current data cannot be statistically validated as being more than the decadal variation associated with these events (Pielke et al., 2005). There is not yet any apparent consensus in the scientific community on what effect increased temperatures have already had, and likely will have in the future, on global weather.

Factors to consider when estimating future hydrologic changes include the effects of rising atmospheric CO_2 levels – and increased temperature – on hydrologic parameters including precipitation totals, frequency, intensity and distribution, evaporation rates, soil moisture levels, groundwater recharge rates, and surface runoff rates. Interestingly, there are no clear indications of what changes may occur in the global hydrologic cycle, with

some scientists claiming temperature induced forces have already resulted in hydrologic changes (Groisman et al., 2004; Liu et al., 2009; Anthes 2006), and others claiming there are no obvious trends (Pryor et al., 2009; Pielke et al., 2005).

Trenberth suggests that a warmer climate will increase the water vapor holding capacity of the atmosphere by a factor of about 7% per degree temperature change (Trenberth et al., 2003). Tropical storms get their energy from moisture convergence, and if there will be more moisture and warmer temperatures, these storms could grow in intensity proportionally with increase in atmospheric water vapor levels. Recent climate modeling research suggests that although the total number of tropical storms may not increase in a warmer climate, the number of major hurricanes may increase significantly (Bender et al., 2010). Curiously, the IPCC climate models predict that the total precipitation change due to a doubling of the GHG levels will increase precipitation totals globally by only 1 to 2% (IPCC, 2007). These results suggest that a warmer future climate may contain a future increase in heavy or extreme storm events with a corresponding decrease in light and moderate sized storms (Trenberth et al., 2003). The combined global effects of these mechanisms could lead to a small and spatially variable increase in regional precipitation totals, a global increase in precipitation intensity, and a spatially variable increase in drought conditions – driven by fewer smaller storms bracketed in time by much larger rainfall events.

Pryor provides a statistical analysis of weather data for 643 weather recording stations covering the continental United States over the period of 1895 to 2002 (Pryor et al., 2009). In this analysis, they were looking for trends in precipitation and in the intensity of extreme events. To be consistent with previous literature, Pryor defined

"extreme events" by several metrics including the 90th and 95th percentile storm return intervals, precipitation from the top 10 wettest days, and the wettest pentad (5 days). He reported that the vast majority of U.S. weather stations showed no statistical trends in total precipitation and in precipitation from extreme events, which suggests that the temperature effects on precipitation in the continental United States is either much smaller than the natural variability in rainfall events (and therefore lost in the "noise" of the natural event), or that there are no correlations (at the 90% confidence level) between temperature increases and rainfall events. For stations showing positive trends in total precipitation over this period, Pryor reported that these increases were manifested in storm events greater than the 95th percentile (Pryor et al., 2009).

In contrast to these findings by Pryor, Groisman presents an alternate statistical analysis of weather data for the continental United States over the same general time span (Groisman et al., 2004). When considering weather changes over this period, he found much more spatial and temporal variability in the precipitation data than the temperature data. Grosiman showed that the annual mean precipitation over the continent increased during the century by 7%, and the total precipitation associated with the most extreme storm events (i.e., the upper 95th and 99th percentile) increased 14% and 20% respectively (Groisman et al., 2004). These findings suggest two things; first that local changes in precipitation parameters may be more dependent on global changes than regional changes (i.e., local precipitation changes were disproportionate with local temperature changes), and second that changes in annual precipitation totals are manifested in larger "extreme" storms.

Both Groisman et al. (2004) and Pryor et al. (2009) report a statistically significant increase in number of wet days (i.e., days where any amount of rain fell), which would also explain some of the reported increase in annual precipitation. However, Pryor suggests that the historic precipitation record may have under-reported light precipitation amounts (less than 0.05 inches), and that the observed increase in number of "rainy days" reflects a change in the record keeping methodology and not in a wetter climate (Pryor et al., 2009).

Liu provides a similar study of global precipitation data for the period 1979 to 2007 (Liu et al., 2009). He reported that for each degree of increase in global mean temperature, there is a 95% increase in the precipitation from the top 10% bin (i.e., the largest 10% of storms) and a corresponding decrease in precipitation from the 30% to 60% bins. The results of these studies tends to support – or in the case of Pryor, does not dispute – the general hydrologic/temperature relational mechanisms proposed by Trenberth.

When considering likely temperature impacts on precipitation in the future, the consortium of available climate models are noticeably divergent for longer time scales, especially in the estimation of precipitation extremes in the tropics (IPCC, 2007; O'Groman et al., 2009). Current GCMs generally show an intensification of precipitation extremes in relation to the increase in atmospheric humidity (O'Gorman et al., 2009; Liu et al., 2009; IPCC, 2007). Even though climate models poorly correlate on the exact manifestation of climate change, there is better agreement that occurrence of extreme events tend to become more positive and stronger than mean precipitation (Groisman et al., 2005). As discussed previously, the general theory of Trenberth et al. (2003) and in

the observational evidence by Groisman et al. (2004) and Liu et al. (2009) suggest that the increase in precipitation intensity is actually not proportional to the increase in atmospheric water vapor levels.

O'Gorman et al. (2009) suggest that the precipitation simulations of the current set of models is not reliable especially in the tropics, and the mechanisms employed should be updated to better describe changes to the wet adiabatic lapse rate during extreme rainfall events. These model changes would include a better description of the physics and thermodynamics involved in the creation and propagation of convective storms in a warmer climate (O'Gorman et al., 2009). Because observed weather responses to regional warming periods (including El Nino) will likely differ from responses to global and long term temperature change, models that reasonably reproduce these short-term events may not accurately estimate the much longer term climate change. According to O'Gorman, the current set of GCMs should be updated to define and estimate more broadly how precipitation events will be influenced by greenhouse warming into the future (O'Gorman et al., 2009).

In summary, it appears from this literature review that although global warming is not in question, its current and future effects on rainfall total and the rainfall intensity of extreme events is poorly understood as modeled by the current general circulation models. There is general agreement that future weather will likely include an increase in annual rainfall for portions of the globe; but this may not mean a wetter environment as the rainfall increase may be contained within larger, relatively infrequent storms surrounding longer periods of drought for much of the world.

2.2 Hurricane Disasters

The human health, economic, political and social impacts of hurricane landfall on the United States coastline have received significant attention in recent years with notable landfalls on the Gulf coast by Hurricanes Katrina and Rita in 2005, and most recently Hurricane Ike in 2008. These storms brought havoc to human social, political and regulatory structures, the aftermath of which has been the topic of much public discussion and academic research (Waugh, 2006; Stehr, 2006; Kousky et al., 2006). In addition, these storms significantly impacted biological and ecological systems in the coastal impact zones, which has received disproportionally less attention. The current coastal population burden, which continues to grow faster than inland areas, places fragile coastal areas under increasing environmental stress.

A few of the identified environmental stressors associated with hurricane landfall include increased aquatic nutrient levels, increased total suspended solids, decreased dissolved oxygen levels, increased pollutant loading, increased coliform and pathogen loading, exotic species expansion, and harmful algal and phytoplankton blooms (Edminston et al., 2008). In addition to these direct water quality impacts, there are specific physical and chemical alterations associated with shoreline morphology and salinity intrusions into brackish, fresh water and terrestrial systems that have significant consequences (Howard and Mendelssohn, 1999; Wang et al., 2006). The complex coastal biological effects resulting from hurricane landfall can have significant negative impacts to individual organisms as well as to whole ecosystems. These negative impacts can be attributed to degradation of water quality – expressed through increased nutrient and BOD loading, mobilization of toxic contaminants, and reduction of dissolved oxygen

levels – to loss of species diversity, to repression of metabolic growth and maintenance capacity, and to physical injury from wave scour or sediment bury. As devastating as these biological impacts can be, it seems that natural systems are surprisingly able to assimilate the physical and water quality changes in a remarkably short time. Studying the coastal biological and ecological systems and how they cope with these significant perturbances may help humans develop building standards and land development strategies that are more resilient to hurricane upsets in the short term and therefore more sustainable and reliable in the long term.

2.2.1 History of Hurricane Disasters

A useful metric to assess social vulnerability to hurricane disasters is the magnitude of the cumulative cost incurred by these events. The higher the total cost attributed to natural disasters, the more vulnerable society is to these events. If society is well prepared for hurricane landfalls, the negative impacts – in terms of loss of life and property – should be acceptably low, the recovery time from the event should be reasonably short, and the economic cost of the event should be sustainably small. Although society can do little to contain and control the destructive forces generated by a hurricane (i.e., hazard mitigation), it can actively decide where and how to develop the coastline, how to get people out of harm's way, and how to design and construct coastal infrastructure to survive impacts (i.e., risk mitigation). All of these risk mitigation measures can be effective in reducing the magnitude of losses in event of hurricane landfall, thereby decreasing social vulnerability.

The National Oceanic and Atmospheric Agency (NOAA) tracks natural disasters

of all kinds. Figure 2.1 shows a summary of weather related disasters across the U.S. for the period spanning 1980 to 2010 that resulted in at least one billion dollars of total losses. A companion NOAA report of billion dollar disasters from 1980 to 2011 notes that 16 of 17 Atlantic and Gulf coastal states were impacted by billion dollar hurricanes, with Maine being the only un-impacted state (NOAA, 2011). There were 24 billion dollar hurricanes in this 31 year period as summarized in Table 2.1.

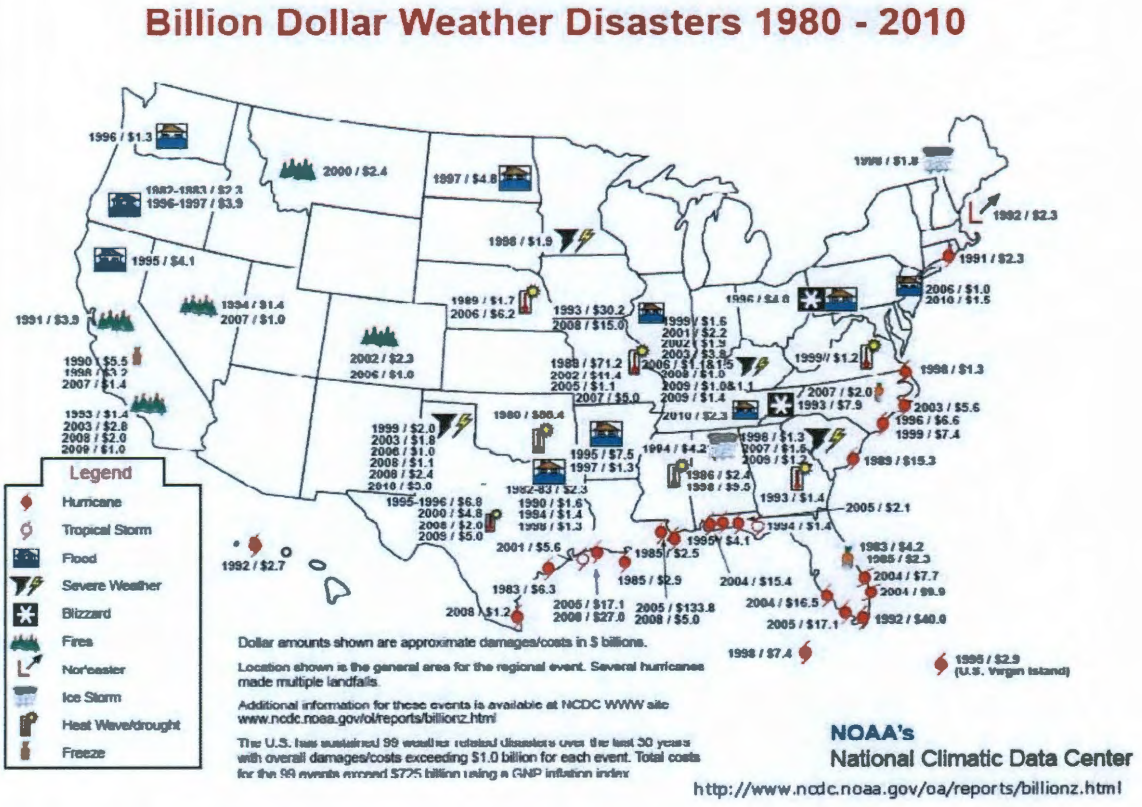

Figure 2.1. NOAA's Summary of Billion Dollar Weather Disasters.
http://www.ncdc.noaa.gov/oa/reports/billionz.html

Table 2.1. U.S. Coastal Hurricanes from 1980 to 2011

Storm Name	Year	Atlantic/Gulf Coastal States Impacted	Total Deaths	Cost (billions)
Irene	2011	NC, VA, MD, NJ, NY, CT, RI, MA	45	7.0
Ike	2008	TX, LA	112	27.0
Gustav	2008	AL, LA, MS	53	5.0
Dolly	2008	TX	3	1.2
Wilma	2005	FL	35	16.0
Rita	2005	AL, MS, LA, TX	119	16.0
Katrina	2005	AL, MS, FL	1,833	125
Dennis	2005	FL, AL, MS, GA	15	2.0
Jeanne	2004	GA, SC, NC, VA, MD, DE, NJ, NY	28	7.0
Ivan	2004	GA, MS, LA, SC, NC, VA, MD, DE, NJ, NY	57	14.0
Frances	2004	FL, GA, SC, NC, NY	48	9.0
Charley	2004	FL, SC, NC	35	15.0
Isabel	2003	NC, VA, MD, DE, NJ, NY	55	5.0
Floyd	1999	NC, SC, VA, MD, NY, NJ, DE, RI, CT, MA	77	6.0
Georges	1998	FL, LA, MS, AL	16	5.9
Bonnie	1998	NC, VA	3	1.0
Fran	1996	NC, VA	37	5.0
Opal	1995	FL, AL, GA	27	3.0
Andrew	1992	FL, LA	61	27.0
Bob	1991	NC, NY	18	1.5
Hugo	1989	SC, NC	86	9.0
Juan	1985	LA	63	1.5
Elena	1985	FL, AL, MS, LA	4	1.3
Alicia	1983	TX	21	3.0

2.2.2 Water Quality Impacts

Nutrient loading to bay and near shore waters can occur through several mechanisms during and shortly after hurricane landfalls. Many investigators have observed the direct input of macro nutrients – the most problematic being organic substrate, nitrate and phosphorus – transported by storm runoff (Zhang et al., 2009; Gierach and Subrahmanyam, 2008; Tilmant et al., 1994; Tomasko et al., 2006). The most common nutrient sources were identified as inorganic fertilizer leachate from urban and agricultural soils, mobilization and transport of nutrient laden soil particles through

surface soil erosion, and contaminated sediment re-suspension by hydrodynamic wave impacts (Zhang et al., 2009; Gierach and Subrahmanyam, 2008). Significant loading can also occur from anthropogenic sources including sanitary sewer spills, runoff from landfill facilities, and from oil or fuel spills. Other natural sources of nutrient loading include suspension and transport of organic material from downed vegetation or peat rich inland soils (Tilmant et al., 1994; Tomasko et al., 2006). The main environmental impacts of this increased nutrient loading is expressed through eutrophication as evidenced by increases in algae biomass and water column turbidity. These high spikes of nutrients following hurricane landfall, however, appear to be assimilated fairly quickly with normal levels of nutrients achieved within two to three months following the perturbation (Zhang et al., 2009).

Contaminant and nutrient mobilization in bay and near shore waters not associated with storm runoff quality are driven by two main mechanical processes; these being water column mixing across stratified layers in deeper water (greater than tens of meters) and mechanical mixing resulting in bottom scour in shallower water (less than ten meters). Each of these mechanisms has biological significance as they can increase nutrient and contaminant levels in the upper surface water by mobilizing previously sequestered compounds found in the lower water layers and benthic zones.

During warm sunny weather, as is prominent during hurricane season, surface waters become stratified. In offshore waters, the resulting thermocline effectively isolates the warm upper layer from the cooler lower layer, thereby preserving dissolved nutrients and contaminants in the underlying layer where low temperature and low sunlight conditions tend to retard biological activity. During hurricane passage, storm

winds generate surface wave currents that move radially away from the hurricane's center of rotation. This distal horizontal surface water movement generates a vertical upwelling from the lower layer and results in a mechanical mixing across the previously impenetrable thermocline. The upwelling water brings with it sequestered compounds that mix across the water column and express their nutrient or toxic influence. Phytoplanktom blooms along hurricane tracks in deeper water are attributed to the nutrient influx into surface waters because of this layer mixing phenomena (Gierach and Subrahmanyam, 2008).

As hurricanes move over shallower water, vertical water column mixing reaches all the way to the benthic layer (Li et al., 2006), scouring and re-suspending sediment along with all sorbed contaminants and nutrients. This action can mobilize and transport great quantities of sediment and can disperse nutrient or toxic benthic compounds throughout the water column (Miner et al., 2009). Many of the sediment contaminants are recalcitrant xenobiotics or heavy metals, so this redistribution will create new toxic effects in the bay and near shore ecosystems that would otherwise not be expressed because the nutrients and contaminants would have remained sequestered. Documentation of nutrient and toxic potential of bay sediments were reported for Galveston Bay on the upper Texas coast of Gulf of Mexico (Carr et al., 1996; Warnken et al., 2000).

A major result of elevated nutrient loading is expressed in low dissolved oxygen (DO) levels in bay and near shore surface water. A study of DO impacts in Charlotte Harbour, FL after a series of three hurricanes in 2004 attributed the depressed DO levels to high biochemical oxygen demand (BOD) and total suspended solids (TSS) loading

from organic matter mobilized by the storms. Long term DO levels that had been typically 4 to 8 mg/l were hypoxic (<2 mg/l) to anaerobic (<0.5 mg/l) for approximately 3 months after the series of hurricanes impacted the watershed (Tomasko et al., 2006). Dissolved oxygen impacts also present through delayed responses as the algal biomass dies and cell decomposition provides additional significant BOD loading to the water column. This low DO effect is magnified by the stratification between freshwater and saline water that occurs as fresh riverine runoff flushes into the brackish bays (Tomasko et al., 2006; Poirrier and Rodriguez del Rey, 2008). Fresh water has a density slightly less than the saline bay water, so a density stratification and low vertical mixing conditions following a hurricane landfall restrict oxygen transfer to the lower sediment rich saline layer. This effect creates hypoxic to anaerobic conditions in the saline layer, displacing natural aerobic microorganisms in favor of opportunistic facultative or anaerobic species. As with the nutrient loadings, DO perturbations were seen to correct themselves within two to three months following the hurricane landfall event (Tomasko et al., 2006).

2.2.3 Salinity Intrusion

Storm surges associated with hurricane landfalls bring saltwater intrusion to the shoreline environment. Localized surge inundation depths of 10 to 20 feet are possible for hurricanes as weak as Category 2 storms as was observed for the Hurricane Ike landfall on the Texas coast in 2008 (East et al., 2008). Storm saltwater inundation can last from several hours to days, giving ample opportunity to fully saturate relatively low saline environments with high doses of saline sea water. These events increase salinity

levels in brackish marsh, freshwater wetland and terrestrial systems, adding additional stress to organisms who must also survive the punishing mechanical shear forces brought by storm landfall. The sudden immersion of an organism into a significantly more saline environment has the biological consequence of increasing internal ion concentrations as the organism attempts to balance osmotic pressure between cells and the environment, a biological attempt to avoid physiological drought and dehydration (Marcum, 2006). Internal accumulation of salt ions can result in toxic levels of ions within the cells, or it can generate a significant energy burden as the cells try to balance concentration gradients by operating membrane ion pumps at the expense of cell maintenance and growth. In turf grasses and trees, the physiological effects of increased salinity include photosynthesis decrease, damage to leaves, decreases in growth rates, and an increase in respiratory cost of maintenance (Epron et al., 1999; Mirck and Volk, 2010).

Storm induced salinity pulses can effect brackish and freshwater wetlands by retarding plant growth as previously mentioned, but can also change relative species concentrations as different species express different levels of salt tolerance. Salinity dose and duration of exposure have retarding effects on growth of the salt tolerant species, and that these exposures can affect ecosystem composition as less tolerant plants are replaced by more salt tolerant opportunistic competitor species. These community composition and structure shifts can be significant in the short term, but have been observed to be short lived with species compositions re-established at pre-landfall equilibrium levels within about a year of the initial perturbation event (Howard and Mendelssohn, 1999).

Coastal estuaries provide important ecosystems for the growth and development of many economically important aquatic organisms including shrimp, oyster, and

flounder. These marine species are generally tolerant of saline conditions up to full strength seawater and therefore are not adversely affected by the surge salinity. However, these species can be negatively impacted by the freshwater flushing resulting from riverine runoff inputs following storm landfall. Edmiston noted an 80 to 90% mortality rate in an oyster population on the Florida coast due to prolonged reduced salinity in an enclosed bay following a tropical storm event (Edmiston et al., 2008). Tolley showed that important oyster biometrics including organism density, biomass and diversity decrease as salinity decreases (Tolley et al., 2005). Palacios found biological stress in shrimp postlarvae when salinity values were lowered, indicating a biological preference for mid to high levels of salinity (Palacios and Racotta, 2007). Sampaio reported that flounder mortality was unaffected by salinity levels in the immediate environment, but growth rates were depressed in fish exposed to prolonged freshwater conditions (Sampaio and Bianchini, 2002).

Terrestrial plants are much more impacted by saline pulses than the oligohaline bay and estuarine species previously discussed. Many tree and grass species commonly found along the Gulf Coast of Texas are surprisingly intolerant of salt pulse events as evidenced by the die-off of many well established Live Oak trees and St. Augustine lawns on Galveston Island following the Hurricane Ike storm inundation. Generally, chloride concentrations in soil pore water around 14,500 mg/l will have a strong negative influence for oak and willow tree species expressed through inhibition of root growth, depression of shoot growth, photosynthesis decrease, and increases in cell maintenance energy requirements (Epron et al., 1999; Mirck and Volk, 2010).

2.2.4 Coastal Morphology

Coastal morphology following hurricane landfall has been the subject of intense investigation in the United States following the 2005 hurricane season in which hurricanes Cindy, Katrina and Rita all made landfall on the upper Gulf Coast. Studies of the Louisiana coast following the 2005 hurricane season estimated approximately 131 million metric tons of inorganic sediment (approximately 50 to 90 million m^3) was washed inland and deposited onto coastal marshes during the Katrina and Rita events, although the source of this volume of sediment was not identified (Turner et al., 2006). Later studies estimated a loss of 9.1 million m^3 of sediment from an ebb-tidal delta in this same area along the Louisiana coast following Katrina and Rita, resulting in a 160 meter landward movement of the inlet (Miner et al., 2009). These two studies suggest that, at least for the 2005 hurricane season along Louisiana, an erosion of near shore, barrier island and beach sediment resulted in a build-up of inland coastal marshes. A possible explanation for these observations is a mechanism where storm landfall mobilizes near shore and beach sediment, storm surge quickly transports the sediment inland, and deposition occurs when the surge slowly retreats. Coastal morphology can induce biological stress through three main mechanisms including physical scouring and removal of organisms, direct bury of organisms following sediment mobilization and deposition, and ecosystem regime changes (i.e., erosion and loss of shore, barrier island and beach ecosystems and filling of inland salt marshes). Anthropogenic modifications to the shoreline through land use modifications or structural encroachments can make

ecological systems more susceptible to these natural morphologic processes (Greening et al., 2006).

2.3 Future Trends

Cumulative social and economic risk is steadily increasing as more of the coast evolves with an increasing density of development (Pompe and Rinehart, 2008). The result is more people and infrastructure in harm's way, and inevitably more losses as future hurricanes make landfall. To frame the expectations about possible future risks, the following sections discuss current trends that will affect society's coastal vulnerability to future hurricanes.

2.3.1 Coastal Population

As referenced in many academic studies, approximately 53% of the entire U.S. population lives in coastal counties along the Atlantic, Pacific, Gulf of Mexico and Great Lakes coastlines. The origin of this estimate comes from a report from the National Oceanic and Atmospheric Administration (NOAA) regarding coastal population trends of the coastal United States. (Crossett et al., 2004). As defined in the NOAA report, a coastal county is one with at least 15% of its surface area contained within a coastal watershed (Crossett et al., 2004). For some purposes, as in the study of water quality along the coast, this may be an appropriate definition – but for others, including studying the impact of hurricanes on coastal populations, this will overestimate the number of people directly exposed to a hurricane disaster (Crowell et al., 2007). Recognizing this distinction, the Federal Emergency Management Agency (FEMA) defined a coastal

county as one that has a coastline bordering the shore of an open ocean or Great Lakes or has high velocity flood zones (i.e., V zones) in its county FIRM floodplain maps (Crowell et al., 2007). Using this more restrictive definition of coastal county, the estimate of coastal population is reduced to 37% of total population (104,990,000 people) residing in 364 counties. Removing those that boarder the Great Lakes, and are therefore not directly vulnerable to hurricane impacts, the coastal population lowers to 30% of total population (85,540,000 people) from 281 coastal counties (Crowell et al., 2007). Similarly, the U.S. Census Bureau defines coastal counties as those that are adjacent to coastal water or territorial sea, and includes 254 counties with an estimated 87,400,000 people (U.S. Census Bureau, 2011), an estimate very similar to FEMA's coastal population. Therefore, for the purpose of this hurricane impact assessment research, it is appropriate to estimate the current population exposed to hurricane hazards at approximately 30% of the total U.S. population

According to U.S. Census Bureau statistics, population growth for the entire U.S. was 64.3% for the period 1960 to 2008, however growth of U.S. coastal counties for the same period was 84.3%, or 30% faster (U.S. Census Bureau, 2011). Figure 2.2 summarizes the relative growth rates of coastal counties, and shows growth rates well in excess of the national average - especially along the New England, Southeastern, Florida, upper Texas and West coasts. It may seem trivial to state, but if the population of coastal areas continues growing at a rate faster than the rest of the country, an even larger percentage of the population will be exposed to hurricane hazards in the future – increasing hurricane risk and losses whether or not hurricane hazards change.

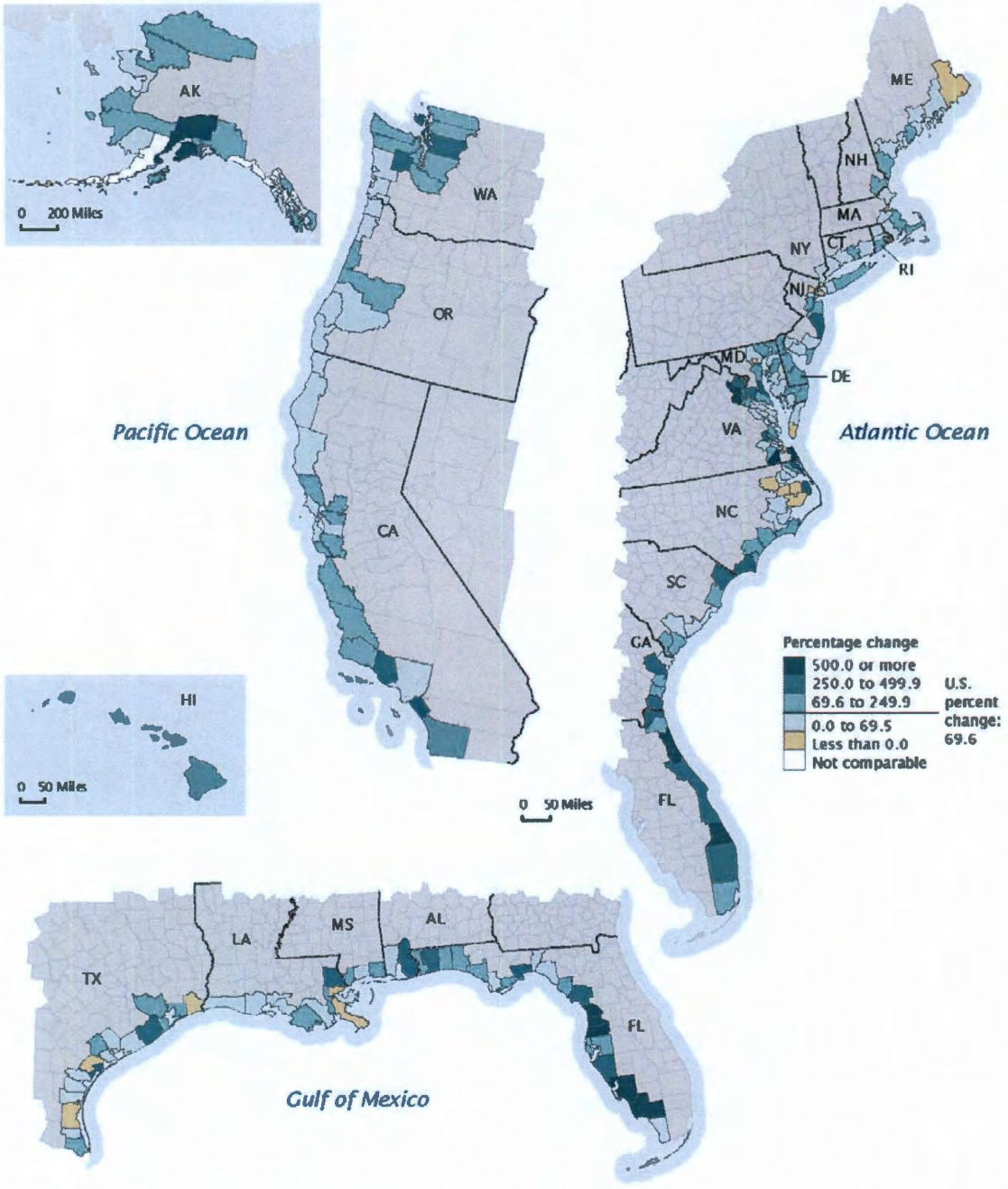

Source: U.S. Census Bureau, Decennial Census of Population and Housing: 1960; Population Estimates Program: 2008.

Figure 2.2. Change in Coastal Population by County: 1960 to 2008

2.3.2 *Relative Sea Level Rise*

Coastal communities could likely see their vulnerability to hurricanes increase over time as the continued and accelerating effects of relative sea level rise (RSLR) manifest. RSLR is the rise of ocean's water surface relative to the coast, and can be attributed to natural and anthropogenic factors. Along the coast of the Gulf of Mexico, RSLR is caused by both an increase in mean sea level (i.e., rise of water surface relative to a constant coastal elevation) and to coastal subsidence (i.e., lowering of the coastal elevation relative to a constant seal level) (Anderson, 2007; Mousavi et al., 2011; Reed, 2002; Smith et al., 2010; Day et al., 2007; Day et al., 2011).

The IPCC working group report attributes an increasing rate of sea level rise to global warming as a result of anthropogenic climate change (IPCC, 2007). Over the last century, sea level has risen at a rate of about 0.17 cm/year, but more recently this rate has increased to about 0.30 cm/year (IPCC, 2007). The vast majority of this increasing rate is attributed to thermal expansion of the ocean as the sea surface temperature (SST) increases, but addition of water from glaciers, polar caps, ice sheets and other land reservoirs also contributes to the rise in sea level elevation (IPCC 2007).

Coastal subsidence is a significant driver of increased vulnerability for some coastal communities (Day et al., 2007; Reed, 2002). The main culprit for this loss of elevation is subsurface fluid removal which decreases pore pressure in the sedimentary geologic formations containing the fluid, resulting in compression of the formation and loss of surface elevation (Anderson, 2007; Kolker et al, 2011). A close association between oil production rates in Louisiana, groundwater withdrawal in Galveston and subsidence rates in each area suggests a correlated relationship at a sub-decadal temporal

scale (Kolker et al., 2011). This is not strictly a Gulf of Mexico problem, as the sinking delta phenomena has been documented in highly populated deltaic regions across the globe (Syvitski et al., 2009). In addition to anthropogenic reasons, natural subsidence can result from natural compaction of sedimentary formations and geologic plate subduction along the coast. Under the influence of subsidence, wetlands convert to shallow open-water, barrier islands submerge, and the coastline moves landward (Day et al., 2007), affecting both the physical character and ecology of the coast.

As the hydrologic systems change, the type of vegetative cover changes. This ecological morphology alters the frictional forces along the water-surface interface, which in turn modifies the hydraulic characteristics of the coastline. Wetland pastures and cypress forests typically have Manning's 'n' values of 0.14 to 0.18; low quality wetlands and salt marshes have 'n' values of around 0.06 to 0.09; and shallow open waters generally have 'n' values of 0.035 to 0.055 (Smith et al., 2010). As the coastline submerges, the lowering Manning 'n' values decrease the frictional force retarding storm inundation and allows hurricane storm surges to propagate further inland. Additionally, the effects of wave impact on the coast are modified. Wave breaking is caused by surface frictional forces acting at the base of the wave opposite the direction of wave movement. With increased water column depth and decreased Manning 'n' values, the waves move further inland before breaking (Smith et al., 2010). These mechanisms result in an increase in the coastal floodplain that is non-linear with increases in RSLR (Mousavi et al., 2011; Reed, 2002; Smith et al., 2010).

Unfortunately, natural processes that act opposite to RSLR can be significantly retarded by anthropogenic activities along the coast. For example, the cumulative effects

of flood control activities, levee maintenance, navigation channel dredging and inland sediment impoundments reduce or eliminate natural sediment aggradation processes around highly populated deltas, which are then not able to keep up with subsidence (Anderson, 2007; Day et al., 2007).

2.3.3 Climate Change and Hurricanes

The scientific community has come to the conclusion that our industrial activity is contributing to measurable cumulative changes in global temperatures. Although scientists have raised the alarm of warming trends, mostly attributed to the release of greenhouse gases and organic aerosols (Anthes, 2006), there is currently little scientific consensus of how the impact of rising global mean temperatures will manifest. Some believe that warmer temperatures will result in dramatically higher sea elevations as polar ice caps melt; some believe that warmer ocean temperatures will increase the frequency and severity of tropical cyclones; and others are not sure if there is enough statistical information to distinguish current weather patterns from the uncertain "noise" found in historic weather records (Anthes et al., 2006; Pielke et al., 2005). Research into the rate of major hurricane landfall events onto the Texas coastline from the late Holocene to the present suggest the rate of hurricane landfall has been constant despite high-frequency climate oscillations during the period (Wallace and Anderson, 2010), so there is uncertainty as to whether the current global atmospheric and SST changes will affect hurricane activity.

With as much at stake in the fate of our environment, speculation and debate over human sponsored weather impact is sure to continue well into the future. Following is a

summary of two contrasting views on the effects of temperature rise on weather patters from teams of scientists who have reached polarized conclusions based upon a common observed data set.

To begin the discussion of future hurricane risks, Pielke describes "event risk" and differentiate this from "outcome risk" as he considers possible effects of global temperature changes (Pielke et al., 2005). Event risk is defined as the risk directly attributable to an event itself. For example, a hurricane season with more frequent and more intense tropical storms than average would have an increased average event risk. This is different from outcome risk, where the magnitude of risk is not completely dependently on the event. As described in Section 1.2, the current trend in hurricane damage is increasing, but it is unclear if this trend is because hurricanes are stronger (event risk) or because there is more development along the coast to be damaged (outcome risk). Pielke notes a recent rise in the number of tropical storms, particularly the number of major hurricanes, but the changes of the recent past are not so large as to unequivocally indicate that anything is going on other than the multidecadal activity cycle (Pielke et al., 2005). While not disputing the apparent temperature effects of greenhouse gases, he states that a causal relationship between temperature rise and short-term increase in hurricane frequency and intensity is not statistically proven given the historic variability of these weather events. Pielke notes the disagreement between researchers and inconsistent future weather forecasts as evidence of a poorly understood, loosely defined causal relationship between weather frequency/intensity and anthropogenic warming. He proposes that any conclusions of direct linkage are

premature, and speculates that those who pioneer these ideas so passionately are possibly doing so to champion a political agenda (Pielke et al., 2005).

A contrasting view presented by Anthes et al.. proposes that the recent hurricane record from 2005 shows strong correlation between temperature rise and event risk. He notes that the 2005 hurricane season had the largest number of named storms, the largest number of hurricanes, the only year with three category 5 storms, the most intense storm on record, the most intense storm in the Gulf of Mexico, and the most costly storm on record. (Anthes et al., 2006). He suggests that articles like those from Pielke are misleading by not considering the short term increase in activity of the 2005 season. Anthes points out the plausible causal relationship between tropical weather events and warmer oceans – which provide the fuel for storm birth, propagation and continuation – and speculates that a warmer and wetter atmosphere would favor enhanced hurricane activity (Anthes et al., 2006). Anthes, referencing the same researchers and future weather forecasts discussed by Pielke, points to their agreement and consistency as overwhelming evidence of a causal relationship between warmer temperatures and event risk (Anthes et al., 2006). He also cites the published work of several scientists with contrasting viewpoints, but he suggests these views are naïve, misleading and potentially dangerous to the public.

Both scientific groups appear to agree that whether or not weather cycles are increasing in frequency and intensity, our society's vulnerability to sever weather events (i.e., outcome risk as described by Pielke) is undoubtedly increasing. Because there is a public perception that, at least in recent years, every hurricane season brings more devastation than the previous, it may be tempting to conclude that the natural disasters

are increasing in intensity and frequency over time. However, as we continue to develop along the coastline, placing billions of dollars of infrastructure and millions of our population in harm's way, society becomes increasingly vulnerable whether or not there are any changes in the weather characteristics.

2.4 Research Objectives

The goal of this research is to investigate and better understand the physical properties of surface water flow at and near the coastal zone during extreme natural disaster events, and be able to predict the impact these events will have on social systems and critical infrastructure. This improved understanding can then be used in the design of coastal infrastructure that is better able to survive hurricane impact, and therefore be better able to protect human health and property from these natural disasters. The end results will include social/political structures that are less vulnerable, economic assets that are more durable, and coastal communities that are less vulnerable in the face of hurricane impact.

Maintaining sustainable coastal communities is becoming more difficult because of increasing pressure of development, the severity of natural disasters, and the consequences of social structure failure – including loss of human lives, destruction of economic base and failure of basic infrastructure systems. Accordingly, engineers, land planners and decision makers must strive to fully understand the physical forces inherent in these events so that appropriate structural flood protection controls may be designed or non-structural solutions created to reduce the social impact when these natural disasters occur.

Structural controls are risk management tools including levees, seawalls, gates, diversion channels, detention reservoirs and other constructed facilities designed to isolate and protect important social assets from the ravages of natural disasters when the hazard and the asset occupy the same space – as when a city is constructed along the coast. Non-structural controls are risk management tools that protect social assets from damage by physically separating them from the natural hazard. Examples of non-structural controls include establishment of laws, codes and ordinances for the preservation of natural barrier islands, establishing or maintaining coastal wetlands and marshes, and implementation of land use controls intended to create hydraulic buffers between social assets and the coastal hazards. The success of these protective measures, structural and non-structural alike, is highly dependent on an accurate understanding of the characteristics of the natural hazards. In the case of hurricane impact, there are hazards associated with torrential rainfall, storm surge propagation onto shore, wave impact on coastal structures, and damage from tropical wind fields exceeding 33 m/s (74 mph).

To improve the understanding of destructive forces at play in the coastal zone, this research presents several dynamic hydraulic system models illuminating the interaction and interdependence of coastal phenomena (tides, currents, hurricane windfields and hurricane storm surge) with riverine flow characteristics (runoff quantity, channel routing and floodplain storage), and determine the impact they have on the coast and coastal infrastructure. This fundamental understanding will be gained through pursuit of the following research objectives:

Objective 1: Determine the hydraulic interaction between coastal waters and channelized runoff at the coastal-riverine interface.

Objective 2: Determine and map the 1% flood hazard and flood risk in the coastal zone considering the uncertainty of natural parameters and the highly dynamic nature of coastal flooding events.

Objective 3: Determine the interdependence and reliability of built hydraulic infrastructure systems in the coastal zone under hurricane impact.

Objective 4: Evaluate current regulatory policy regarding delineation of coastal floodplains, administration of FEMA's flood insurance program, and water system reliability in Texas in light of the hydrodynamic research presented here.

2.5 Advanced Coastal Hydraulic Research Topics

The research presented here is by no means an exhaustive evaluation of all hydraulic characteristics found in the coastal environment. However, by generating a better understanding of the hydraulic characteristics at the coastal interface, within the coastal floodplain, and upon the coastal infrastructure, scientists and engineers can develop more sustainable social and infrastructure systems to benefit a less vulnerable coastal society.

2.5.1 Hydraulic Modeling at the Coastal-Riverine Interface

Research begins in Chapter 3 by investigating the hydraulic properties of surface water flow in the coastal zone where inland riverine systems interact with coastal waters.

Current hydraulic analyses within the coastal zone typically uncouple the coastal hydraulic processes from the riverine processes to consider each independently. This is done to satisfy regulatory requirements and to simplify analysis complexity, but is not hydraulically appropriate for reasons presented. To illustrate this point, an unsteady hydraulic model of a typical coastal-riverine drainage system was developed to investigate flow properties at the coastal interface. This model is then utilized to estimate the operational parameters and effectiveness of a proposed structural flood protection levee and channel gate at the coastal interface.

2.5.2 Modeling the Coastal Floodplain

Chapter 4 investigates the development of probabilistic flood hazard and flood risk delineations as improvements to standard floodplain maps for coastal watersheds. Current floodplain maps present 1% flood hazards as polygon features developed using deterministic, steady-state models that do not consider data uncertainty or natural variability of input parameters. Using the techniques presented here, a standard binary deterministic floodplain delineation is replaced with a probabilistic flood inundation map showing the underlying flood hazard structure. Additionally, the hazard probability is further transformed to show flood risk as a spatially distributed probable flood depth using concepts familiar to practicing engineers and software tools accepted and understood by regulators. A case study of the proposed hazard and risk assessment methodology is presented for the Dickinson Bayou Watershed – a Texas coastal watershed draining into Galveston Bay – which shows that storm duration and stage boundary conditions are important variable parameters, while rainfall distribution, storm

movement and roughness coefficients contribute less variability. The probabilistic floodplain for this coastal watershed shows the highest variability in the tidally influenced reaches and shows little variability in the inland riverine segments. Additionally, comparison of flood hazard maps to flood risk maps demonstrates that they are not directly correlated as areas of high hazard do not always represent high risk, an important distinction for floodplain managers with limited resources charged with reducing social risk. The information in Chapter 4 has been submitted for peer review and possible publication as:

> Christian, J., A. Teague, L. Duenas-Osario, Z. Fang, and P. Bedient, 2011. Uncertainty in Floodplain Delineation: Expression of Flood Hazard and Risk in a Gulf Coastal Watershed. *Journal of Hydrological Processes*. Accepted with revisions February 2012.

2.5.3 Modeling of Water Infrastructure Reliability

The research presented in Chapter 5 considers the application of novel hydraulic modeling technique to a small town water distribution network to determine infrastructure reliability given a direct hit from a hurricane. In this system simulation the water network proved to be reliable under storm impact when studied in isolation, but ultimately proved to be vulnerable because of water network dependence upon the electrical grid to provide operating power for water system pumps. To consider the interdependencies between the power and water networks, this research introduces a scenario-based, two-stage simulation method to decouple system interdependencies, increase analysis flexibility and effectively reduce the computational complexity. The electrical grid and water network reliability realizations generated by this method are used as input to a hydraulic model to simulate the resulting water system pressure at

consumption nodes throughout the network. Simulated system pressures are compared against a regulatory minimum pressure criteria to determine if the water network is reliable or not. As this work demonstrates, survival of the electrical system network is the most important factor in determining the reliability of the water system. Utilizing the results from this case study, the local water system operator and emergency responders can become better prepared for future disaster events, and the community can be more confident that minimum water services can be provided as future hurricanes make landfall. A manuscript with the information in Chapter 5 has been developed and is in final stages of internal review. It will be submitted for peer review and possible publication as:

Christian, J., K. Rokneddin, M. Ouyang, L. Duenas-Osorio, and P. Bedient, 2012. Water System Reliability Under Hurricane Impact Considering Electrical Grid Interdependency. *Journal to be Selected.*

Chapter 3

Coastal-Riverine Hydraulic Interface

The "coastal-riverine interface" is defined here as the transitional hydraulic domain between gravity driven flow of inland river systems and tidal, wave, current and surge driven flow present at the coast. Boundaries of this transition zone are difficult to delineate because the interface can exhibit hydraulic properties of both inland and coastal environments depending upon other temporal and spatially variable environmental parameters. At times, the channels, ditches and bayous in the interface zone will act like upland drainage facilities that collect and convey inland rainfall runoff toward the sea. Other times, these hydraulic structures may reverse flow and carry significant quantities of sea water inland, as when approaching hurricanes bring significant storm surges to the coastline. Still other times, there may be a balance of hydraulic forces such that surface flow does not occur in any significant quantity in either direction, as when unusually high tides or on-shore winds raise the elevation of near shore waters for extended periods, surcharging drainage channels at the coast.

Understanding the properties of these coastal drainage features becomes critically important in the planning and design of coastal communities because of the overwhelming hydraulic forces associated with hurricane impact. The following research

considers the current approach to analysis of the coastal-riverine interface and to the design of constructed improvements therein. To investigate the flow properties at this interface and to illuminate specific characteristics of coastal hydraulic systems, an unsteady hydraulic model of the lower San Jacinto River and Houston Ship Channel was constructed and analyzed. These two channels are significant tributaries to Galveston Bay, Texas and drain most of the Greater Houston metropolitan area. Figure 3.1 is the vicinity map of the hydraulic model domain, and Figure 3.2 shows the aerial extent of the watersheds served by these channels.

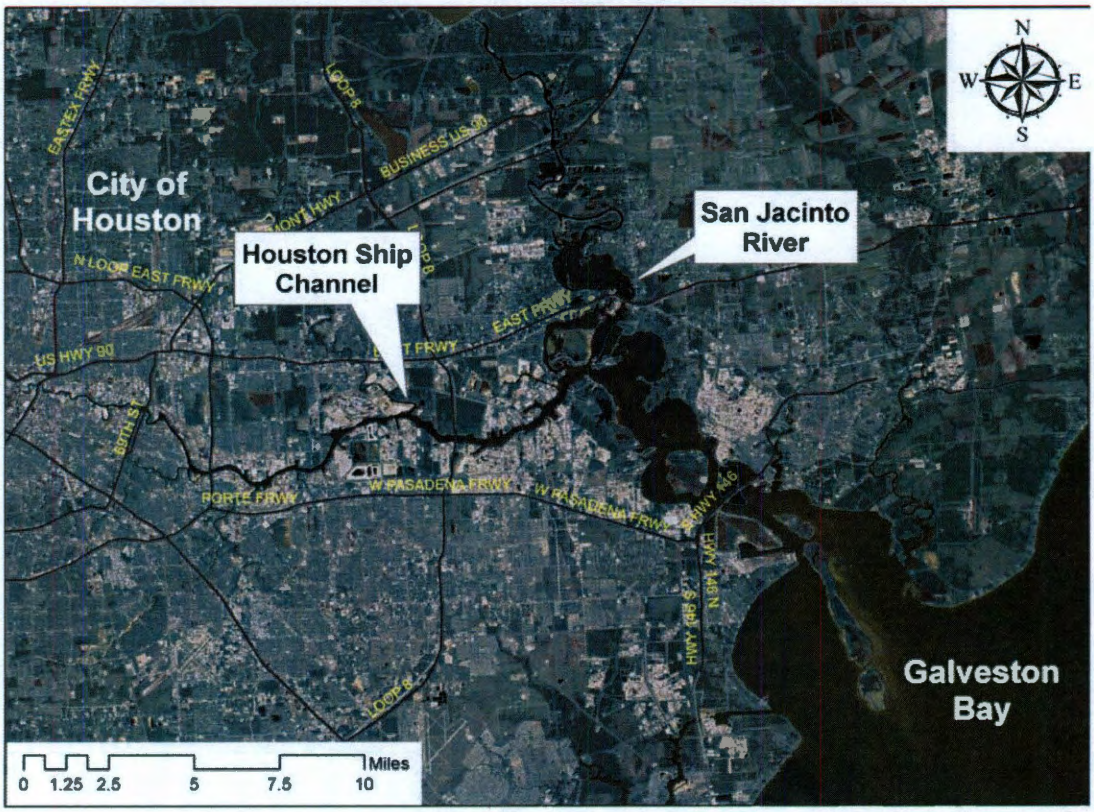

Figure 3.1. San Jacinto – Houston Ship Channel Model Domain

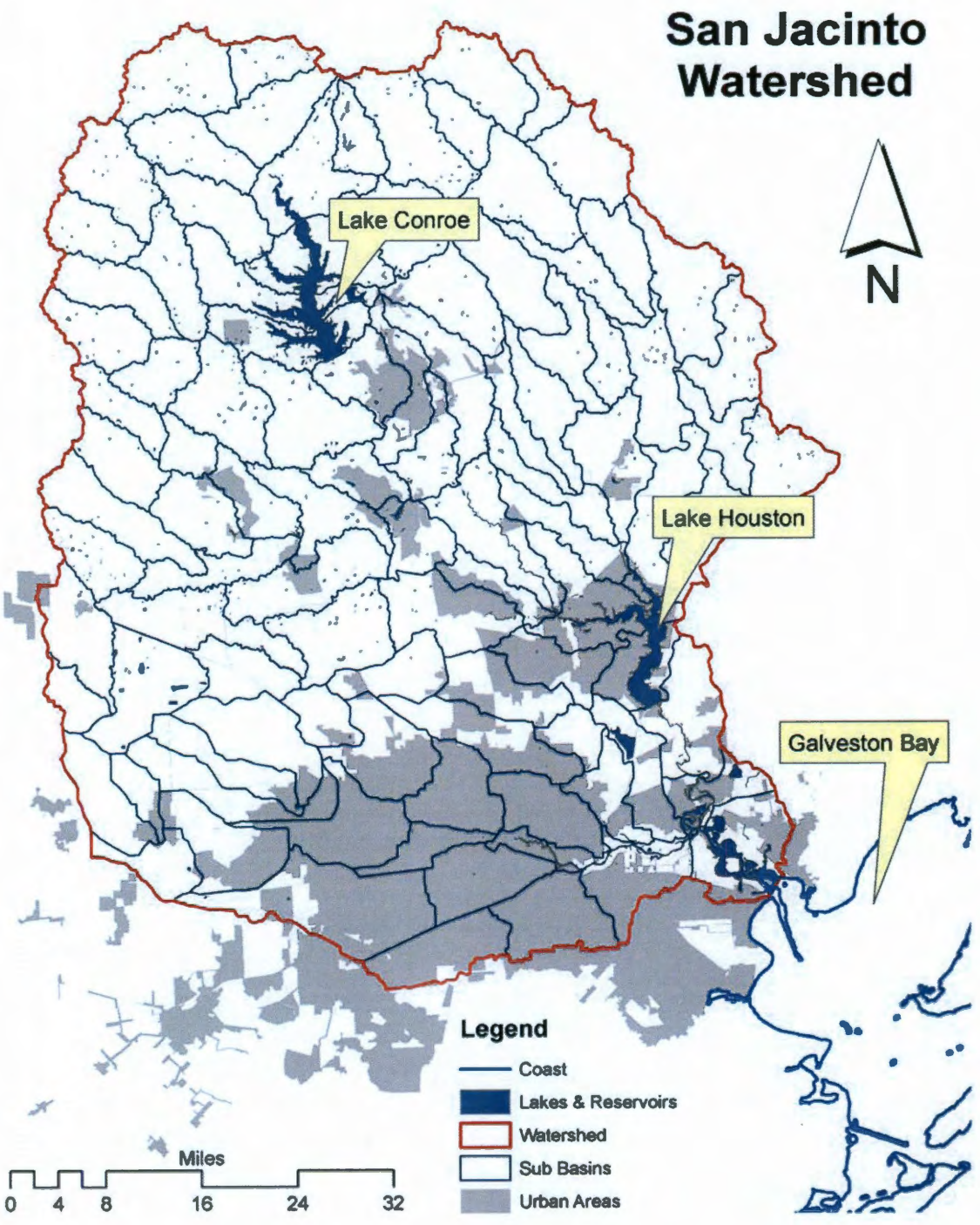

Figure 3.2. San Jacinto – Houston Ship Channel Watersheds

The San Jacinto watershed drains approximately 10,400 square km (4,015 square miles) of mixed agricultural, rural and dense urban development along its 160 km (100 mile) channel. The watershed contains Lake Conroe and Lake Houston, which are the main sources of surface drinking water for the Cities of Conroe and Houston. It also contains most of urban Houston and all of Katy, Conroe, Humble, The Woodlands and Spring, Texas. This watershed is typical of Texas Gulf coast watersheds with a flat surface gradient, highly impermeable surface soils, significant flooding issues, and vulnerability to hurricane storm surge. Output from this San Jacinto hydrologic model was used as input to the hydraulic model of the lower San Jacinto River shown in Figure 3.3. This hydraulic model is an dynamic, one-dimensional HEC-RAS model constructed using current topography/bathymetry and is intended to capture important temporal characteristics of the hydraulic system such as how the stage boundary condition interacts with the hydrologic loading in the coastal interface.

Section 3.1 considers the physics of surface channel flow in the coastal-riverine interface and discusses characteristic flow properties – including quantity, velocity, and depth – as well as the timing of events in this hydraulic domain. Sections 3.2 discusses appropriate computer models used in the analysis within the interface zone, and Section 3.3 summarizes considerations in the appropriate selection of design storms.

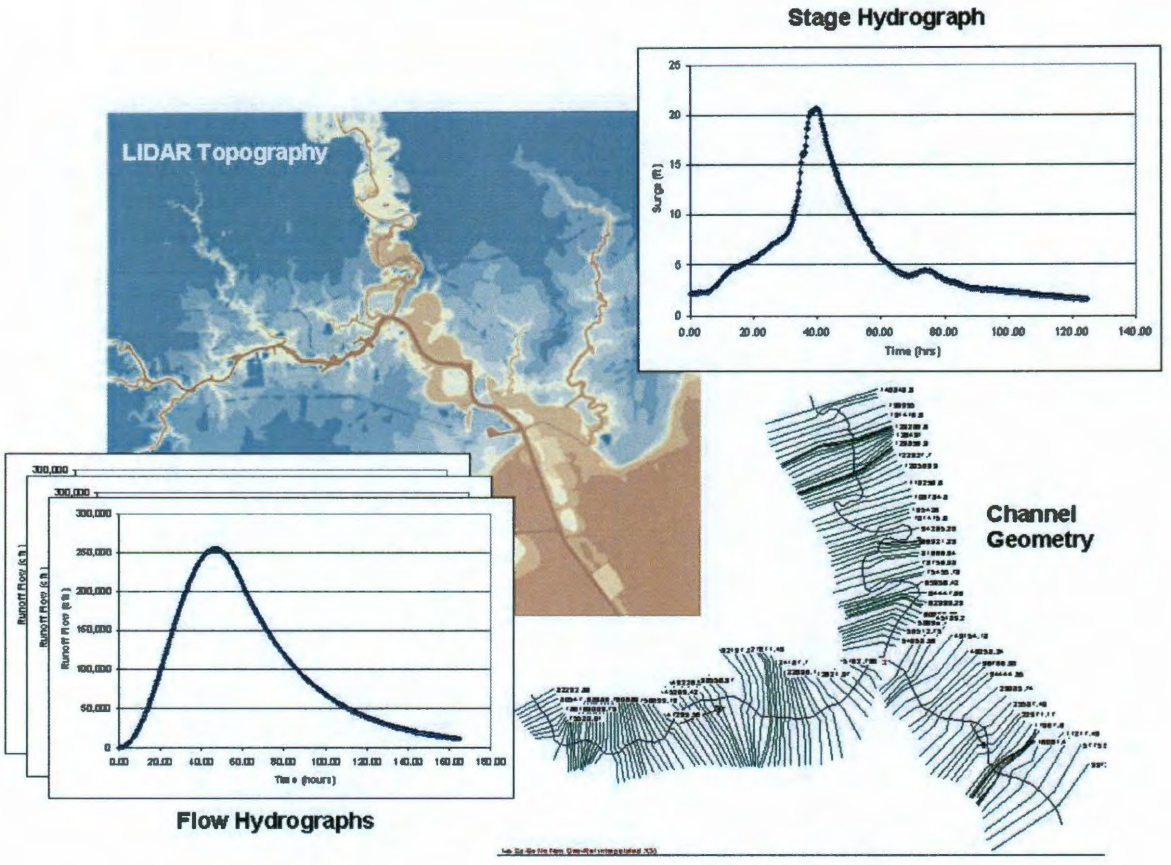

Figure 3.3. Unsteady HEC-RAS Model Schematic

3.1 Hydrology & Hydraulics at the Coastal Interface

Current hydraulic analyses of the coastal zone typically uncouple the coastal hydraulic components (including tides, waves and storm surge) from the riverine components (rainfall runoff, surface routing, and channel storage) to analyze each independently. An example of this process is the creation of regulatory flood insurance rate maps (FIRM) floodplain maps for coastal counties. According to FEMA methodology, the riverine floodplain is modeled and mapped using prescribed methods and hydraulic models that consider rainfall induced flooding of areas along drainage channels (FEMA, 2003). A separate coastal analysis effort is conducted to estimate still

water surge depths and wave impact zones along the coastline, and these results are also mapped (FEMA, 2003). In a final step, the riverine floodplain map is projected onto the coastal and the union of the two delineated floodplains are combined into one flood hazard map (FEMA, 2003). While this process considers flooding potential from coastal surge and river flooding as if they occur independently, it does not consider any hydraulic synergistic or antagonistic interactions between the two processes if they happen concurrent with each other, as occurs in hurricane landfall.

Consider the flow and stage hydrographs shown in Figure 3.4 extracted from the unsteady hydraulic model of the Lower San Jacinto River at its discharge point into Galveston Bay. The storm surge shown was recorded by USGS during the passing of Hurricane Ike in August of 2008 (USGS, 2009). The flow hydrograph shown is an estimate of rainfall runoff associated with Hurricane Ike, presented as it would appear without any influence from surge in Galveston Bay (i.e., the flow hydrograph has no knowledge of the downstream stage condition). Because the peaks of each event would occur 23 hours apart if they were hydraulically disconnected as shown, it may seem reasonable to conclude the two events are temporarily separate and can be uncoupled without introducing significant model error.

Figure 3.5 presents the results of a hydraulic model that considered coupled runoff and surge components from Hurricane Ike. In this figure, the stage hydrograph appears exactly as it did in Figure 3.4, because the volume of water flowing through the San Jacinto River at the time of surge peak has negligible effect on the depth of Galveston Bay (estimated to be less than an inch). However, the flow hydrograph is highly impacted by the coupled stage boundary condition. The coupled peak channel

flow rate increased approximately 110% from the uncoupled peak (190,000 cfs to 400,000 cfs), and the hydrograph is modified so that the peak flow occurs simultaneous with the maximum stage depth at the interface. Additionally, the flow hydrograph has two distinct peaks, one as the surge forces water inland and one as the channel drains after the surge abates. When viewing the results of this coupled analysis, it becomes apparent that the stage boundary condition induces flow in the channel that is not considered in the uncoupled approach. Therefore, the assumption of independence between riverine and coastal processes does not capture the correct fluid flow dynamics occurring at the interface when the two occur together. Any inferences about the characteristics of channel flow derived from the uncoupled model would be incomplete at best and incorrect at worst. Similarly, any coastal infrastructure design based upon the uncoupled model approach would be potentially flawed and subject to premature failure during hurricane impact events.

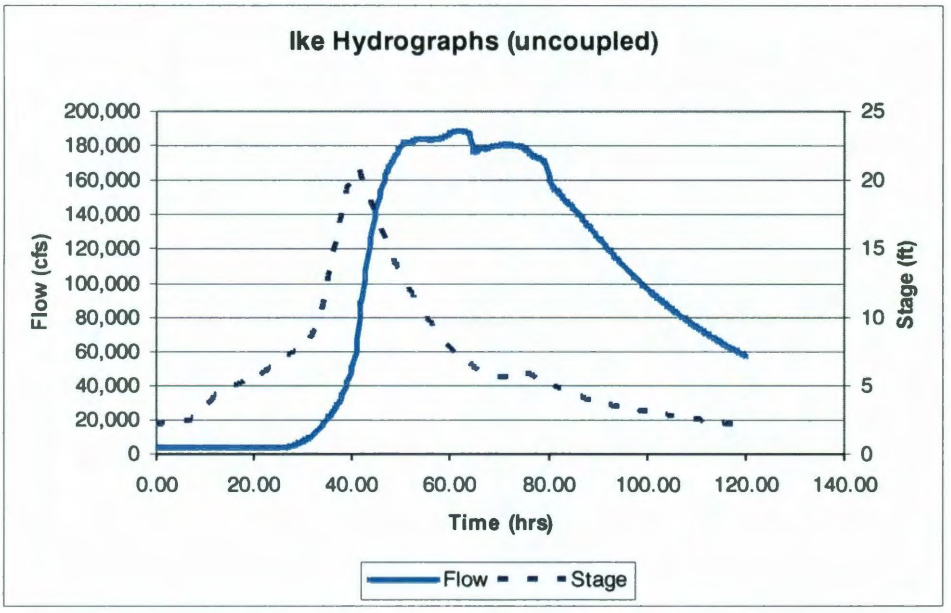

Figure 3.4. Uncoupled Flow and Stage Hydrographs

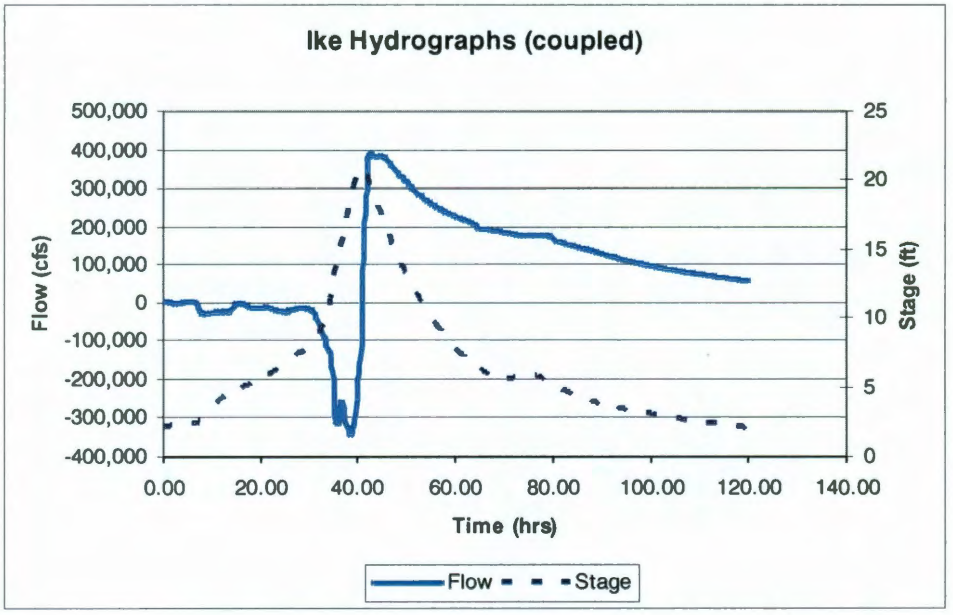

Figure 3.5. Coupled Flow and Stage Hydrographs

A similar analysis of channel flow velocity under uncoupled and coupled conditions gives results shown in Figure 3.6. While the magnitude of instantaneous peak

flow velocities are reasonably the same (at least in the positive flow direction), the uncoupled model does not capture the largest magnitude flow velocity (-4.8 fps) as the surge propagates inland. Channel scour and sediment transport effects of the coupled velocity field are dramatically different from the effect of the uncoupled, and could have significant impacts on analysis of foundation design, sediment and contaminant mobilization and channel morphology in the interface zone.

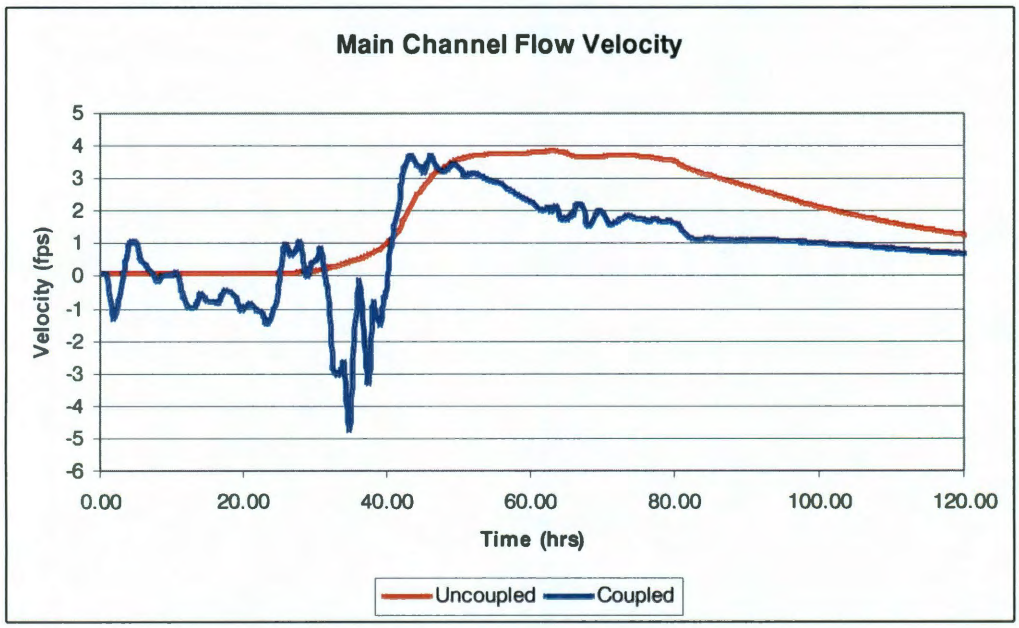

Figure 3.6. Lower San Jacinto Flow Velocity - Coupled vs. Uncoupled

3.2 Hydraulic Modeling of the Coastal Interface

On the inland side of the coastal interface, riverine models are employed to estimate hydraulic properties including flow, flow depth and depth averaged velocity for use in delineating floodplains, sizing bridge openings, determining minimum bridge deck height, and the estimating effects of levee systems for flood protection. Additionally,

channel floodways (i.e., the minimum flow width that will result in a maximum one foot rise in flow depth) can be delineated with these widely used models. Because of the complexity of fluid flow on the coastal side of the interface, two-dimensional unsteady hydraulic models are typically used for analysis of coastal flow fields and floodplains, wave propagation and dissipation, and coastal structural design. The predominant models available to scientists and practitioners provide finite element or finite difference solutions of the shallow water equations. The following sections introduce the unsteady equations and solution techniques utilized by specific software packages. Information presented here is a summary only, more information and detail can be found in the respective technical manuals provided by the software authors.

3.2.1 One-dimensional Riverine Models

One-dimension steady state models are routinely used for river analysis problems, however improvements in computer processing speed and computational capacity have made access to, and use of unsteady models more common for the previously mentioned uses as well as for channel bed scour, sediment transport, water quality analysis, flood control detention and flood diversion analysis. Industry standard computer software used in one-dimensional, steady and unsteady riverine modeling include, most notably, the Hydrologic Engineering Center's River Analysis System (HEC-RAS) (USACE, 2010a). The unsteady flow solution provided by HEC-RAS is achieved by simultaneous solution of the continuity equation and momentum equation for each cross-section at each time step (USACE, 2010b).

The continuity equation provides a conservation of mass in the one-dimensional

form shown in Equation 3.1.

$$\rho \frac{\partial A_t}{\partial t} \Delta x = \rho \left[\left(Q - \frac{\partial Q}{\partial x} \frac{\Delta x}{2} \right) - \left(Q + \frac{\partial Q}{\partial x} \frac{\Delta x}{2} \right) + q_l \Delta x \right] \tag{3.1}$$

Where ρ is fluid density, t is time, A_t is flow cross-sectional area at time t, x is length along the channel centerline, Q is flow rate through the cross-section, and q_l is the unit lateral inflow into the channel segment Δx. Assuming that the density of fluid is constant, dividing each side by $\rho \Delta x$ simplifies the continuity equation as shown in Equation 3.2.

$$\frac{\partial A}{\partial t} + \frac{\partial Q}{\partial x} - q_l = 0 \tag{3.2}$$

The conservation of momentum equation is an expression of Newton's second law of motion. In this conservative equation, the momentum flux entering the channel segment plus the sum of all external forces (i.e., pressure, gravitational, and frictional) is equal to the rate of accumulation of momentum, which is set to zero. Equation 3.3 is the conservation of the momentum equation:

$$\rho \Delta x \frac{\partial Q}{\partial t} + \rho \frac{\partial QV}{\partial x} \Delta x + \rho g A \frac{\partial h}{\partial x} \Delta x + \rho g A \frac{\partial z_o}{\partial x} \Delta x + \rho g A S_f \Delta x = 0 \tag{3.3}$$

Where V is velocity, g is gravitational acceleration, z_o is the channel flowline elevation, and S_f is the slope of the hydraulic grade line (frictional slope). The water surface elevation z is equal to the channel flowline elevation plus water depth, and differentiating with respect to x gives Equation 3.4.

$$\frac{\partial z}{\partial x} = \frac{\partial h}{\partial x} + \frac{\partial z_o}{\partial x} \tag{3.4}$$

Substituting Equation 3.4 into Equation 3.3 and dividing by $\rho \Delta x$ yields Equation 3.5.

$$\frac{\partial Q}{\partial t} + \frac{\partial QV}{\partial x} + gA \left(\frac{\partial z}{\partial x} + S_f \right) = 0 \tag{3.5}$$

The final solution of flow (Q) and flow depth (h) are achieved for each section at each time step with a simultaneous implicit finite difference numerical scheme. More detail about the derivation of the conservation equations and application of the numeric solution can be found in the HEC-RAS technical reference manual (USACE, 2010b).

3.2.2 Two-dimensional Coastal Models

Historic coastal surge models include finite difference approximations of storm surge as in the Sea, Lake and Overland Surges from Hurricane (SLOSH) model (USDOC, 1992). SLOSH was developed by the National Hurricane Center (NHC) in the early 1970's for estimating the depth and area of inundation from long-period gravity waves, and ignores shorter period wind waves, tides and run-up (USDOC, 1992). The SLOSH documentation suggests the model results may contain errors in the range of ±20% (USDOC, 1992), and post Katrina surge studies suggest the SLOSH models underestimated storm surge by approximately 40% in Harrison and Jackson Counties, Mississippi (Melton et al., 2010). Recent significant research effort has been placed into development of the Advanced Circulation Hydrodynamic Model (ADCIRC), a finite element, discontinuous Galerkin solution for the shallow water equations coupled with wind, wave, tide, atmospheric pressure and Coriolis forces (Luettich and Westerink, 2006; Dawson et al., 2011). The ADCIRC models represent a significant improvement to the estimation of storm surge, and FEMA is currently validating the model's results against a list of historic storms – but these results have not yet been published. These recent surge estimate improvements do come at a significant cost as these models are computationally expensive especially for large domains or complex bathymetry.

Similar to the one-dimensional model, the two-dimensional models also solve conservation of momentum and continuity equations. The Navier-Stokes equations for incompressible flows are presented below. These equations are also known as the shallow water equations because the depth dimension is orders of magnitude smaller than the horizontal dimensions for open water environments. The continuity equation (conservation of mass) assuming an incompressible fluid is shown in Equation 3.6.

$$\nabla \bullet \tilde{u} = 0 \tag{3.6}$$

Where $\tilde{u}$ is a two-dimensional fluid velocity vector and ∇ is the gradient operator. Application of Newton's second law of motion (the conservation of momentum) is applied in Equation 3.7.

$$\frac{\partial \tilde{u}}{\partial t} + \tilde{u} \bullet \nabla \tilde{u} - f - \nu \nabla^2 \tilde{u} = 0 \tag{3.7}$$

Where f is a sum of all body forces on the fluid element (including Coriollis, pressure, surface friction, tidal potential, etc.), and υ is fluid kinematic viscosity. In Equation 3.7, the second term represents advective forces and the fourth term represents diffusive forces.

3.2.3 Coupling 1D and 2D Models

Both of the state-of-the-art models discussed (i.e., HEC-RAS and ADCIRC) allow the coupling of riverine and coastal flow properties through appropriate selection of boundary conditions. For example, applications of ADCIRC models to the near shore and coastal environment can incorporate riverine flow as a boundary condition to its model domain (Luettich and Westerink, 2006). Use of this feature allows a more appropriate approximation of flow rates, velocities and currents in the coastal interface

for reasons discussed in Section 3.1. Likewise, applications of unsteady HEC-RAS models to primarily one-dimensional domains in channels and tributaries in the coastal interface can incorporate dynamic stage conditions at the downstream boundary (USACE, 2010). The effect is the same either way, coupling the riverine and coastal flow properties together to achieve a more correct approximation of fluid flow physics at the coastal hydraulic interface.

3.3 Design Storm Selection

Use of numeric models to analyze the coastal flow environment requires the incorporation of appropriate boundary conditions derived from a design storm, or from analysis of a suite of design storms. Selection of design storm(s) is not a trivial matter because selection must satisfy numerous and potentially competing stakeholder interests.

In well researched areas of study (i.e., open channel design and floodplain delineation), regulators may have already established and published storm criteria for use in design and analysis. In areas of new or innovative research (i.e., as in the design of coastal storm surge barriers), there may not be any regulatory guidance as each analysis is highly site specific. Critical to the selection of an appropriate design storm is public discussion, involving all stakeholders, of the following questions:

1. What risk or hazard should the proposed flood control facility/improvement mitigate?
2. To what standards should it perform, including what level of protection should it provide potential receptors?
3. What is the consequence of is potential failure?

With the answers to these questions, an appropriate design storm can be identified and the performance characteristics of the proposed flood control improvement can be assessed. Depending upon the specific application, sources of design storm parameters can include observed historic storms, results from probabilistic analysis of historic weather data, or combined characteristics of different historic and probabilistic storms to create unique design storms.

3.3.1 Design to Historic Storms

When considering new and innovative modeling projects, there may be little or no regulatory guidance to specify design storm selection criteria. In this case, a reasonable analysis approach is the use of an historic storm. An example is the analysis and design of flood protection improvements for the Texas Medical Center in downtown Houston, Texas using observed hydrologic parameters from Tropical Storm Allison as the design event (Bedient et al., 2007). Under these conditions, recorded precipitation intensity, distribution and duration are combined with observed channel stage conditions to evaluate proposed flood improvements. Generally, the use of historic events can be justified because they represent storms that have actually occurred, and therefore have a demonstrated probability of occurrence in the area of interest. However, because extreme storms occur so infrequently, there may not be a record of observations long enough to determine the probability of occurrence for the actual event – resulting in uncertainty in the level of protection the designed system will provide.

3.3.2 Design to a Synthetic Storm

If a sufficient record of historical weather observations exists, a statistical analysis can be performed on the data to generate recurrence intervals for specific events, including extreme events. Many of the regulatory jurisdictions along the upper Texas coast have determined the 1% rainfall event (i.e., the event that statistically occurs, or is exceeded, once in one hundred years on average) to be the basis of most flood control designs, including Harris County Flood Control District (HCFCD, 2009) and City of Houston (COH, 2011). Regulatory guidelines from these flood plain jurisdictions provide statistical tables describing the design rainfall intensity (or depth) for different rainfall durations and return frequencies. A description of methodology utilized to determine appropriate statistical descriptors of rainfall parameters is given by Koutsoyiannis (1994). Similarly, sources and methodology for the analysis of surge depth return frequencies along the Gulf coast include research provided by Irish et al. (2011) and Keim and Muller (2007).

3.3.3 Coupling of Hurricane Rainfall and Storm Surge

Care must be taken in the selection of synthetic design storm for a coupled coastal-riverine interface hydraulic model discussed here. For example, a user that wants to evaluate a 1% event with a coastal-riverine model may be tempted to utilize a 1% rainfall event in development of the upstream hydrologic flow boundary condition and also use a 1% surge event to create the downstream stage boundary condition. However, this approach assumes that rainfall and surge are independent storm variables. In this case, the user is actually specifying a design storm with a 0.01% (one in ten thousand)

probability of occurrence – much more restrictive than the intended 1% event. Instead, the user should employ a methodology to define and characterize a "combined" storm which recognizes that rainfall and surge components are actually dependent storm parameters.

Proposing appropriate design storm characteristics for analysis within the coastal-riverine interface is beyond the scope of this research, but determining an evaluation methodology to review and select appropriate design storm parameters is of critical importance as the design storm characteristics should be rigorous enough to meet stakeholder requirements and fully explore the performance of the proposed coastal improvement. One possible way to achieve this requirement is to couple rainfall and surge components through another storm parameter – the tropical storm's windfield for example. Current research by others is exploring the coupling of tropical storm wind with surge (Dawson et al., 2011; Luettich and Westerink, 2006) and tropical storm wind with rainfall (Langousis and Veneziano, 2009; Jiang et al., 2008), so definition of a design synthetic windfield could provide the coupling mechanism from which the model surge and precipitation inputs could be derived.

3.4 Modeling a Surge Control Structure for the HSC

Following is an application of a coastal-riverine coupled model for the evaluation of a proposed levee and gate system protecting the Houston Ship Channel from hurricane landfall. The proposed levee is approximately 3 miles long, connecting topographic ridges on either side of the lower San Jacinto River with elevation of 7.6 m (25-foot) msl. The levee would contain a major gate structure in the vicinity of the Fred Hartman bridge

(SH 146) so that shipping traffic and storm runoff would not be restricted. Figure 3.7 shows the preliminary location of this proposed structure.

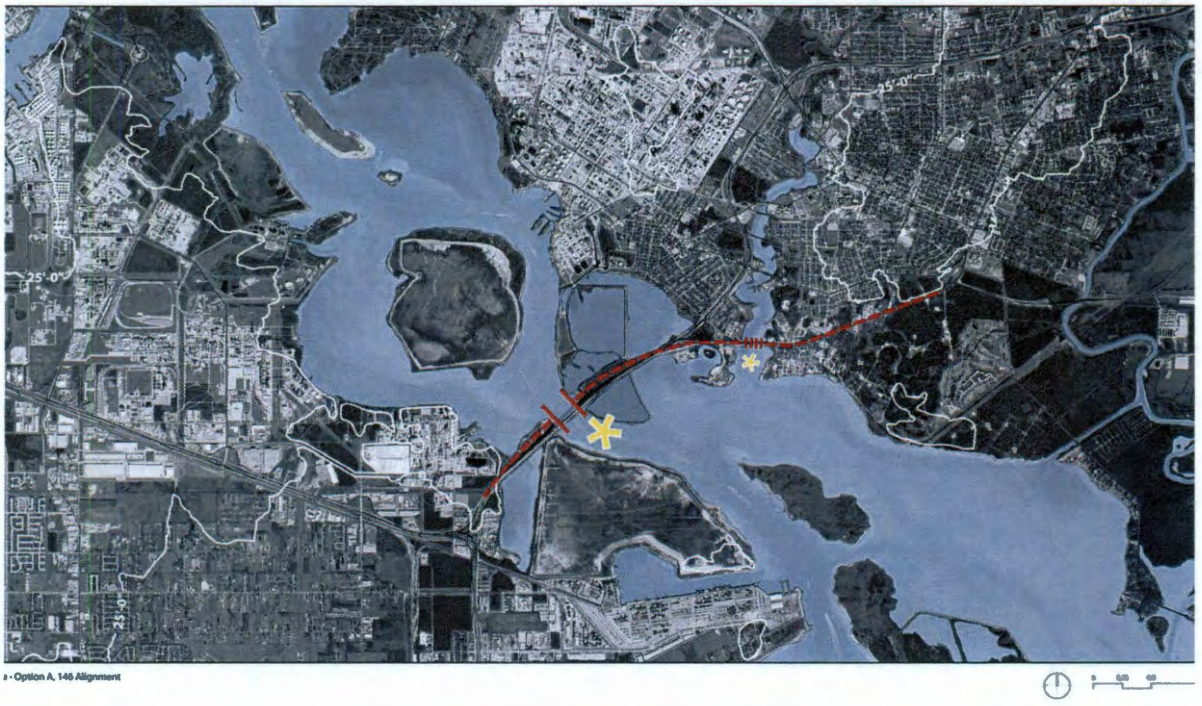

Figure 3.7. Location of Proposed HSC Levee and Gate Structure

3.4.1 Operational Characteristics of the Proposed Gate & Levee

Currently, all the industrial developments along the Ship Channel are responsible for their own flood protection, so the protective standards vary from site to site. The topographic elevation of some of the most critical facilities along the HSC are extremely low, and existing flood protection levees may not protect facilities to reasonably acceptable standard. Figure 3.8 contains an example of the environmental hazards present along the HSC banks. This figure shows the presence of a petrochemical storage tanks (red dots) located at elevations varying from 0.6 m (2 feet) to 6.1 m (20 feet) above sea level (TCEQ, 2011). This facility has a protective levee around the most vulnerable

of the tanks with a maximum elevation of around 4.3 m (14 feet). However, the design standard, construction methods and maintenance history of this levee are not publicly available, so the true risk of discharge from this tank farm is not readily known.

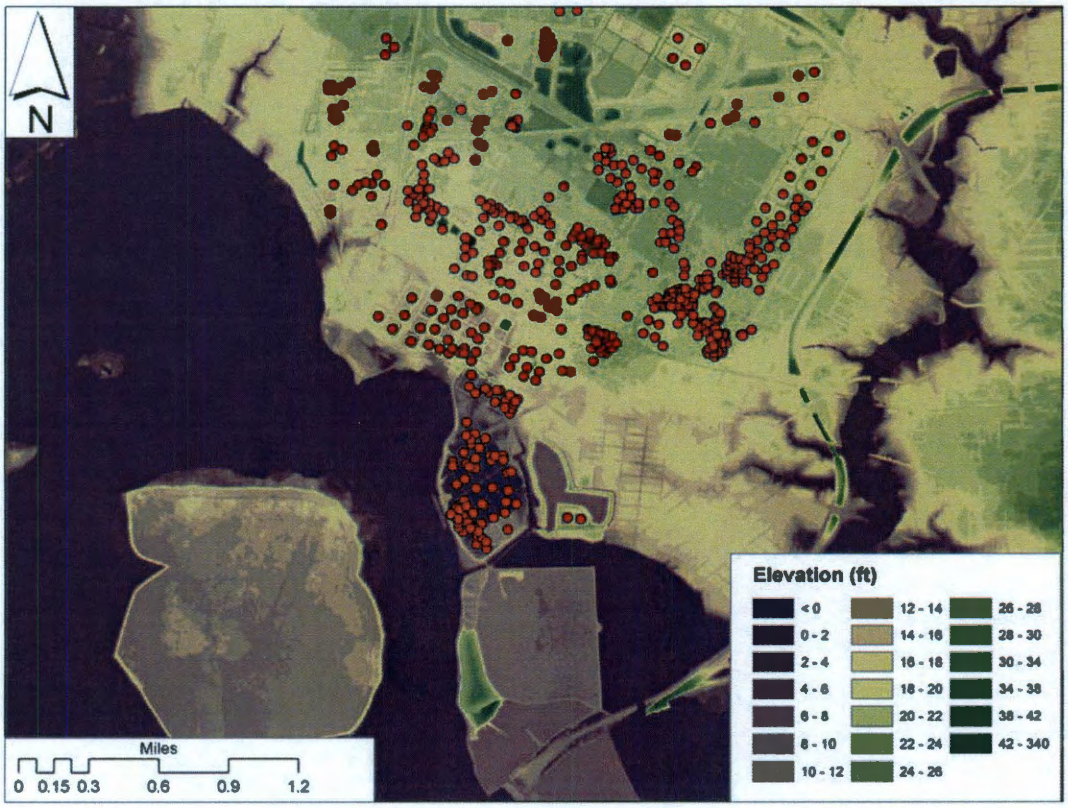

Figure 3.8. Example of an Environmental Hazard Along the HSC

In contrast to the individual protective measures provided by each facility to protect their assets, the HSC levee and gate structure would offer a uniform protective benefit to all industries along the HSC in the event of hurricane landfall into Galveston Bay. Ultimately, the height of the proposed levee and gate would be based on a cost-benefit analysis that balances the construction and maintenance cost with flood protection benefits. For the purposes of this preliminary analysis, a design height of 7.6 m (25 feet) was selected for consideration to take full advantage of the adjacent topography.

3.4.2 Model Constraints

To be an effective surge barrier, the proposed gate structure would have to completely block the San Jacinto River – which drains approximately 10,400 km^2 (4,000 $miles^2$) including all of downtown Houston, Texas. With the gate structure closed, runoff from the upstream watershed will accumulate in the channel until the gate is re-opened and the flow is released into Galveston Bay. With the conceptual design of a simple levee and gate (no pumping station is currently being considered), there is only a finite time the gate can remain closed without causing collateral flooding from rainfall runoff accumulation in the channel upstream of the gate structure. The model must be able to determine the tolerable length of gate closure and estimate the resulting backwater depth in the HSC resulting from operation of the surge gate.

3.4.3 Model Calibration

To assure reasonable model results, the hydraulic model shown in Figure 3.3 was calibrated against an observed hurricane landfall event. Hurricane Ike provided a direct hit into Galveston Bay in September 2008, and there are well documented water depth recordings by the U.S. Geological Survey and Harris County Homeland Security and Emergency Management across this model domain (USGS, 2008; HCHSEM, 2011) as summarized in Table 3.1. USGS collected water elevations at a recording station located near the discharge point of the San Jacinto River into Galveston Bay (known as Morgan's Point), and this data was utilized as the downstream stage boundary condition in the hydraulic model. Additionally, water depth data collected by Harris County at the

upstream ends of the San Jacinto River and Houston Ship Channel are used for model calibration at locations just downstream of Lake Houston on the San Jacinto River and at the Turning Basin on the Ship Channel. After running the hydraulic model calculated flow depths at the upstream ends of each tributary are compared against the Harris County observed data. Figure 3.9 contains the calibration results for the San Jacinto River location, and Figure 3.10 shows results for the Ship Channel.

Table 3.1. Stage Observation Locations for Hurricane Ike

Location	Channel	Site ID	Reference
Morgan's Point	San Jacinto, lower	SSS-TX-HAR-004	USGS, 2008
US90 Bridge	San Jacinto, upper	G720-SanJac_US90	HCHSEM, 2011
Turning Basin	Ship Channel	G2210-BufBayou	HCHSEM, 2011

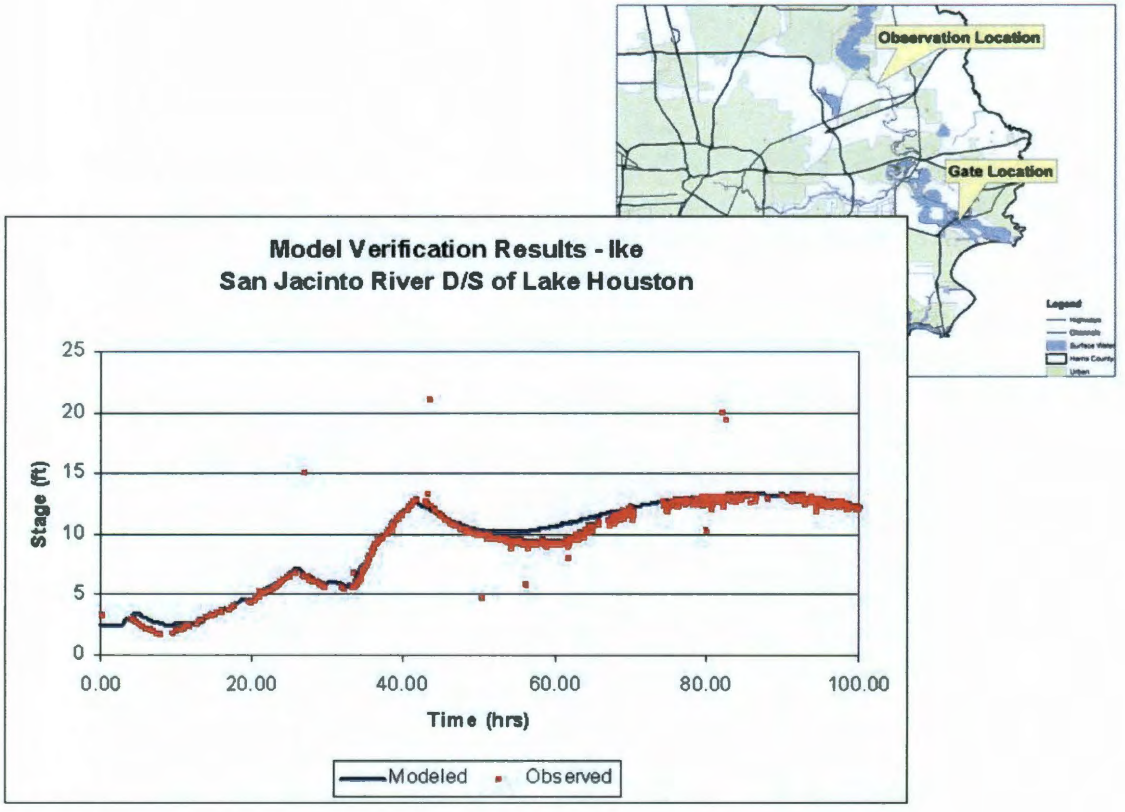

Figure 3.9. Model Calibration at San Jacinto Boundary

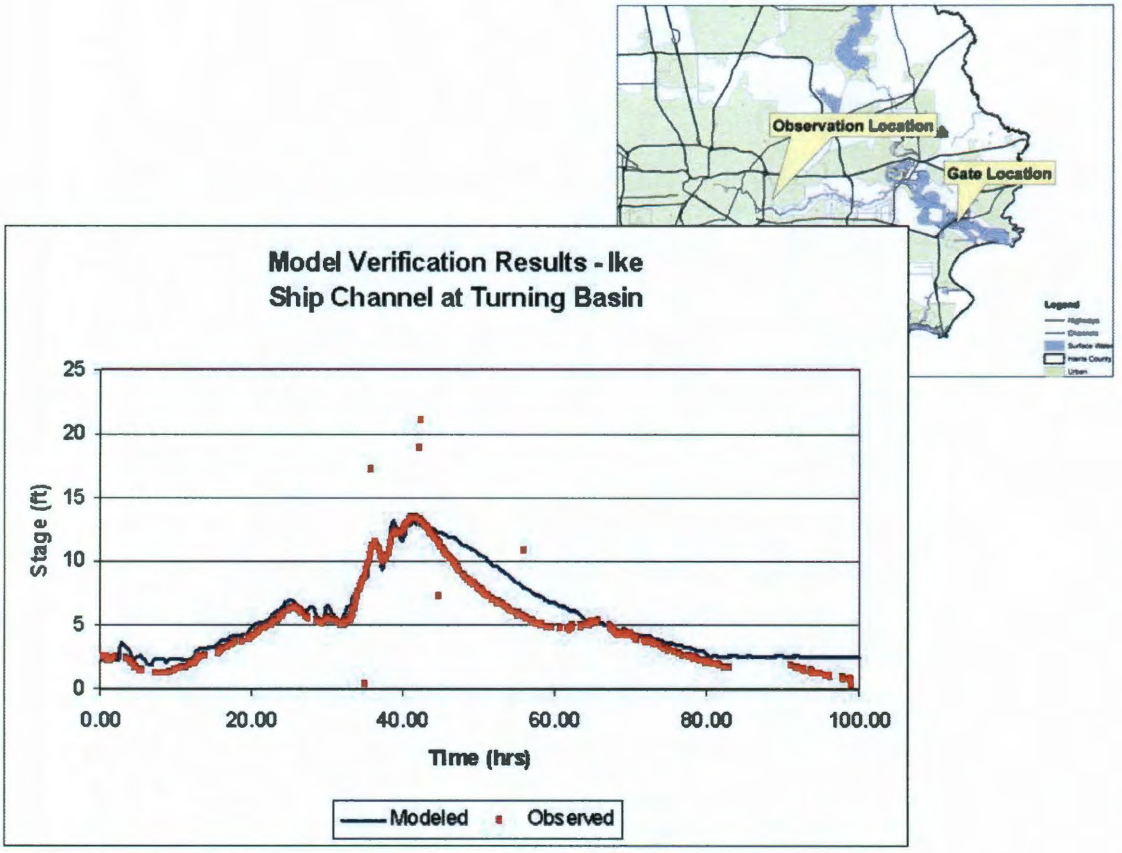

Figure 3.10. Model Calibration at Ship Channel Boundary

For each tributary, the unsteady model approximated the surge propagation effects (time 0 to 40 hours) quite well. There was more variation from observed data after time 40 hours (especially in the HSC tributary), and this is attributed to uncertainty in the hydrologic flow inputs to the model. Loss of power across much of the watershed during hurricane landfall resulted in an incomplete precipitation data set. Even though hydrologic model input is not certain, the general hydraulic response of the model agrees closely with observed stage data as shown in Figures 3.9 and 3.9, and there is high confidence in the ability of the hydraulic model to correctly estimate the hydraulic

processes occurring during a coastal surge event.

3.4.4 Selection of Design Storm

Two design storm scenarios were selected to analyze the effectiveness of a hurricane surge levee and gate after carefully considering the purpose of the analysis (i.e., a preliminary engineering assessment of the proposed structure) and the availability of design surge and rainfall data. The first analysis scenario considered was the Hurricane Ike event that occurred in September, 2008. This historic storm was selected for use because it was a well observed event, with stage observation stations occupying strategic locations as shown in Table 3.1. Additionally, because the memory of this event is still fresh in the minds of many decision makers, comparisons between actual events and computational results from the model can have meaning far beyond those from hypothetical event scenarios.

The second design storm considered is intended to be an approximation of a 1% event, with a characteristic 21 foot storm surge and a 10 inch uniform rainfall across the entire watershed. To achieve this synthetic design storm, the observed Hurricane Ike stage hydrograph from the USGS recording station at Morgan's Point was scaled-up to achieve a maximum 21 foot surge depth, and the 100-year, 24-hour hydrographs from Tropical Storm Allison Recovery Project (TSARP) hydrologic models were scaled down to approximate a 10 inch rainfall. This combination of storm surge and runoff hydrographs is identified for analysis based on professional opinion that it is representative of a plausible 1% design storm event. Additional design storm events could be easily specified and analyzed considering other storm characteristics, if desired.

3.4.5 Analysis Results

Each of these design storm events was analyzed using the hydraulic model under existing conditions (i.e., no levee or gate structure) and under conditions with the proposed levee and channel gate. This analysis quantifies the flood protection benefit in terms of reduction in maximum water surface elevation under the specific design storm conditions being considered. Additionally, the unsteady hydraulic models estimate the operating parameters of the gate including the conditions under which the gate should close and how long the gate must remain closed to maximize the flood protection benefit. Table 3.2 summarizes the analysis results for the Hurricane Ike landfall scenario. The difference between the maximum water surface elevation (WSEL) columns containing the "No Gate" and "With Gate" scenarios shows the net reduction of flood depth associated with operation of the gate and levee. The "Max Surge Reduction" column shows the benefit of the gate structure at the time the peak surge occurs. The optimal time that the gate structure should remain closed under Hurricane Ike conditions is approximately 39 hours.

Table 3.2. Hurricane Ike Design Storm Analysis Results

Observation Location	Maximum WSEL		Max Surge Reduction (feet)
	No Gate (feet)	With Gate (feet)	
Hartman Bridge	12.33	9.03	8.12
SanJac-HSC confluence	12.38	9.29	8.06
Beltway 8 Bridge	12.49	9.63	7.71
US-90 Bridge	12.64	11.76	7.89

As the results indicate, the gate and levee structure can reduce the 12.3 foot MSL surge

event by approximately 8 feet at the confluence of the San Jacinto River and the Ship Channel, resulting in a water elevation of about 4.3 feet MSL at the time of peak surge. However, during the time that the surge gate remains closed, accumulation of rainfall runoff behind the gate raises the water elevation to approximately 9.3 feet MSL resulting in a net reduction in the flood plain of around 3 feet.

Results for the 1% design storm event show a much better flood protection benefit as summarized in Table 3.3. Under this design storm event, the proposed structure would reduce the 21 foot MSL surge by over 12 feet at the confluence of San Jacinto and HSC. During the approximate 38 hours of gate closure in this design storm, runoff accumulation will increase water depth to about 15 feet MSL, resulting in a net flood reduction benefit of around 6 feet. Although beyond the scope of this initial investigation, future model runs could consider the benefit of a pumping station at the gate structure, providing an additional level of protection by allowing continuous discharge of rainfall runoff and reducing the accumulation depth of runoff behind a closed gate.

Table 3.3. 1% Design Storm Analysis Results

Observation Location	Maximum WSEL		Max Surge Reduction (feet)
	No Gate (feet)	With Gate (feet)	
Hartman Bridge	21.08	14.45	14.08
SanJac-HSC confluence	21.10	14.95	12.34
Beltway 8 Bridge	21.36	15.42	13.37
US-90 Bridge	21.79	18.78	10.98

Chapter 4

Coastal Floodplains

Standard floodplain delineations along the U.S. Gulf Coast are performed according to Federal Emergency Management Agency (FEMA) guidance using deterministic, steady state hydraulic models incorporating assumed stage boundary conditions, peak flow rates occurring simultaneously throughout the system, and average values for roughness coefficients uniformly applied throughout the hydraulic models (FEMA, 2003). Flow input for hydraulic models is generated from hydrologic models, either lumped or distributed, that routinely assume a spatially unvarying precipitation depth, duration, and rainfall pattern. The net result of these practices is the delineation of a floodplain hazard that is independent of the natural variability inherent in actual flooding events. Typically, these flood hazard assessments communicate a "binary" hazard state – a location is either inside the delineated floodplain, or it is outside the floodplain. In reality, uncertainty in event and watershed parameters means that the floodplain depth and extent are also uncertain. Therefore, the floodplain is not a binary feature, and there is no singular floodplain depth for any specific location. Instead, the flood hazard is better described as a range of flood depths with an associated probabilistic distribution varying continuously across the topography (Kousky and Kunreuther, 2010).

Variability in floodplain model results are influenced by a number of factors including data uncertainties, model uncertainties, and natural variability. Data uncertainties result most commonly from sample sizes too small for the population they represent and sampling bias introduced through a simplistic or inadequate data collection plan. Generally, data uncertainties – commonly referred to as epistemic uncertainty – can be minimized by improvements in the data collection and estimation process (Liu and Gupta, 2007). There can also be significant amounts of analytical model uncertainties – also epistemic uncertainties – which are present if the mathematical models do not adequately describe the physics behind the natural processes taking place (Pappenberger et al., 2007). Refining the mathematical models and assumptions utilized can reduce this error source. Finally, some sources of variability are naturally occurring and cannot be eliminated or reduced with any amount of planning, sampling or modeling effort. These uncertainties – also called aleatory uncertainty – represent parameters that can take one of many values through natural random processes. Although model parameters may be classified, sorted and tracked as either epistemic or aleatory, the essence of uncertainty, and how a modeler manages them, depends solely on the context of the application (Der Kiureghan and Ditlevsen, 2009). In the framework of simulations presented here there is no benefit for distinction between epistemic or aleatory parameters, as both were treated in the same manner in the model realizations. Therefore, the term "uncertainty" will be used for the remainder of this paper to describe the effects of both error types.

Previous work in flood analysis incorporated parameter uncertainty through statistical analysis methods where a confidence level is calculated for the delineated floodplain based upon the uncertainty of input parameters (McBean et al., 1984;

Kunstmann and Kastens, 2006). Specific examples of statistical approaches include application of standard least squares (SLS), weighted least squares (WLS), Bayesian total error analysis (BATEA), and non-probabilistic information gap analysis (Hine and Hall, 2010; Thyer et al., 2009). While these methods allow for incorporation of uncertainty in the analysis through calculation of a confidence interval, the floodplain is still presented as a binary feature with the many associated drawbacks identified by Kousky and Kunreuther (2010). Additionally, there is little evidence that these techniques are porting over to practical applications because of difficulties with educating practitioners in using these statistical techniques and acceptance by regulators of unfamiliar statistical concepts and computer models.

Alternatively, stochastic analysis methods have been used to incorporate variable and uncertain parameters directly into the analysis (Di Baldassarre et al., 2010; Roth, 2009a) allowing expression of the floodplain uncertainty as a collection of possible floodplains, usually acquired at a high computational cost. For example, Smemoe et al. (2007) evaluated the impact of variability in sub-basin curve number (CN) for a lumped hydrologic model; McMillan and Brasington (2008) employed a stochastic description of rainfall duration and basin discharge with an unsteady hydraulic model; Werner et al. (2005) analyzed unsteady hydraulic models with variable but spatially homogeneous roughness coefficients; Brown et al. (2007) studied the floodplain impact of variability in stage boundary conditions and roughness coefficients; and Pappenberger et al. (2006) incorporated uncertainty in the upstream flow boundary. Each of these studies considered certain parameters as stochastic variables, either because of data uncertainty or natural variability, and presented the results as probabilistic floodplain delineation

maps illustrating the underlying hazard structure of the floodplain based upon the variability of the input parameters. This paper expands upon this previous research by considering uncertainty in parameters presumed to be important to coastal watersheds, developing a flood hazard map incorporating that variability, and calculating a flood risk map given the hazard uncertainty and coastal topography. The work presented here takes advantage of existing software tools commonly used in practice to incorporate, process and communicate hydrologic variability. However, this work is not a study in demonstrating commercial software features. It is a critical appraisal of existing flood delineation methodology and suggests alternative ways to incorporate uncertainty to extract useful results, including the delineation of risk maps, given existing tools.

4.1 Traditional Floodplain Analysis Procedures

Analysis of floodplain requires two distinct steps: a hydrologic analysis to convert precipitation hyetographs into flow hydrographs incorporating the effects of physical processes such as surface impoundments, soil infiltration, overland routing and accumulation in channels; and a hydraulic analysis to determine the characteristics of that flow in the channel including the depth, velocity, width of flow, hydraulic gradient and other parameters. The following paragraphs discuss each of these steps including common analysis practices and assumptions utilized by engineers and regulators.

4.1.1 Hydrologic Analysis

Design storms used for floodplain delineation generally have a prescribed uniformity including a return frequency (1% probability of occurrence per year), a

duration (24-hours) and homogeneous spatial extent (uniformly applied to the entire watershed) (FEMA, 2003). Compliance with these regulatory requirements effectively removes variability associated with the design storm event. While this may enhance consistent application of the floodplain delineation process among multiple researchers and practitioners across varying locations, it introduces un-quantified analysis error in the model results. For example, not all 1% events have a 24-hour duration and a uniform spatial characteristic. In fact, the compounded requirements for a specific return interval, duration and spatial distribution result in a design storm that has an extremely low probability of occurrence – much less frequent than the 1% regulatory requirement. In addition to the uniformity of the design storm event, several basin hydrologic characteristics are frequently considered to be unchanging throughout the system. Hydrologic parameters including soil moisture, sub-basin time of concentration, overland slope, channel slope, among others, are assumed to be known and unvarying over time and space. In reality, each of these parameters could be considered as an uncertain parameter existing within a range of possible values.

4.1.2 Hydraulic Analysis

Although not a specific regulatory requirement, most current floodplain delineations are conducted using deterministic, steady state hydraulic models. In application of these deterministic models, uncertain parameters are replaced by representative point values selected from the range of possible values. In practice, these point values are selected with a bias that tends to maximize the calculated floodplain depth, so as not to underestimate the delineated floodplain. This error is compounded as

multiple conservative parameters are incorporated into the hydraulic models and their cumulative bias is propagated through the analysis. While it is generally acceptable to be conservative in administration of the floodplain, this current process does not quantify how much of the floodplain estimate is true hazard and how much is analysis error attributable to conservative inputs.

From a hydraulic perspective, these steady state floodplain models are relatively easy to construct and execute, extremely stable, and for the reasons stated provide a conservative floodplain estimate. However, they do not incorporate dynamic hydraulic effects of either hydrograph summation or flow routing. By ignoring these dynamic characteristics, steady state models tend to introduce additional analysis error, especially as hydrograph timing becomes more variable (McBean et al., 1984). While it would be difficult and cost prohibitive to generate probabilistic hydrologic and hydraulic floodplain models incorporating uncertainty in all input parameters, completely ignoring uncertainty may not be a reasonable practice given the software tools and data sources currently at our disposal.

4.2 Floodplain Uncertainty Analysis

Development of the hydrologic and hydraulic models utilized in this paper's flood hazard and flood risk assessment is achieved in three distinct steps. The first step includes defining the hydrologic and hydraulic parameters to be considered uncertain and designing an analysis plan to appropriately consider reasonable combinations of these parameters. This work considers storm duration, spatial rainfall distribution, roughness coefficients, stage boundary conditions, and hydraulic timing as important sources of

uncertainty in coastal watersheds based upon professional opinion that these are important characteristics in this coastal watershed. Recognizing that other parameters also contribute to floodplain variability, this analysis only considers these parameters.

Regulatory flood design guidance from the jurisdictional drainage district serving this area establishes 1% event as a minimum depth of rain falling during a prescribed duration (GCDD1, 2007). Table 4.1 shows the rainfall-duration combinations representing 1% storms for this watershed. Values for the additional parameters (i.e., storm speed, rainfall distribution and stage boundary conditions) are specified with reasonable combinations of values once duration is identified. Acknowledging uncertainty in just these few variable parameters generates an infinite number of possible 1% events for consideration given that the parameters are continuous in time and space, and each combination of parameter values generates a unique runoff response, distinct from all other possible 1% storm events. To reduce computational complexity, the analysis plan identifies a sub-set of possible storms that will specifically be incorporated in this uncertainty analysis. This design storm selection process joins reasonable combinations of parameters to create unique and plausible design storm conditions in accordance with the logic shown in Figure 4.1. For the purposes of this analysis, 24 unique design hydrologic events are selected for incorporation in the models.

Table 4.1. 1% Rainfall Events for the Case Study Watershed

Storm Duration (hours)	**Total Rainfall (cm)**
3	17.45
6	21.95
12	27.43
24	34.14

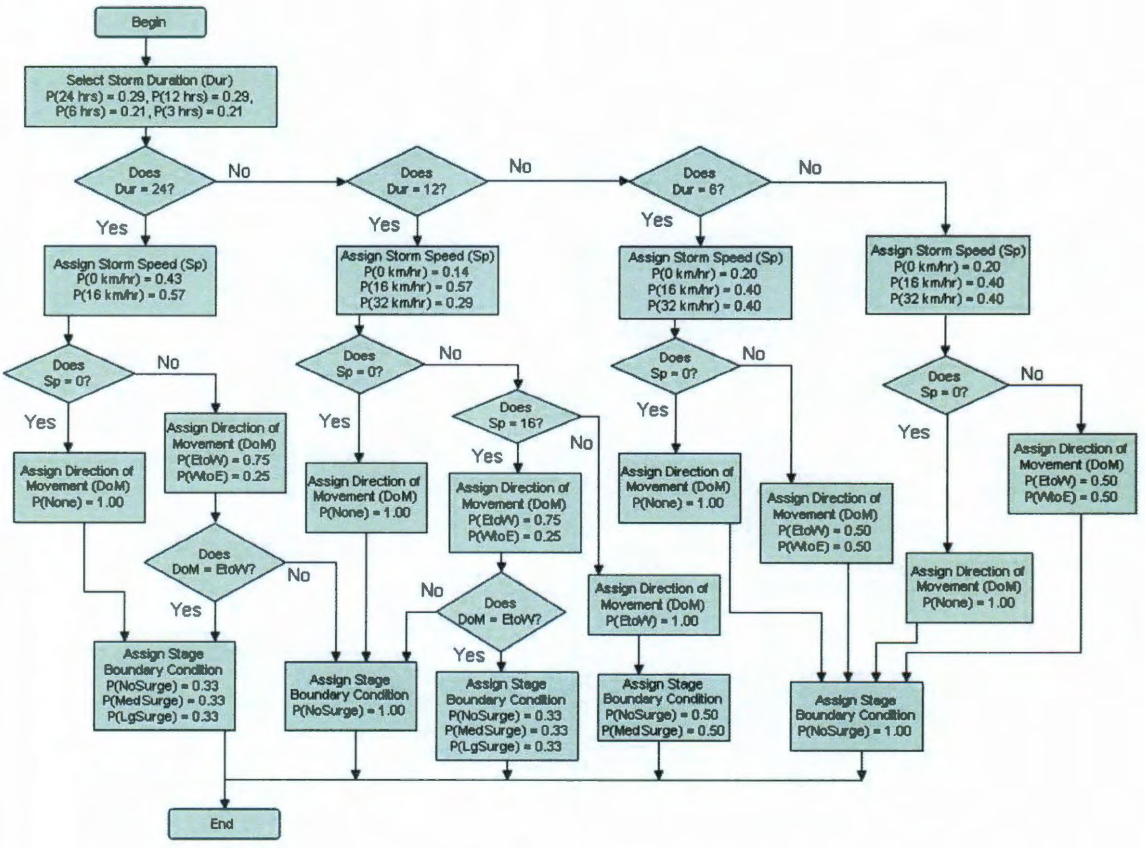

Figure 4.1. Design Storm Selection Decision Tree

The second step of floodplain delineation includes conducting a hydrologic analysis to generate flow hydrographs incorporating the variable hydrologic parameters identified in the previous step. In this step, hydrologic simulations of the design meteorologic events are conducted, and the derived flow hydrographs are extracted for use as input to the hydraulic analysis. The last step includes the formulation of an unsteady hydraulic model to assess riverine dynamic responses in a more robust manner than is available in the steady state models. Steady state hydraulic models are ubiquitous in industry and in many circumstances may be appropriate for use, such as in analysis of

short channel segments with well documented boundary conditions (Di Baldassarre et al., 2010). However, as the complexity of the watershed increases and channel segments lengthen, the potential analysis errors introduced by the steady state assumption grows. The current version of HEC-RAS (USACE, 2010) has the capability of modeling both steady state and unsteady hydraulic behavior utilizing a common geometry, and regulators have a high level of familiarity with this software's capabilities. Because the requirements for steady and unsteady geometries in HEC-RAS are essentially the same, most steady state HEC-RAS models are good potential candidates for an "upgrade" to unsteady models. The authors have found that well constructed steady state models can be run in unsteady mode with a reasonable investment of time.

4.2.1 Flood Hazard Assessment

A hazard is defined as a condition that has the potential to cause some consequence, where the consequence is an event that would preferentially be avoided (Haddow and Bullock, 2006). In this context, the process of delineating a floodplain is considered a "hazard assessment" as it determines the areas that are susceptible to flooding under prescribed hydrologic conditions. Current binary floodplain maps (FEMA FIRM maps for example) do not capture epistemic or aleatory uncertainty, and they convey a confidence of results that is not representative of the uncertain parameters upon which they are based.

Incorporation of parameter uncertainty in the analysis process can be accomplished in many ways, however stochastic numerical simulation techniques are generally easy to understand and implement. In this uncertainty simulation, multiple

realizations of the hydrologic and hydraulic models are executed with input parameters varying in accordance with user defined distribution. Each individual realization of the base deterministic model provides one possible result, and running multiple realizations with variable input parameters results in an ensemble of plausible outcomes. Studying the distribution of the outcomes gives an indication of the variability of the system representative of the uncertainty in input parameters. These simulations are flexible and robust techniques that can handle large and complex systems for which there are no good approximate analytical methods. One major drawback is that this technique is computationally expensive to run because of the number of realizations required. An appropriate number of model runs is dependent on the total variability of the system and the desired level of confidence and can be estimated by the following equation described by Eng (2003):

$$N = \frac{4 \times \sigma^2 \times Z_{crit}{}^2}{D^2} \tag{4.1}$$

Where N = required sample size, σ is the standard deviation of the population (usually approximated by the standard deviation of the sample set), Z_{crit} is a critical value of the standard normal deviate and is a function of a user defined confidence interval, and D is the desired confidence interval width. This method does not require knowing the number or characteristics of uncertain input parameters affecting the output population mean. It is simply an estimate of minimum sample size required given an estimate of variability in the parameter being considered. In future work , if probability distribution functions (PDFs or joint PDFs) can be derived for these input parameters, a true probabilistic analysis can be performed and a sufficient number of realizations made to fully describe probabilistic uncertainty in the coastal floodplain.

Once derived, the data set can be queried using frequency analysis techniques to reveal the relationship between flood depth and exceedence probability throughout the model domain. Each flood depth can be mapped with its associated probability of occurrence to show the floodplain hazard as a collection of possible 1% floodplains differentiated by the probability of their occurrence. Presentation of floodplain hazard maps utilizing high resolution digital topographic data and GIS mapping techniques are quite effective for presenting this type of probabilistic information (Roth, 2009a, 2009b).

4.2.2 Flood Risk Assessment

For floodplain managers there is an important distinction between floodplain "hazard" and "risk" concepts. In practice, it may not be possible, advisable or economically feasible to manage flood hazards (i.e., insure that 1% events can be completely confined to channels, detention ponds or other flood control structures), however it may be quite possible to effectively manage flood risk by protecting people and development from areas of high hazard. Given the previously determined uncertain flood hazard showing frequency of surface inundation, the next logical step is to combine this probability of occurrence (i.e., the hazard) with inundation depth into one parameter in some meaningful and useful way. This probability-weighted flood depth parameter is defined in this work as a proxy for flood risk. This flood risk can be calculated as a continuous spatial variable using the Fractile Method (Haimes, 2004) utilizing Equation 4.2, where the variable 'x' is flood depth above the ground surface and f(x) is the probability that depth x will occur, and the integral is evaluated over the total depth of the water column.

$$Risk = \int_{0}^{Depth} x \times f(x)dx \tag{4.2}$$

The integral risk equation can be approximated by Equation 3, when an empirical PMF is available, where $p_i = p(x_i)$, and Risk = $\sum$(Depth $\leq x_i$) where n is the number of percentile bins used in the analysis.

$$Risk = \sum_{i=1}^{n} x_i \times p_i \tag{4.3}$$

Once calculated, this risk variable can be mapped and used for many purposes including formulation of informed public policy decisions, setting flood insurance premium rates based on actual risk, development of land use and land control ordinances to minimize possible exposure to areas of elevated risk, and assessing the impact of regional drainage and flood control facilities, among other uses.

4.3 Probabilistic Floodplain Delineation

The modeling approach discussed here was applied to the Dickinson Bayou watershed, a complex but typical watershed in the Texas Gulf Coast plains located south of Houston, Texas and discharging into Galveston Bay, as shown in Figure 4.2. This watershed covers 250 km^2 (95.5 square miles), it is approximately 27 kilometers (17 miles) long and generally flows from west to east. Characteristics of this watershed include a flat topography (less than 0.025% slope on average), highly impermeable surface soils, and mixed land uses including agricultural, rural residential and urban developments. Figure 4.3 shows the extent of a classical steady state floodplain delineation for Dickinson Bayou. The floodplain is a prominent feature of the watershed as it covers approximately 78 km^2 (30.25 square miles), representing 32% of the

watershed's total area. The floodplain heavily impacts the City of Dickinson, Texas which straddles the banks of Dickinson Bayou near its outfall into Galveston Bay (inset area in Figure 4.3). An expanded view of the inset in Figure 4.4 shows the standard 1% floodplain delineation as a binary hazard with no means to differentiate areas of unequal hazard and associated risk.

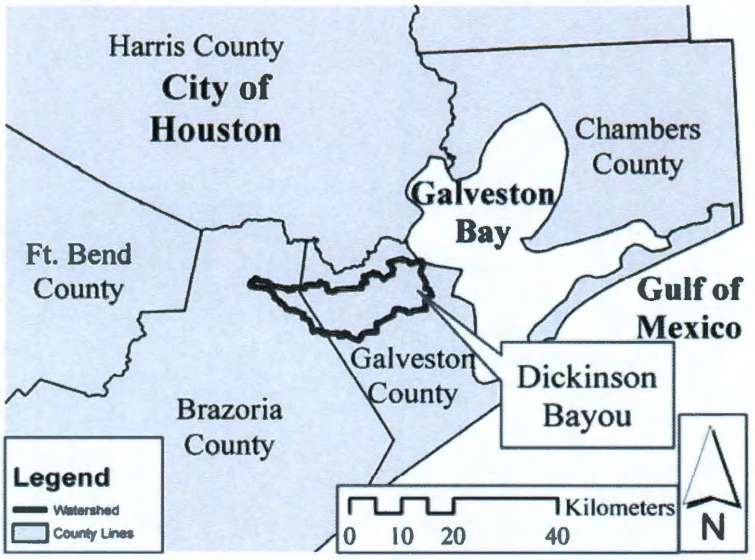

Figure 4.2. Dickinson Bayou Vicinity Map

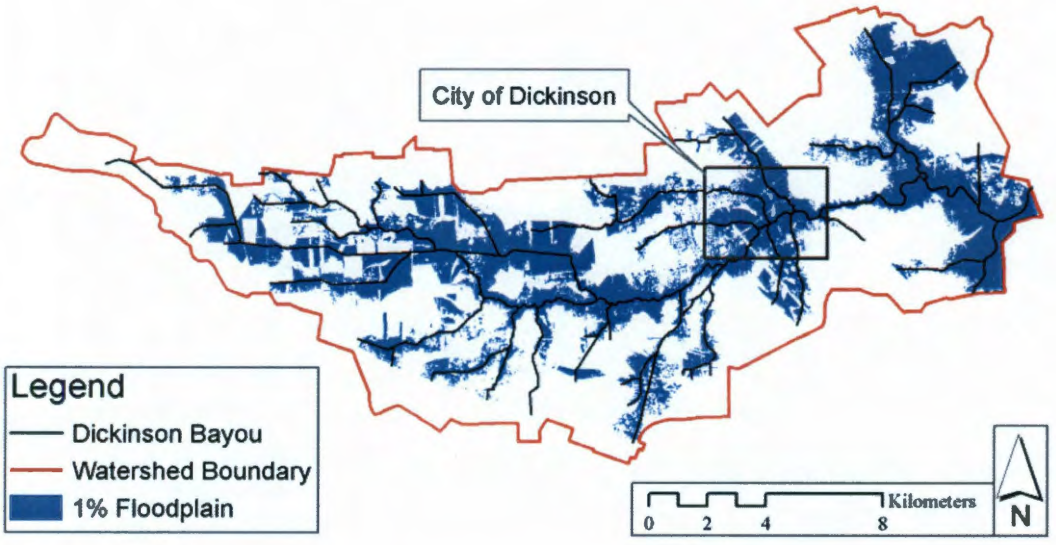

Figure 4.3. Dickinson Bayou Watershed and Floodplain

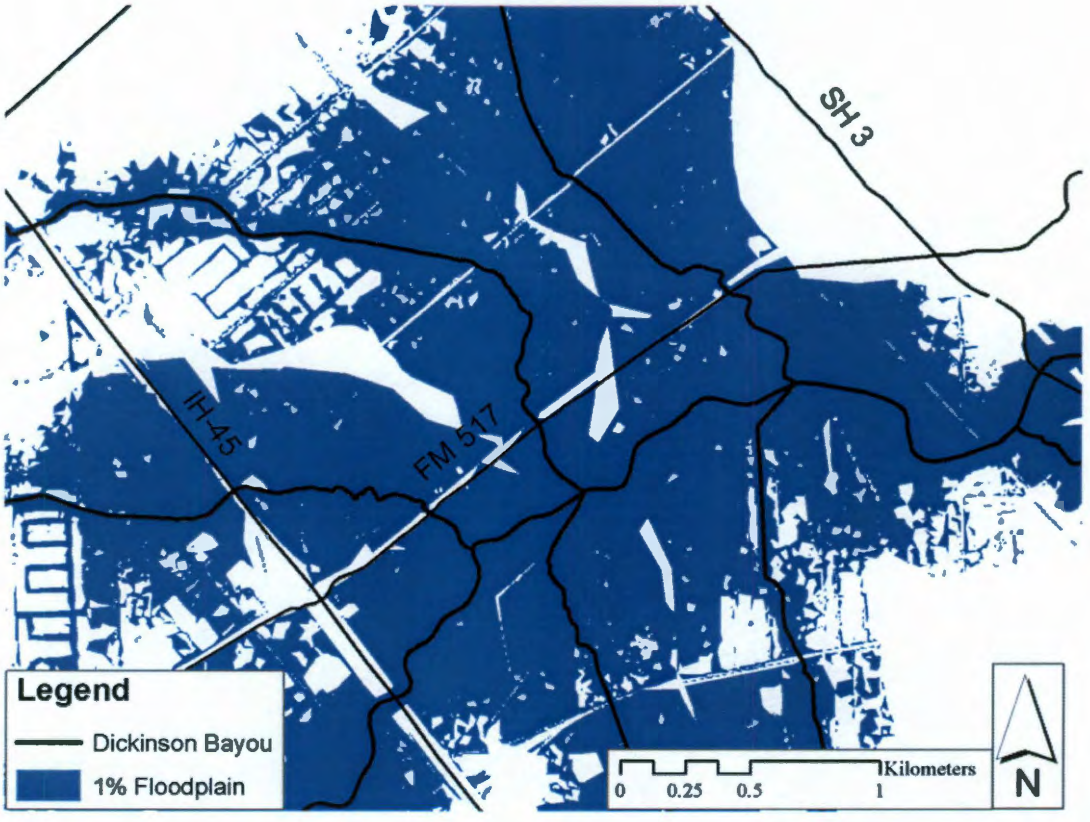

Figure 4.4. City of Dickinson Floodplain

This case study utilized existing lumped parameter hydrologic and steady state hydraulic models as the starting point for a probabilistic flood hazard assessment (GCDD1, 2008). In this uncertainty assessment, hydrologic parameters of storm duration and rainfall distribution are considered to be variable. Uncertain hydraulic parameters included roughness coefficients and downstream boundary conditions, and an unsteady hydraulic model is implemented. An analysis plan is formulated that included reasonable combinations of parameter values, as summarized in Table 4.2 with the full range of values included in this assessment. For comparison purposes, Table 2 also contains the deterministic parameter values commonly used in this watershed for floodplain delineation.The specific scenarios identified in the analysis plan were not selected naively from the infinite number of possible events, but were selected intelligently based upon reasonable combinations of the uncertain variables. In accordance with the analysis plan, if the preliminary modeling results suggested that uncertainty of floodplain variability required more than these scenarios, an additional number of scenarios would be included as warranted by the variability of the data set. Assignment of design storm parameters occurs according to the logic flow shown in Figure 4.1, and justification for specific hydrologic parameter values used in the analysis are described in the following paragraphs.

Table 4.2. Uncertain or Variable Model Parameters.
The numbers in parenthesis show the number of scenarios containing each uncertain parameter value.

Hydrologic/Hydraulic Parameter	Deterministic Value	Uncertain or Variable Parameter Values
Storm Duration	24 hours	3 (20), 6 (20), 12 (28) or 24 (28) hours
Storm Movement Velocity	None	0 (24), 16 (48) or 32 (24) km/hour
Storm Movement Direction	None	E-W (48), W-E (24) or None (24)
Roughness Coefficient	Average	Average (24) or Random (72)
Stage Boundary Condition	Normal Depth	Normal Depth (68) or Surge (28)

4.3.1 Storm Duration

In contrast to the standard deterministic floodplain analysis which only consider a 24-hour rainfall event, this analysis considered multiple events ranging from 3 hours to 24 hours. These durations represent design storm lengths commonly used in flooding studies in this watershed. This watershed is large enough that rainfall durations less than 3 hours would not cause significant basin wide riverine flooding and therefore were not considered. Likewise, 24-hour durations were considered a reasonable upper bound because of the way design storm hyetographs are constructed – longer storm durations would not yield rainfall hyetographs inherently different from the 24-hour storms being considered. Design storm hyetographs for each of the storm durations modeled assumed a normal distribution with maximum precipitation intensity occurring at 50% of the storm duration. Hyetograph shape could have actually also been included as an uncertain parameter with a range of front-loaded and rear-loaded shapes included in the analysis, and future uncertainty assessments may consider hyetograph shape as a naturally variable parameter.

4.3.2 Storm Rainfall Distribution

Typical deterministic floodplain delineations assume a uniform precipitation across the entire watershed. This assumption forces the hydrologic modeler to apply precipitation to the watershed with spatial homogeneity – as would result from a very large storm cell with little to no movement. While the Texas Gulf Coast experiences storms with these characteristics, they are no more certain than smaller storm cells with discernable movement patterns. Accordingly, this uncertainty analysis selected both storm speed and direction of movement as uncertain parameters. Values of 0 km/h (i.e., a stationary storm), 16 km/h (10 mph) and 32 km/h (20 mph) were considered. The authors expected that slow moving storms starting upstream and moving toward the outlet would be more likely to combine peak flows from contributing sub-basins, resulting in larger channel flow rates and a deeper floodplain as compared to uniform storms. Similarly, events starting at the outlet and moving upstream were expected to be less likely to add peak flows, generating a shallower floodplain. This variation in the timing of sub-basin contribution is the mechanism expected to add uncertainty for speed and direction of movement parameters.

Forward storm speeds in this geographic area can easily approach 80 km/hr (50 mph), or more. However, during fast moving storms, the time differential between when sub-basins contribute flow is small and the watershed response looks similar to a homogeneous storm with no movement. Therefore, faster moving storms were not independently considered as the expected differential runoff response diminishes as the storm speed increases. For these reasons, values of 0 km/h (i.e., a stationary storm), 16 km/h (10 mph) representing a slow moving storm, and 32 km/h (20 mph) representing a

moderate storm movement were considered in this work. Uncertainty in movement direction is also included with storms having no movement, some moving West-to-East (W-E) and some East-to-West (E-W). Because of the long and relatively narrow geometry of this watershed (see Figure 2), it was assumed that runoff from storms with North and South movements would not differ significantly from the uniform storms considered, so they were not explicitly included in the analysis.

4.3.3 Channel Roughness Coefficients

Typically in a hydraulic analysis, whether it be steady state or unsteady, average values of roughness coefficients are applied uniformly across the entire hydraulic model. In other uncertainty studies (Di Baldassarre et al., 2010; Smemoe et al., 2007), this parameter was allowed to vary across a reasonable range but was applied with a spatial homogeneity throughout the model. Functionally, there is no way to determine an exact value for this parameter across the entire watershed, and in the case of natural channels is almost certainly not homogeneous. Even if a snapshot distribution could be determined, it would change randomly over time as vegetation grows and dies, overbank areas are cleared and developed, and channel morphology results in bank erosion in some areas and sediment deposition in others. To incorporate this natural variability, a stochastic modeling approach was employed and three different hydraulic model geometries were generated with randomly assigned Manning's '*n*' values at each hydraulic cross-section.

According to literature, specific values of Manning's '*n*' for natural channels can span from 0.025 to 0.060 (Bedient et al., 2008, Linsley et al., 1982). For the purposes of this stochastic analysis, parameter values are selected from a normally distributed set

with a mean (μ) of 0.045 and a standard deviation (σ) of 0.008, which gives a confidence interval of 95% that the selected value falls within the range of 0.029 to 0.061 (i.e., $\mu \pm 2\sigma$) for this assumed distribution. As would be expected with a random assignment, some adjacent cross-sections are randomly assigned significantly different roughness values which contributed to numeric instability in the unsteady model. In these rare instances of numeric instability, non-random adjustments to the assigned values are made – just enough to address the numeric instability while preserving the overall normal distribution of this parameter in the model. In addition to the three random geometries, a fourth geometry containing a spatially uniform and average roughness (i.e., n = 0.045) is created and utilized in the analysis. Of the storm scenarios analyzed, each of the four model geometries described was utilized in one-quarter of the scenario realizations.

4.3.4 Stage Boundary Condition

Finally, an improvement to the arbitrary "normal depth" stage boundary condition utilized in most floodplain delineation models is desired. In this coastal watershed, 1% events are frequently, but not always, accompanied by elevated stage conditions in Galveston Bay. These conditions occur as tropical storms bring both torrential rains and coastal surge as the storms make landfall. There is an absence of literature regarding return frequency and storm surge depths for locations along the Gulf Coast, and there is no definition of a 1% surge in Galveston Bay. Accordingly, surrogate surge profiles from actual storms are utilized in this analysis.

Hurricane Ike was a strong category two storm when it made landfall into Galveston Bay in 2008, and the resulting storm surge in Galveston Bay tested the design

limit of many of the protective dikes along the shoreline. In this event, a surge profile just outside Dickinson Bayou outfall generated a maximum height of 3.8 meters (12.5 feet) with a duration of around 60 hours (USGS, 2008). The surge created by Hurricane Ike was considered an average surge event for the purposes of this analysis, and several scenario runs utilized the Ike surge data as the downstream boundary condition. An additional surge boundary condition was created by scaling the Ike surge event by a factor of 1.25, to represent landfall of a stronger hurricane. Figure 4.5 shows the stage hydrograph utilized for the Ike surge boundary condition, constructed of idealized tide and surge components and shown in comparison with the observed surge for Hurricane Ike at USGS site SS-TX-GAL-019 (USGS, 2008).

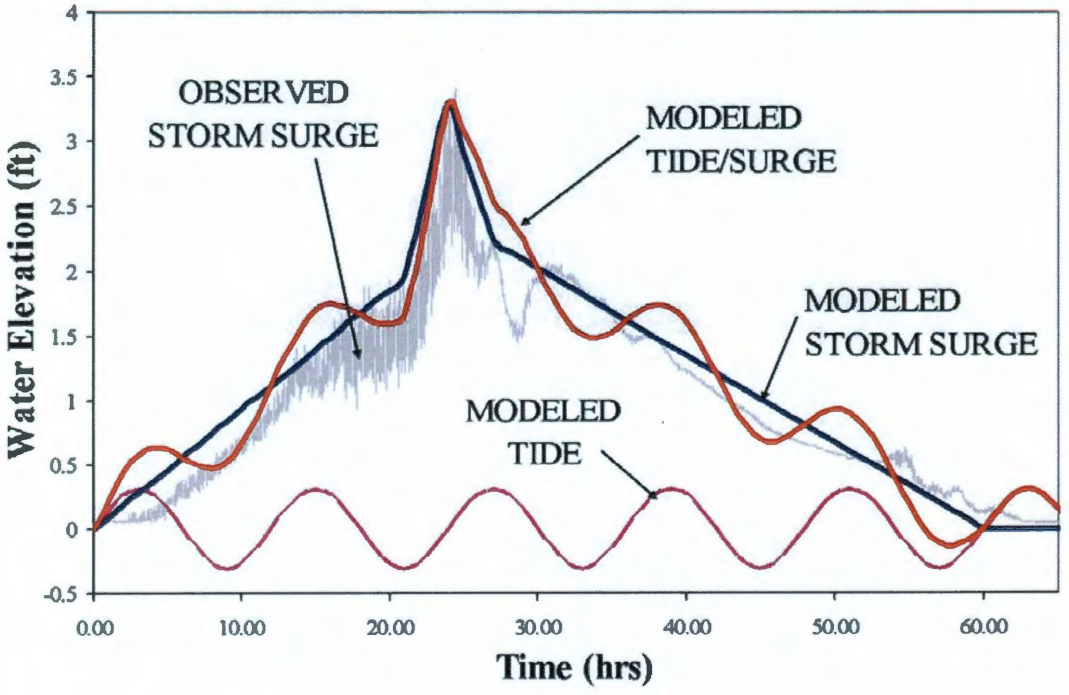

Figure 4.5. Hurricane Stage Boundary Condition

4.3.5 Design Storm Scenarios

Having identified the parameters to be considered as uncertain, representative values of these parameters were combined in unique scenarios to create the set of design storms used in this uncertainty analysis according to the logical steps shown in Figure 4.1. Combinations of uncertain parameters were not truly random and required some amount of engineering judgment. For example, no west-to-east moving storms (i.e., storms originating over land and moving seaward) would be capable of creating surge boundary conditions, therefore no combinations of eastward movement and surge boundary conditions were utilized. Likewise, a storm capable of creating a surge would likely have a longer duration than 3 or 6 hours, therefore all scenarios with surge boundary conditions also had durations of 12 or 24 hours. Using this methodology, 24 unique hydrologic events applied to 4 different channel geometries result in 96 individual storm scenarios used as a representative sub-set of possible 1% events for this watershed. Application of Equation 1 to the hydraulic cross-section with the largest standard deviation (σ = 0.13 m) results in a minimum sample size estimate of 72 using Z_{crit} = 1.960 (for a 95% confidence interval) and D = 0.06 m.

4.4 Floodplain Delineation Results and Discussion

The aggregate results from the 96 storm events hold interesting information about the underlying structure of the floodplain in Dickinson Bayou. As detailed in Figure 4.6, there were three major regions in the lower portions of the Dickinson Bayou main channel including a "tidal zone," a "transition zone" and an "inland zone." The tidal zone is defined by a relatively high channel aspect ratio (channel width divided by

channel depth) and is consistent with the tidally affected portion of Dickinson Bayou. However, this variability is not attributed solely to tide as tide is not a component of the normal depth boundary conditions and therefore could not contribute variability in those realizations. Figure 4.6 shows that floodplain depth in the coastal zone has a variability of approximately 1.2 m (4 ft) when considered independently of surge boundary conditions, and a maximum of 3 m (10 ft) when storm surge is considered. In the upper portion of the coastal zone, model results generally tended to cluster by storm duration, with the shortest storm duration (3 hours) being the lowest grouping followed by 6 hours, 12 hours and 24 hours at the upper end. The intra-group variability (i.e., group band width) was generally around 0.08 meters (0.25 feet) while the inter-group variability (i.e., depth spanned by groupings) was approximately 1.0 m (3.5 feet). These results suggest that for the lower portions of Dickinson Bayou, the most important variable parameters were the model stage boundary condition and the design storm duration. Other uncertain parameters, including storm movement speed and direction and channel roughness, contributed some variability to floodplain depth, but these parameter effects were approximately an order of magnitude less.

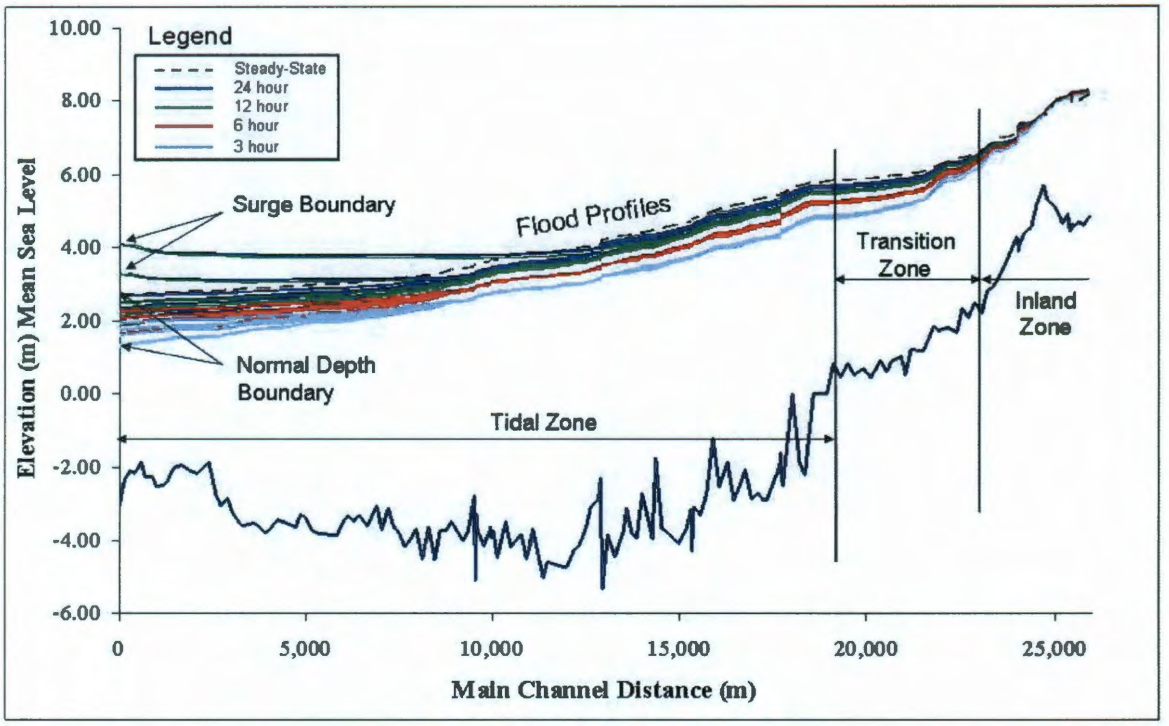

Figure 4.6. Main Channel Flood Depth Profiles

In Dickinson Bayou, the transition zone begins at the upper extent of tidal influence. In this zone, the analysis results maintain their banded nature with intra-band variability remaining relatively constant at 0.08 meters (0.25 feet) and inter-band variability reducing to 0.6 m (2.0 feet) on average. Again, the shortest duration storms represented the lower end of the floodplain variability, with the longer duration storms comprising the upper end. In the transition zone for the main channel, no effects of surge boundary conditions were evident, leaving storm duration as the only uncertain parameter providing significant variability of results in this coastal watershed.

The inland zone is characterized by a tight grouping of all scenario results with little expression of variability regardless of values used for the uncertain parameters. In

this region, the total variation including the influence of all uncertain parameters is on the order of 0.15 meters (0.5 feet). It appears that for the inland riverine segments of this coastal watershed, uncertainty in model parameters analyzed does not contribute much variability to the solution of the floodplain delineation and the steady-state deterministic model provides an adequate approximation of the floodplain.

4.4.1 Flood Hazard Delineation

After generating results for all model scenarios to capture uncertainty, flood depth values were aggregated by cross section, and specific percentiles of the data set were determined. Flood depth values for the 90^{th}, 75^{th}, 50^{th}, 25^{th} and 5^{th} exceedence probabilities at each model cross section were exported and mapped to a surface model of the watershed using GIS mapping techniques. This effort resulted in a distributed flood hazard showing the frequency that the surface will be inundated by a 1% event. Figure 4.7 shows an expanded view of the floodplain hazard for the inset area accounting for uncertainty, and shows the underlying structure of the floodplain hazard as compared to the binary hazard shown in Figure 4.4. Using this technique, the 1% floodplain can be sub-divided into hazard areas that are inundated with a relatively high frequency (i.e., high hazard areas shown with darker colors) and those that are affected by relatively few of the possible 1% events (low hazard areas shown with lighter colors).

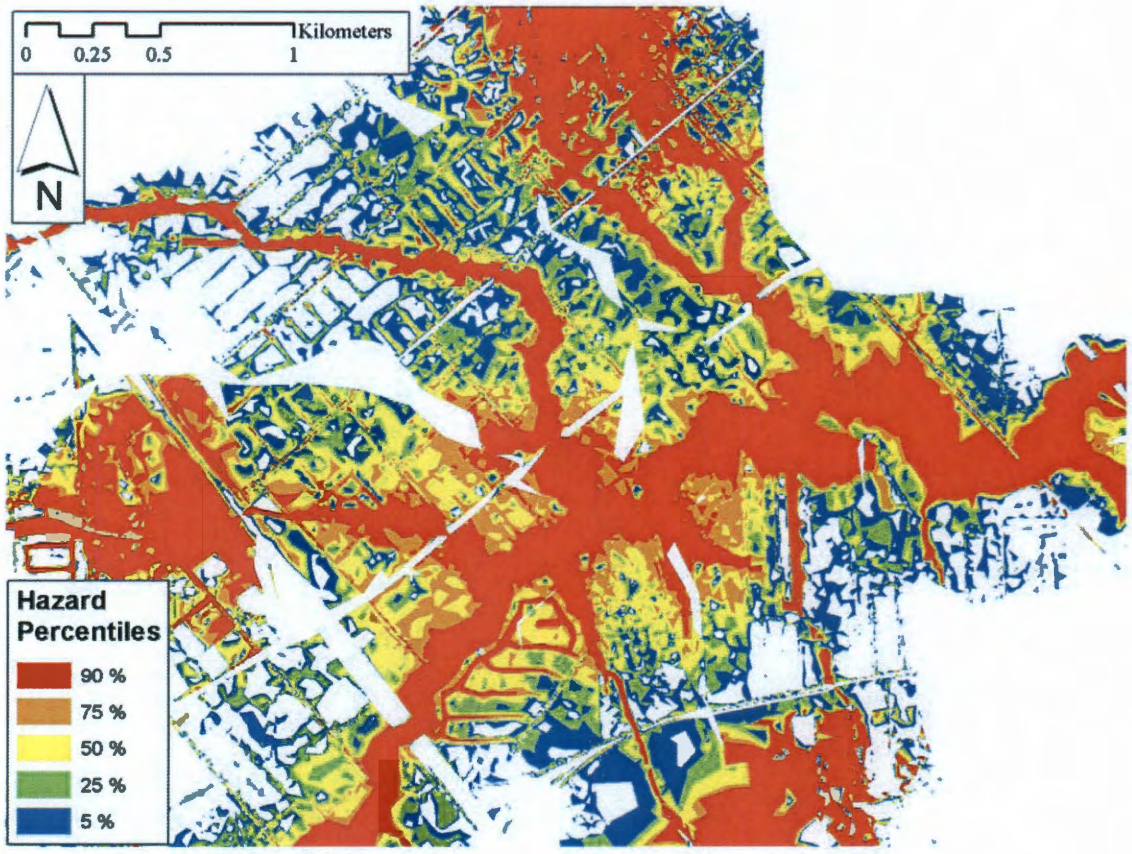

Figure 4.7. Flood Hazard Map for City of Dickinson

4.4.2 Flood Risk Delineation

Knowing the flood hazard structure within a floodplain is informative, but the true advance in floodplain delineation with explicit treatment of uncertainty comes with the ability to express that hazard as a risk, because it is the risk that is problematic and must be managed. Calculation of risk is relatively straightforward given a hazard probability distribution. As an example of these calculations, Equation 4.3 is applied to the point labeled A on Figure 4.8, with actual values for hazard depth given in Table 4.3.

Table 4.3. Parameter Values for Risk Calculation at Point A in Figure 4.7.

Parameter Description	Water Depth (m)
Minimum Flood Depth (min)	1.40
10% Hazard Depth (D10)	1.44
25% Hazard Depth (D25)	1.73
50% Hazard Depth (D50)	1.98
75% Hazard Depth (D75)	2.14
95% Hazard Depth (D95)	2.38
Maximum Flood Depth (max)	2.42

Equation (4.3) is expanded to:

$$Risk = \left(\min + \frac{D10 - \min}{2}\right) \times 0.10 + \left(D10 + \frac{D25 - D10}{2}\right) \times 0.15 + \left(D25 + \frac{D50 - D25}{2}\right) \times 0.25$$
$$+ \left(D50 + \frac{D75 - D50}{2}\right) \times 0.25 + \left(D75 + \frac{D95 - D75}{2}\right) \times 0.20 + \left(D95 + \frac{\max - D95}{2}\right) \times 0.05 = 1.93$$

This calculation can be easily applied using available GIS software to create a continuous risk distribution for the entire floodplain. Comparing Figure 4.8 (flood risk) to Figure 4.7 (flood hazard) shows the benefit of the more detailed delineation, especially where areas of high hazard do not represent high risk. Using this information, areas delineated as high risk can be the focus of floodplain managers as they attempt to apply limited resources for maximum benefit.

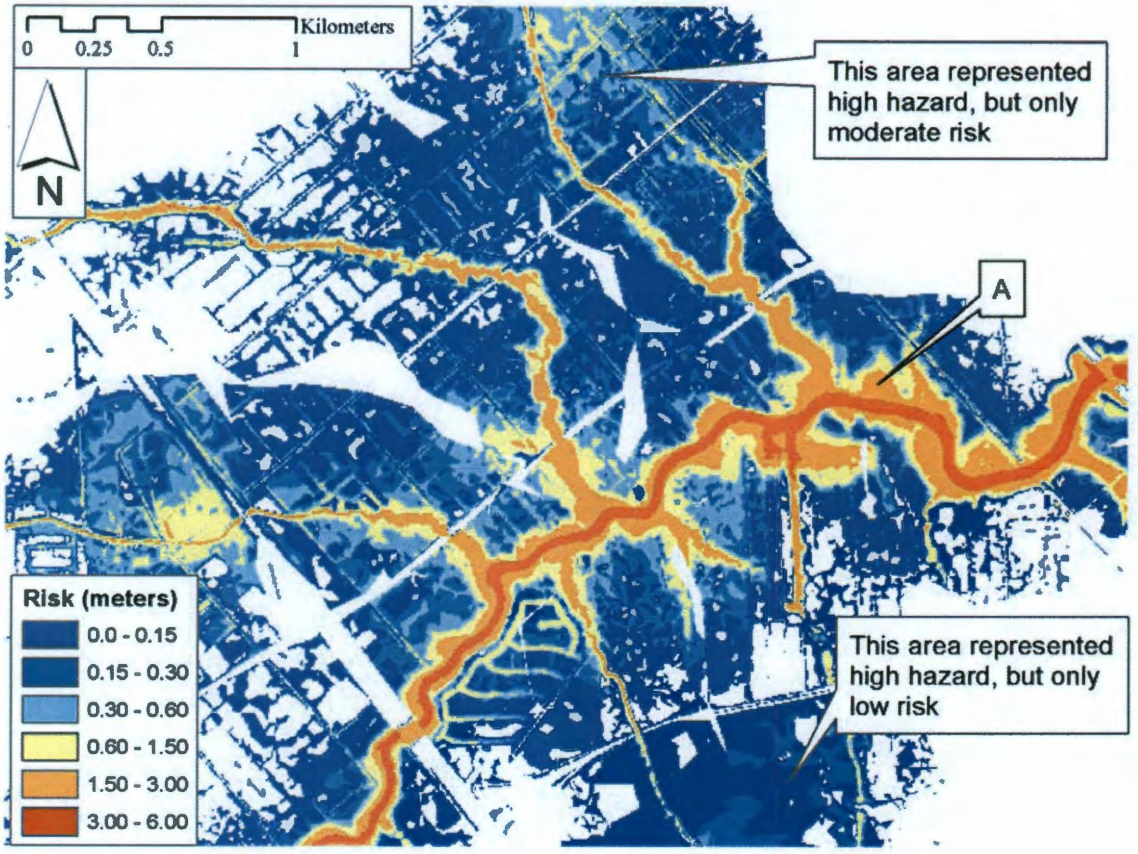

Figure 4.8. Flood Risk Map for City of Dickinson

4.5 Floodplain Delineation Conclusion

Hydraulic and hydrologic parameter uncertainty drive uncertainty in delineating the extent and depth of floodplains. Standard deterministic floodplain delineations mask this uncertainty by assuming point estimate values for all uncertain parameters and projecting the flood hazard as a binary feature. This process can be improved as epistemic and aleatory uncertainty are included in the analysis, and the resulting floodplain is viewed as an aggregate of several possible floodplains. Parameter uncertainty for the Dickinson Bayou watershed was assessed for storm duration, rainfall spatial distribution, roughness coefficients and stage boundary conditions, and an

unsteady hydraulic model was applied to address uncertainty in the timing of hydrologic events. Results of this case study suggest that stage boundary condition and storm duration contribute to most of the floodplain uncertainty in the tidal and transitional sections of the coastal watershed, and that none of these parameters contributed significant variability to the floodplain in the inland riverine segments.

Expression of floodplain hazard as a distributed probability provides important information about the floodplain structure and can differentiate relative hazards based upon parameter variability and topographic characteristics. Additional transformation of this hazard into a risk distribution provides the most meaningful tool for floodplain management under uncertainty, as it highlights differences between hazard and risk – especially where areas of high hazard do not correlate to areas of high risk. This transformation also allows a focused and efficient expenditure of limited resources on those areas that represent the most risk. Potential applications for probabilistic floodplain analysis include predicting repetitive loss properties based upon flood hazard delineation, prioritizing flooding problems based upon the magnitude of flood risk, setting flood insurance premiums based on actual flood risk, development of local land use ordinances and emergency plans, and evaluation of regional flood risk reduction projects. As this case study demonstrates, advanced analysis methods incorporating unsteady and uncertain hydrologic and hydraulic parameters can be readily performed using commonly available software with the framework of existing regulatory requirements. Future work in this area could include development of probability distribution functions for the most important coastal parameters (i.e., storm duration and stage boundary condition), assessment of other potentially significant uncertain parameters on coastal floodplain

variability, and the use of probabilistic flood risk in development of infrastructure damage models.

Chapter 5

Coastal Water Infrastructure Reliability

Communities located along the Gulf of Mexico are uniquely vulnerable to disruptive events associated with hurricane activity in the Gulf. In 2005, landfall of Hurricanes Katrina and Rita on the Louisiana and Texas coasts brought public attention to the overwhelming destructive power of hurricane events and to the impacts they can have on local and regional infrastructure networks including highways and bridges, electrical generation and distribution, oil and gas production, sanitary sewer collection, wastewater treatment and water distribution (Kwasinski et al., 2009; Ataei et al., 2010; Comfort, 2006; Kaiser et al., 2009). Similarly in 2008, Hurricane Ike hit the Texas coast and heavily damaged most every major infrastructure system in its path – bridges were destroyed, railroads and highways were buried in debris, power distribution lines were downed and airports were submerged (Miller et al., 2011; Byers, 2011). While it is not physically possible to eliminate the hazard of hurricane impact along the Gulf coast, it may be possible to increase the reliability of infrastructure systems by determining vulnerabilities and hardening the systems against those vulnerabilities. This research proposes a novel analysis methodology to achieve this goal for water distribution networks.

5.1 Hurricane Hazards and Water Infrastructure

Water distribution networks, like all coastal infrastructure systems, are vulnerable to hurricane induced damage. Key water system components including elevated storage tanks, ground storage tanks and pumping stations are potentially vulnerable to damage from wind, debris impact and flooding. Unlike many other infrastructure systems the majority of water system components, such as water pipes and fittings, enjoy protection from hurricanes because they are located underground – away from the effects of hurricane winds and debris impact. For those components located above ground, operators can take reasonable protective measures including designing elevated storage tanks to withstand hurricane wind loads, completely filling ground storage tanks prior to landfall to reduce buoyancy in the event of surface flooding and placing pumps and electrical controls at elevations above reasonable flood depths as required by industry standards and building codes (AWWA, 2011; ICC, 2012).

Unfortunately, even if the water distribution network survives the impact of the hurricane, its dependence on the electrical grid to power its pumps leaves the water system vulnerable. Equipping pumping sites with back-up generators to provide emergency power may not fully address this vulnerability issue because of the limited amount of fuel that can be stored on-site, the likelihood of power outages lasting on the order of weeks to months, potential problems with securing dependable fuel sources in times of emergency, and the likelihood of transportation disruptions (Kwasinski, 2009). For these reasons, any evaluation of the water system reliability would be incomplete without a similar consideration of the electrical network and their interdependence. To demonstrate this point, Section 4.2 contains a description of analysis results showing the

dependence of the water system on the electrical power grid for the water distribution system considered in this work.

Resilient communities depend upon competent, reliable and sustainable water system. Accordingly, the State of Texas requires that each water system operator in the state develop an emergency preparedness plan that details steps the operator will take to provide a minimum operating pressure of 240 kPa (35 psi) under emergency conditions, including natural disasters (TAC, 2011). Typical deterministic hydraulic models, such as EPAnet, can be used to estimate system performance under normal operating and fire flow conditions when topology, geometry, demands and sources are defined by the user (USEPA, 2000). However in the event of random disruptions caused by hurricane impact, the water system evaluator can not know the ultimate status of each system component *a priori*. Therefore, analysis by conventional deterministic hydraulic models is not helpful for this type of reliability analysis. Additionally, assessing the impact to the water system in isolation does not fully answer the question of water system reliability because of interdependencies between water and electrical infrastructure networks. These power-water system interdependencies have been studied elsewhere for seismic hazard where their influence on the performance of the water distribution system is emphasized (Adachi and Ellingwood, 2008; Hernandez-Fajardo and Duenas-Osorio, 2011). This research proposes a novel analysis methodology to assess the probabilistic pressure distribution within water distribution networks under hurricane impact.

5.2 Analysis Methodology

This paper evaluates the reliability of a water distribution system subjected to hurricane hazard by probabilistic methods, specifically Monte Carlo simulations. A decoupled method is used to simulate the state of the components in the electrical and water distribution systems under hurricane scenarios, and hydraulic analysis follows to estimate water pressures throughout the network. Figure 5.1 presents the flow chart of the decoupled method to simulate realizations of the state of the system. The decoupled method assumes a unidirectional relationship between the power grid and the water network in which the latter is dependent upon the former for operating power, but no dependence exists in the other direction. Accordingly, failures in the electrical network can be simulated prior to failures in the water network. This method is further justified because the reaction of power grid components to failures is significantly faster than water network components, and therefore, the spread of damage in the water network can be assumed to start after the power grid has reached a steady state. This decoupled approach reduces the complexity of simulating the state of the system which in turn makes the reliability analysis more applicable to real water distribution systems.

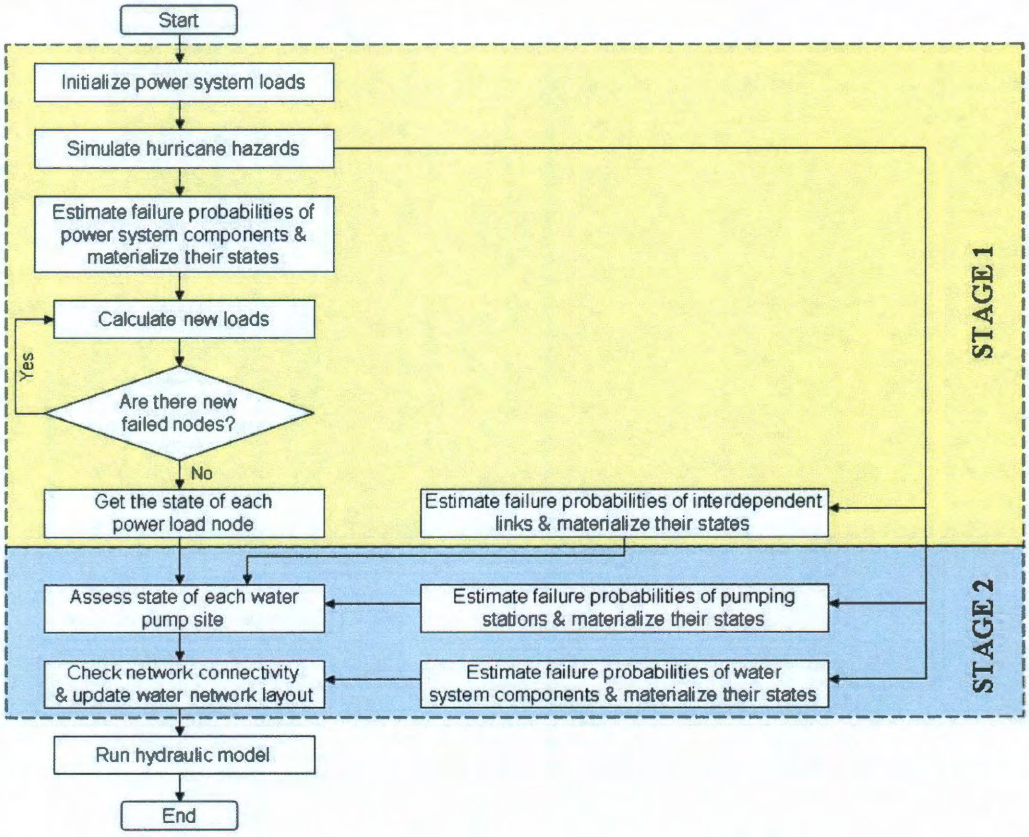

Figure 5.1. Decoupled Analysis Method Flow Chart

5.2.1 Stage 1- Power Grid Outage

For the power grid in the study area, only the asset inventory of generators and transmission level facilities are identifiable from available data sources (FEMA, 2008). The corresponding electric distribution network is typically not documented due to security concerns, but its layout is estimated by inspection through several site visits. A topological representation of the power grid serving the area is shown in Figure 5.2, where power load substations are modeled as nodes and power lines are shown as connecting links. There are six nodes linked as a connected graph through five edges with an average node degree (i.e., the average number of links attached to a node) equal

to 1.67. Nine power distribution lines from the load substations to water pump stations (i.e., the interdependency lines) were also identified through several site visits and included in the system model. Due to unavailability of power generation and line flow data, this paper uses node betweenness to approximate the power flow, where betweenness is a proxy for the amount of current passing through network elements, and it is computed as the number of shortest paths that pass through every node when connecting generators with load substations (Winkler et al., 2010). The initial load of a substation equals its betweenness in the initial power network. A disruptive event can cause the failure of some power substations and alter the network topology, which further changes all substation betweenness values. If a substation betweenness exceeds its maximum capacity defined as the product of its initial betweenness and a tolerance parameter (*tp*), the substation fails operationally. This outage model has been used to analyze the cascading failure process of many real power transmission grids, such as the North American Power Grid (Kinney et al., 2005), Italian Electric Power Grid (Crutitti et al., 2004), the IEEE 118 and 300 bus test systems (Dueñas-Osorio and Vemuru, 2009), and Harris County power system (Ouyang and Dueñas-Osorio, 2011).

To simulate a hurricane scenario, the wind gusts are assumed uniform for all nodal locations as the system covers a relatively small area compared to the spatial extent of the hurricane windfield. This research investigates the hurricane risk in terms of sustained wind speeds expressed as hurricane categories 1 to 5. For each hurricane category, the sustained wind speed in a specific hurricane event is assumed to follow a uniform distribution within the corresponding category wind speed range shown in Table 5.1.

Table 5.1. Wind Speed by Hurricane Category

Category	1	2	3	4	5
Wind Speed (m/s)	33-42	43-49	50-58	59-69	>70

Given the wind speed at each component site, the failure probabilities of power substations, electric transmission lines, and interdependency lines are evaluated based on the fragility models considered by Winkler et al. (2010). Comparing these probabilities with uniformly distributed random variables $\chi \in [0, 1]$ determines the damage state realization per component. Subsequently, running the power grid outage model provides the steady states of power load nodes, presented by a binary number for each node (1: operational, 0: failed). These reliability results are then used as input for Stage 2 of the decoupled method to simulate failures in the water distribution network.

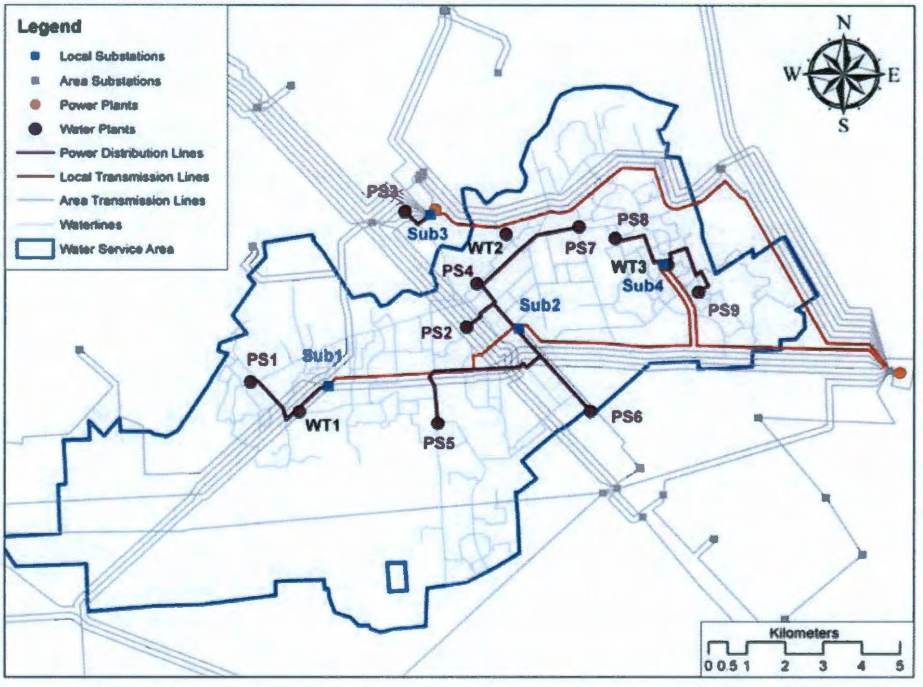

Figure 5.2. Electrical Network Topology

5.2.2 Stage 2- Water Network Failure

The same wind gusts are applied to simulate the direct wind-induced states of water distribution system components. However, much of the water system components are buried below ground and therefore not subjected to direct wind loading. For those above ground components (i.e. ground and elevated water storage tanks and pumping stations) there are no structural fragility curves available for estimating their reliability under wind loading. To account for this unknown structural reliability, a sensitivity analysis was conducted that assumed reliabilities of 0.95, 0.98 and 1.0 for the water system components under wind load.

In addition to the damage state of water components, the state of water pump stations also depends on the state of their corresponding power load substation and the interdependency lines (simulated in Stage 1). Water pump failures thus occur if either of the corresponding load substation, the interdependency line, or the water pump structure fails. For each hurricane category, one hundred realizations of the state of system components are generated by Monte Carlo simulations. For each realization, the water distribution network is then updated to reflect the new layout of the system after component failures.

Hydraulic analysis to estimate the nodal water pressures is performed on the updated network for each realization. The system reliability to satisfy the state requirements is subsequently evaluated from the resulting one hundred realizations for each hurricane category. This methodology is novel in that it utilizes both network and hydraulic analysis techniques to assess probable water system performance given a

highly stochastic natural disaster event and a dependence on another infrastructure system which is also subject to the same highly stochastic natural disaster event.

5.3 Water System Description

This research considers the water distribution system of a small community that is home to approximately 70,000 residents located in the Greater Houston metropolitan area. This community owns and operates its own water distribution system, and its water sources include surface water purchased from the City of Houston and groundwater drawn locally. Figure 5.3 shows the city's actual water distribution network containing 5 to 107 cm (2 to 42 inch) diameter pipes with a total length of 502 km (312 miles), 9 ground storage/booster pump sites (PS1 to PS9), and 3 elevated storage tanks (WT1 to WT3).

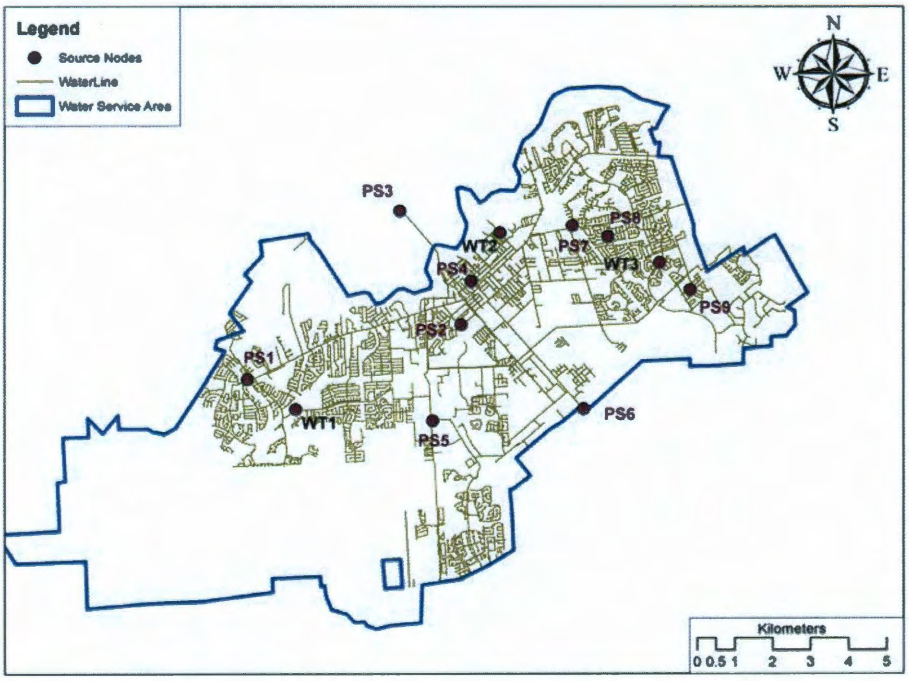

Figure 5.3. Water Distribution Network Topology

This distribution system, even though it serves a relatively small community, is a complex network with approximately 17,200 individual pipes. To facilitate the analysis, the actual water distribution network is simplified to only include the most important components, as represented by the network shown in Figure 5.4. This simplification preserves the essential topological characteristics of the network, as described in this section. The simplified version of the city's distribution system contains 316 links representing approximately 209 km (130 miles) of pipes connecting 221 vertices including the 12 supply nodes. The hydrologic software used in this analysis is EPANet v2.0 (USEPA, 2000).

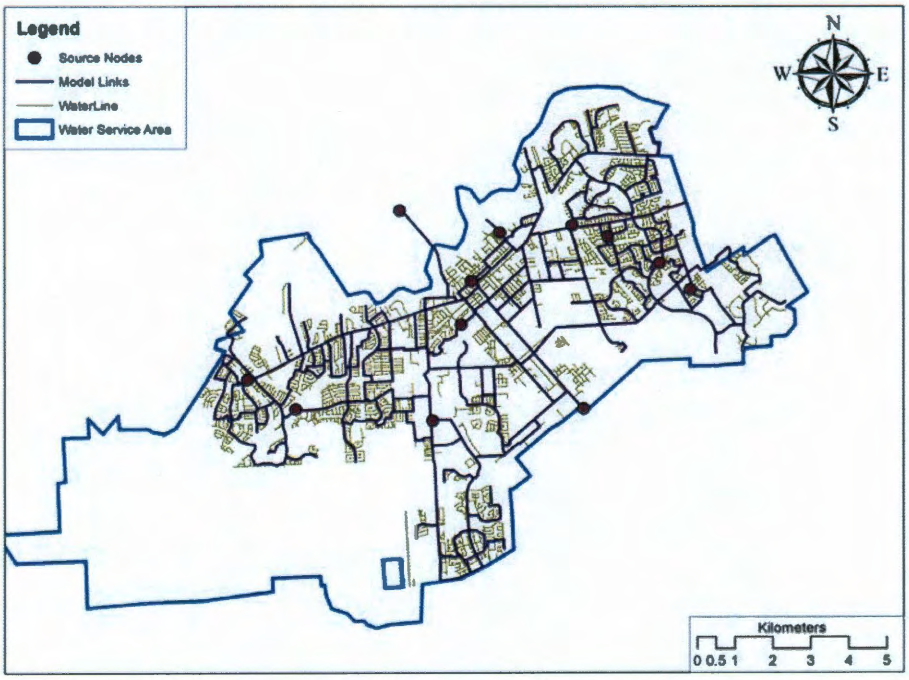

Figure 5.4. Simplified Water Distribution Network Topology

5.3.1 Water Demand Allocation

To implement this hydraulic model, water demands are applied in two parts consisting of "base flow" and "luxury flow" components. This modeling technique mixes demand-driven analysis to enforce minimum flows that must be provided with pressure-driven analysis to account for additional demands that can be met if sufficient system capacity is available. The benefits of analyzing under pressure-driven conditions are discussed in the literature (Ang and Jowitt, 2006; Tanyinboh and Templeman, 2010), and incorporation of a pressure-driven component into this analysis adds the capability of modeling a system that meets a minimum public health and safety flow, but can also account for other less-essential and non-essential uses including debris cleanup, car washing, and landscaping if excess capacity and system pressure is available.

The base flow demand is calculated as the average daily residential demand (380 liters/person/day or 100 gallons/person/day) multiplied by the number of estimated residential users assigned to each node. The luxury flow demand is implemented using the EPAnet emitter feature which applies a variable demand as a function of system pressure. Recognizing that in disaster conditions some citizens will evacuate and the city would likely implement water use restrictions, a full "peak daily" demand scenario is not considered appropriate because it does not replicate the expected demand characteristics following a hurricane impact as recognized in the regulatory requirements (TAC, 2011). Using this two part demand allocation, the hydraulic model approximates system demand, and therefore the system response, in a more realistic manner.

5.3.2 Summary of Network Topologic Properties

Water distribution systems are modeled as spatially distributed networks of pipe segments (network links) and pipe fittings/pump stations (network nodes). The network representation provides valuable insight that is otherwise subtle in the study of the infrastructure systems, as the topological layout of networks strongly influences their functionality and reliability of performance. To illustrate the adequacy of the simplified water network to represent the unabridged system, its topological characteristics are compared against those of five water distribution systems from around the world (Table 5.2). The networks of Colorado Springs (CO, USA), Richmond (Yorkshire, UK), Anglian Region (East Anglia, UK), and Kumasi (Kumasi, Ghana) are adopted from Yazdani and Jeffrey (2011). The Harris County network represents part of the water distribution system in Houston metropolitan area, which is close to the location of the area under study in this research. Following is a general summary of topologic parameters and the information contained in these metrics.

The variables m and n are the size and order of the network, representing the number of links and nodes in the network, respectively. All nodes in the presented networks are located inside one giant cluster, meaning that every node is accessible from every other node in the network before disruptions. The node degree is the number of links connected to a node, and the average node degree $<k>$ is the mean value from all node degrees. The clustering coefficient (C) is a measure of redundancy in the paths connecting any pair of nodes in the network. Redundancies are measured as the number of triangles in the network layout, and a small clustering coefficient value suggests lack of triangle formations. Path redundancy (loops among node triplets) has important

implications for the reliability of the network as nodes are less likely to be isolated by link failures because of the redundant links. However, designing and maintaining a network with high redundancy may not be economically feasible due to the increased number of pipes. Values in Table 5.2 suggest that the simplified network contains more redundancies than the other five networks, making it more resilient to component failures. The efficiency metric (E) is an indicator of flow efficiency between nodes in the network, and is given by Equation 5.1:

$$E = \frac{1}{n-1} \sum_{i,j(i \neq j)} \frac{1}{d_{ij}} \tag{5.1}$$

in which d_{ij} denotes the shortest distance between nodes i and j. In case node j is not accessible from node i, d_{ij} approaches infinity and its contribution diminishes. Larger values of E suggest better communication between nodes on average, resulting in more efficient flow in the network. This value is normalized for the order of the network so that it is comparable among different networks. The abundance of redundancies evident from the clustering coefficient value cause shorter paths among nodes on average, contributing to higher network efficiency.

The meshedness coefficient (M) was introduced by Buhl et al. and is a more general metric to quantify the contribution of cycles – and not just triangles – in planar networks (Buhl et al., 2004):

$$M = \frac{m+n-1}{2n-5} \tag{5.2}$$

with m and n defined as before. The value of M varies in [0, 1], where the lower and higher limits denote lack of cycles and maximum possible number of cycles in a planar network, respectively. Although the simplified network is in a comparable range with

other networks, the simplified network ranks first in meshedness coefficient, with the network in Harris County a close second.

Finally, the central-point dominance (c_b') measures the uniformity in the criticality of nodes in a network in terms of facilitating the flow throughout the network, and is defined in Equation 5.3 (Freeman, 1977):

$$c_b' = \frac{1}{n-1}\sum_i (b_{\max} - b_i) \tag{5.3}$$

in which b_i is the betweenness centrality of node i and b_{max} is the maximum betweenness centrality value in the network. Because the critical nodes are important in raising the efficiency of the network, their failure generally induces more severe disruptions in flow distribution. Therefore, networks without a clear hierarchy (such as mesh-like structures) are more resilient to targeted attacks directed toward the critical nodes.

This topological comparison highlights the similarities between the simplified network and the network of Harris County. While the simplified network seems to be better structured, this study confirms that its essential characteristics are close to those of the similarly designed network, and therefore the simplified layout of the understudy network is appropriate for use in the reliability analysis under hurricane hazard.

Table 5.2. Topological Characteristics of Water Distribution Networks

Network	*n*	*m*	<*k*>	*C*	*E*	*M*	c'_b
Simplified Network	221	316	2.86	0.0490	0.129	0.220	0.270
Harris County, TX	3,926	5,555	2.83	0.0320	0.047	0.208	0.345
Colorado Springs, CO	1,786	1,992	2.23	0.0005	0.052	0.058	0.416
Richmond, VA	872	957	2.19	0.0240	0.036	0.049	0.558
Anglian Region, UK	755	768	2.03	0.0000	0.046	0.009	0.362
Kumasi, Ghana	2,799	3,065	2.19	0.0094	0.040	0.048	0.455

n: total number of nodes (network order)
m: total number of links (network size)
<*k*>: average node degree
C: global clustering coefficient
E: efficiency
M: meshedness coefficient
c'_b: central-point dominance

5.3.3 Reliability of Water System Components

To assess the survival of the water system given a highly dynamic hurricane event, reliability values are assigned to each of the water network's components and a Monte Carlo analysis is conducted to determine the probable system connectivity. As discussed in the following paragraphs, the reliability of water system pipes, fittings and storage tanks is calculated as a product of reliability against direct hurricane damage and reliability against random failure due to condition and age. Similarly, the reliability of pump sites is a product of reliability against direct damage and the reliability of uninterrupted power supply.

Because of a lack of information regarding reliability of water system components against direct hurricane damage, the base analysis assumes the water system is completely protected from damage as most of the system is underground and therefore out of harm's way. While there are conceivable failure modes including pipe displacement by tree uprooting or by erosion/liquification of supporting soil structure due to wave action, there is little in the literature quantifying the probability of such failures. To test the consequence of this assumption, a sensitivity analysis is conducted where the

damage reliabilities of pipes, tanks and pumps are assigned values of 0.95 and 0.98 to compare against the base scenario where damage reliability is assumed to be 1.0. The results of this sensitivity analysis are discussed in later sections.

Nodal Reliability

Nodes in the hydraulic analysis model include water system pipe fittings, ground storage pump sites and elevated storage tanks. Because the fittings are underground and protected from storm damage, they are assumed to maintain their functionality and not be affected by hurricane impact. Accordingly, a structural reliability of 1.0 is assigned to each node that represented a water system fitting under all analysis conditions. The reliability of the remaining nodes (i.e., pump sites and elevated storage tanks) in the simplified network is calculated by Equation 5.4, where the total nodal reliability (R^n) is a function of the node's reliability against direct damage from the hurricane event (R^n_{damage}) and for the pumping sites, the reliability of the power grid providing electricity to that site (R^n_{power}).

$$R^n_i = R^n_{damage,\,i} \times R^n_{power,\,i} \tag{5.4}$$

Generally, because the elevated tanks, ground tanks and pump control houses are designed to withstand hurricane force winds as required by local building codes, the reliability against storm damage is assumed to be 1.0 in the base analysis. A sensitivity analysis presented in Section 5.4 considers the significance of the reliability assumption. Table 5.3 summarizes the reliability of the nine pump sites in the base analysis and shows the variability of reliability given differing hurricane winds. Notice the dramatic general decline in pump site reliability between category 3 and 4 storms that is attributed to loss

of transmission and distribution lines in the power grid as wind speeds exceed 58 m/s (130 mph).

Table 5.3. Water System Pump Station Reliability

Pumping Site	Cat 1	Cat 2	Cat 3	Cat 4	Cat 5
PS1	0.68	0.62	0.35	0.09	0.01
PS2	0.80	0.61	0.63	0.17	0.01
PS3	0.96	0.98	0.90	0.59	0.17
PS4	0.74	0.71	0.47	0.18	0.01
PS5	0.74	0.66	0.49	0.16	0.00
PS6	0.78	0.68	0.53	0.15	0.00
PS7	0.70	0.63	0.45	0.15	0.00
PS8	0.86	0.79	0.75	0.38	0.06
PS9	0.88	0.74	0.66	0.37	0.08

Pipe Reliability

Pipe reliability (R^p) in the simplified network is calculated by Equation 5.5, where the total pipe reliability is a function of the pipe's reliability against direct damage from the hurricane event (R^p_{damage}) and the reliability against random failure due to pipe condition ($R^p_{condition}$).

$$R^p_i = R^p_{damage,\,i} \times R^p_{condition,\,i} \tag{5.5}$$

Pipes making up this water system, like the system nodes discussed earlier, are buried components that are generally protected from the forces of hurricane impact. As with the water system nodes, the pipes in this base analysis are assumed to be protected from direct hurricane damage and a damage reliability of 1.0 is assigned to each pipe. A sensitivity analysis considers the impact of this assumption on analysis results.

The pipe condition reliability is attributed to deterioration caused by pipe age and overall condition. Several examples in the literature consider the reliability of water system pipes and draw conclusions as to pipe failure rates as a function of pipe age, material, diameter, length and previous repairs (Boxall et al., 2007; Berardi et al., 2008; Rajani and Tesfamariam, 2007; and Xu et.al, 2003). Water pipes in this water network are generally either asbestos cement (AC), cast or ductile iron (CI/DI), steel reinforced concrete (RC), or polyvinyl chloride (PVC) material. The water system owner does not have sufficient maintenance records to construct a statistical failure analysis on its components, so surrogate studies from areas with similar climate and soil conditions are used instead. The asbestos cement pipe, much of it installed between 1960 and 1980, is relatively fragile due to its age and material properties of the cement binder. The ductile and cast iron pipes were generally installed between 1960 and 2000, and are susceptible to failure from corrosion as the iron oxidizes over time. Finally, the PVC pipe represents the modern solution to pipe technology, and much of this pipe was installed between 1990 and the present. There are only very few pipes in the City's system that are of different materials than those discussed here or that were installed prior to 1960.

Burst rates (*BR*), defined as the number of expected failures per year, are calculated for each pipe based upon the pipe's diameter (*D* in mm), age (*A* in years), length (*L* in km) and material type. Generally, increased age and length of pipe as well as decreased diameter all contributed to higher burst rates for each material type. Because the age of pipe is included in its burst rate calculation, this parameter is continually changing and the calculation must be updated periodically to account for the aging system. Burst rate calculations are made using equations differentiated by pipe material

type as shown in Table 5.4. Once burst rates are estimated for each pipe (i) in the model system, a pipe reliability can be calculated as a Poisson process using Equation 5.6 where time (t) is in units of years. In this form, the reliability (R_i) is the probability that pipe i will not fail.

$$R_i = \exp(-BR \times t) \tag{5.6}$$

Table 5.4. Pipe Burst Rate Calculation Equations

Pipe Type	Burst Rate Equation (failures/year)	Reference
AC	$BR = \exp(-2.89048 - 0.0093D + 0.5651 \times \log(L) + 0.01056A)$	Boxall et al., 2006
CI/DI	$BR = \exp(-0.5913 - 0.00721D + 0.76727 \times \log(L) - 0.01682A + 0.00012A^2)$	Boxall et al., 2006
RC	$BR = 0.084904 \times \frac{AL}{D^{1.5}}$	Berardi et al, 2008
PVC	$BR = 0.084904 \times \frac{AL}{D^{1.5}}$	Berardi et al, 2008

5.4 Case Study: Reliability, System Dependency and Sensitivity Analysis

In this reliability analysis we estimate the pressure distribution in a system subjected to a highly dynamic disruptive event. To achieve this result, a Monte Carlo analysis is implemented using a hydraulic model of the water distribution system to determine a probabilistic pressure distribution for the entire system. For each hydraulic realization, the pressure at each node is calculated and compared against the regulatory requirement. If all nodal pressures within the system are greater than 240 kPa (35 psi), the system is in compliance with the regulatory requirement for that realization and is classified as reliable. If some, or all, of the distribution nodes do not provide a pressure

of 240 kPa (35 psi), the system is considered unreliable for that category of hurricane in that realization. Upon completion of all realizations for each category of hurricane, a failure probability is calculated as the number of failed scenarios divided by the total number of model realizations. The end result is a probability that at least one node in the system will not meet the minimum pressure requirement (i.e., the failure probability). If the probability of failure is unacceptably high, the water system owner could then develop and implement system improvements to rectify the short-comings.

5.4.1 Hurricane Reliability

Figure 5.5 shows the probabilistic pressure distribution across this water distribution network for Category 1 through 5 hurricanes for the base study, and scenario results are summarized in Table 5.5. As the results indicate, this system performs acceptably for Category 1 and 2 hurricane impacts, with marginal performance during Category 3 events. However, under Category 4 and 5 hurricane impacts, the system is clearly not able to reliably meet the regulatory requirement of 240 kPa (35 psi) due mainly to loss of power at the water pumping sites.

Table 5.5. Water System Response to Hurricane Impact by Category

		Most Vulnerable Node	
Hurricane Category	**System Failure Probability**	**Mean Pressure (kPa)**	**Standard Deviation (kPa)**
1	0.37	314	96
2	0.45	296	103
3	0.64	245	104
4	0.95	108	109
5	1.00	13	38

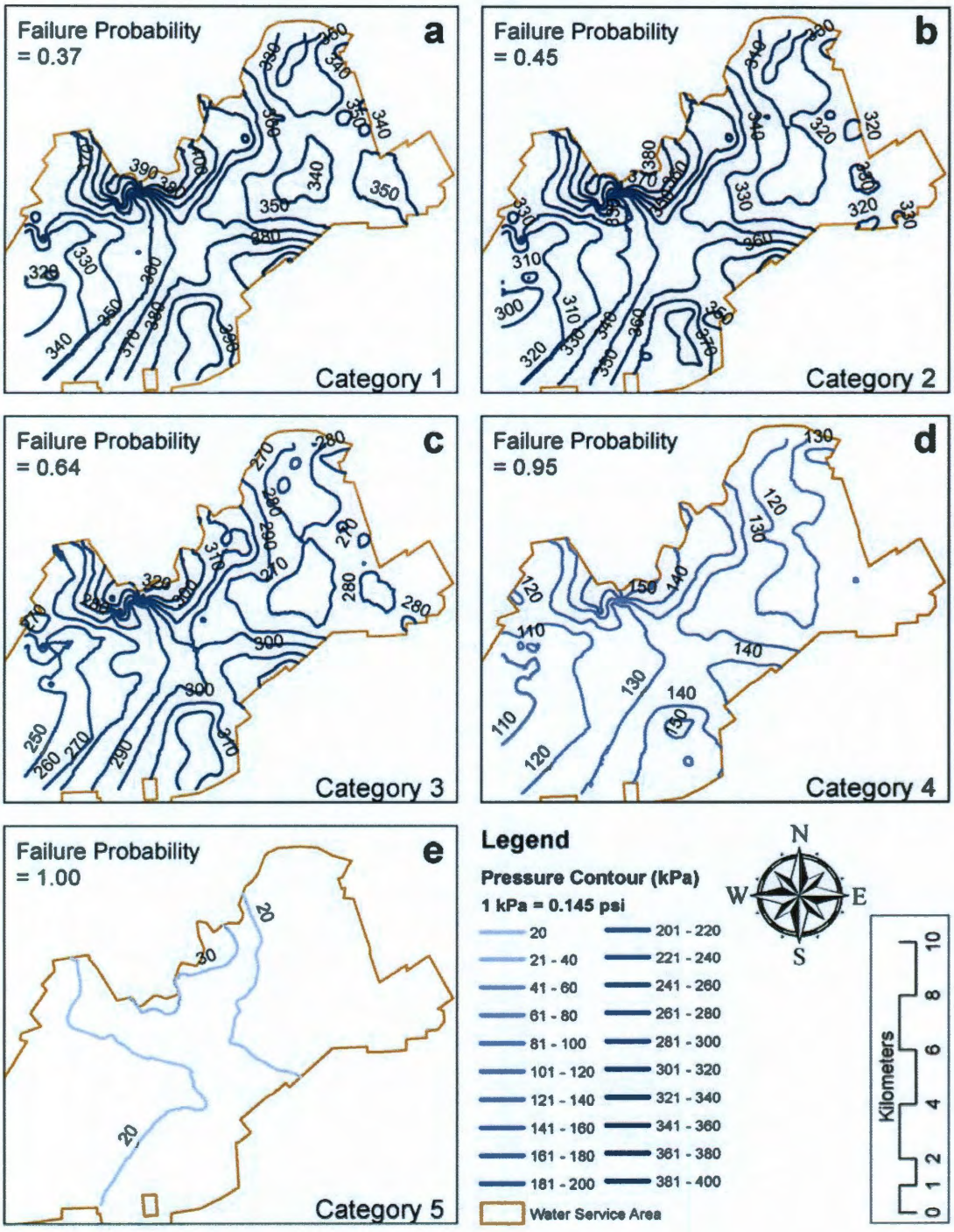

System pressure distribution for (a) Category 1, (b) Category 2, (c) Category 3, (d) Category 4 and (e) Category 5 hurricanes.

Figure 5.5. Hurricane Impact Assessment Results

5.4.2 System Dependence

To quantify the extent of water system dependence upon the electrical network, the impact of a Category 3 hurricane event on the water system is assessed assuming total independence from the electrical grid, shown in Panel (a) in Figure 5.6, and for the water distribution network dependent on the electrical grid, shown in Panel (b). In this exercise, the structural reliability of water system components to hurricane damage was assumed to be 0.98 in both the dependent and independent scenarios.

Results indicate that if this system has an independent, uninterruptable power supply for each of its pumping sites, it would have a probability of failure of 0.56 for a Category 3 hurricane. On average, the most vulnerable node has a mean pressure of 385 kPa (55.8 psi) and a standard deviation of 89 kPa (12.9 psi). Results for the dependent system analysis indicate the probability of failure is 0.76 for a Category 3 hurricane. As shown, the dependent system has a significantly degraded capacity to withstand the event, and the mean pressure at the most vulnerable node drops to 237 kPa (34.4 psi) with a standard deviation of 116 kPa (16.8 psi).

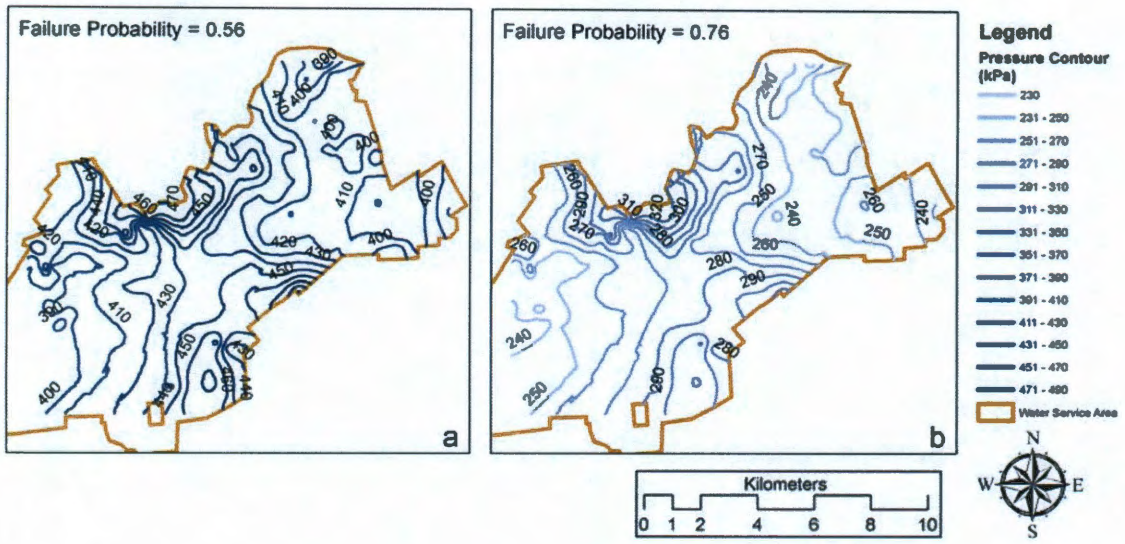

System pressure distribution for (a) independent water-power systems, (b) dependent water-power systems

Figure 5.6. System Dependence Analysis Results

5.4.3 Structural Damage Sensitivity Analysis

As introduced earlier, there is uncertainty about water system component reliability against structural damage resulting from hurricane impact. Based upon professional experience and direct observation following Hurricane Ike, it is expected that this component structural reliability is very high, approaching 1.0. A sensitivity analysis is conducted under Category 3 hurricane conditions to assess the water system response to alternate structural reliability values of 0.95 and 0.98 as compared to the base case where structural reliability is assumed to be 1.0. Results are shown in Figure 5.7 and summarized in Table 5.6. As the sensitivity analysis results show, a component structural reliability as low as 0.98 will significantly increase the expected failure probability of the entire system. Therefore, the presented results in this study are only

accountable if the structural failure probability of system components is negligible, and additional research should be conducted to assess the actual structural reliabilities for these components under hurricane impact.

Table 5.6. Structural Reliability Sensitivity Analysis Results

Assumed Structural Reliability	System Failure Probability	Most Vulnerable Node	
		Mean Pressure (kPa)	Standard Deviation (kPa)
1.0	0.64	245	104
0.98	0.76	236	116
0.95	0.94	177	146

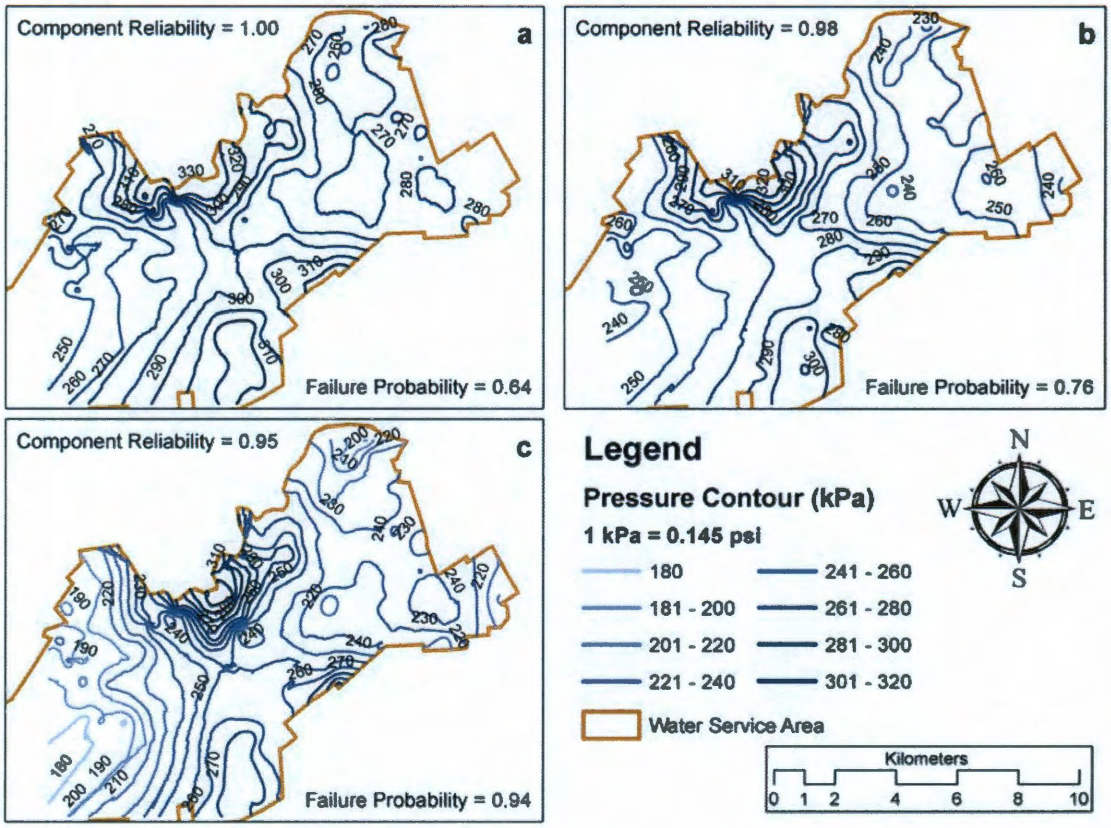

System pressure distribution for water component structural reliability (a) equal to 1.0, (b) equal to 0.98, and (c) equal to 0.95.

Figure 5.7. Structural Reliability Sensitivity Analysis Results

5.5 Water Reliability Analysis Conclusions

This study considered the application of a novel network analysis technique to a water distribution network to quantify system reliability under hurricane impact. This work is unique in that it utilizes both network and hydraulic analysis techniques to assess probable water system performance given a stochastic natural disaster event and a dependence on another infrastructure system which is also subject to the same event. In this system simulation, the water network itself proved to be reliable following storm impact in that the damage to the water system components was minimal under all storm landfall scenarios.

Because the water network is dependent upon the electrical grid to provide operating power for its system pumps, failure of the electrical grid will adversely impact water system performance. To quantitatively consider the interdependencies between the power and water networks and the resulting impact to system water pressure, this paper introduces a scenario-based, two-stage simulation method to decouple system interdependencies, increase analysis flexibility and effectively reduce the computational complexity.

The reliability of the electrical grid is quantified using Monte Carlo analysis techniques driven by wind loading failure modes for each of five hurricane categories. Next, a Monte Carlo reliability model is implemented for the water system which considered survivability of water components driven by routine pipe failures related to pipe age, length, diameter and material. A final Monte Carlo analysis is conducted using a hydraulic model of the system in which water system components (i.e., pipes and

pumps) were considered active or failed according to the reliability probabilities quantified in the first two steps. The results from this hydraulic analysis yield a probabilistic pressure distribution map of the impacted water system under each of the hurricane categories analyzed. This analysis suggests that the residual water system would, on average, meet the regulatory minimum water pressure requirements under hurricane category 1 and 2 landfall events, with marginal results in a category 3 hurricane. This model also suggests that the water system would not likely meet minimum water pressure requirements under category 4 or 5 events due mainly to catastrophic damage to and failure of the electrical grid. As this work demonstrates, survival of the electrical network is critical to the reliability of the water system. This finding highlights the interdependence of the water and power networks and suggests that complete failure of one system can be largely attributed to vulnerabilities and failures in another.

There was a general lack of information regarding the structural reliability of water system components to direct damage by hurricane wind, debris impact and flooding. Therefore, an assumption was made that the components would be extremely reliable based upon professional opinion and observational experience with past hurricane events. However, sensitivity analysis results suggest that this component reliability parameter can have a significant impact on the reliability of the network as a whole, so future research in this area is warranted to better quantify this uncertain parameter.

This level of quantitative information can assist the city planners and emergency managers in hardening its infrastructure systems against hurricane disasters by identifying weak links in and across infrastructure systems. It can also help developing

and implementing a responsive and appropriate disaster management plan based upon the size of the approaching storm and the city's ability to provide basic services in the immediate aftermath.

Chapter 6

Conclusions

The cumulative economic and social consequences of past hurricane disasters demonstrates that our coastal communities are not sustainable. Engineering standards historically applied to the design and construction of coastal infrastructure systems have proven to be inadequate to withstand these disasters, leaving the social systems dependent upon them at significant risk of failure. Understanding the hydraulic processes present at the coastal-riverine interface and understanding the vulnerability of our infrastructure systems to these hydraulic processes are of paramount importance to the development of a less vulnerable coastline in the future. The ability to withstand hurricane disasters is required to meet the challenges of a growing national population base and aging coastal infrastructure.

6.1 Hydraulic Modeling at the Coastal-Riverine Interface

Understanding the properties of coastal drainage infrastructure becomes critically important in the planning and design of coastal communities because of the importance of adequate drainage in the coastal environment.. The research presented here considers the current approach to analysis of the coastal-riverine interface and to the design of constructed coastal improvements. Current hydraulic analyses within the coastal zone typically uncouple the coastal parameters (waves, currents and wind) from the riverine

parameters (flow, velocity, depth, channel storage) to consider each independently. This is not hydraulically appropriate for many reasons, as the assumption of independence between riverine and coastal processes does not capture the correct fluid flow dynamics occurring at the interface when the two occur simultaneously. Any inferences about the characteristics of channel flow derived from the uncoupled model would be incomplete at best and incorrect at worst. Similarly, any coastal infrastructure design based upon the uncoupled model approach would be potentially flawed.

To illustrate this point, an unsteady hydraulic model of a typical coastal-riverine drainage system was developed to investigate flow properties at the coastal interface. This model was analyzed under historic storm conditions (i.e., Hurricane Ike) to show how natural systems respond under conditions found during landfall of hurricanes onto the coastline. This model is then utilized to estimate the operational parameters and effectiveness of a proposed structural flood protection levee and channel gate at the coastal interface.

6.2 Modeling the Coastal Floodplain

Data uncertainty and parameter variability drive uncertainty in delineating the extent and depth of floodplains. Current floodplain maps present 1% flood hazards as polygon features developed using methods and models that do not adequately consider data uncertainty or natural variability of input parameters in a highly complex and dynamic hydraulic environment at the coastal/riverine interface. These standard deterministic floodplain delineations mask this uncertainty by assuming a point estimate value for all variable or random parameters and projecting the flood hazard as a binary

feature. This process can be improved as data uncertainty and parameter variability are included in the hydraulic analysis, and the resulting floodplain is viewed as an aggregate of several possible 1% floodplains. Using the techniques presented here, a standard binary deterministic floodplain delineation is replaced with a probabilistic flood inundation map showing the underlying flood hazard structure. Additionally, the hazard probability is further transformed to show flood risk as a spatially distributed probable flood depth using concepts familiar to practicing engineers and software tools accepted and understood by regulators.

In a case study presented, the hydraulic effect of parameter uncertainty is assessed for storm duration, rainfall distribution, channel roughness coefficients and stage boundary conditions. Additionally, another source of uncertainty (i.e., event timing) is addressed through application of an unsteady hydraulic model. Results of this case study suggest that stage boundary condition and storm duration contribute to most of the floodplain uncertainty in the tidal sections of the coastal watershed, and that none of these parameters contributed significant variability to the floodplain in the inland riverine segments.

Expression of floodplain hazard as a distributed probability provides important information about the floodplain structure and can differentiate relative hazards based upon parameter variability and topographic characteristics. Additional transformation of this hazard into a probabilistic risk distribution provides the most meaningful tool for floodplain management, as it highlights differences between hazard and risk, especially where areas of high hazard do not correlate to areas of high risk. This transformation also allows a focused and efficient expenditure of limited resources on those areas that

represent the most risk. Potential applications for probabilistic floodplain analysis include predicting repetitive loss properties based upon flood hazard delineation, prioritizing flooding problems based upon the magnitude of flood risk, setting flood insurance premiums based on actual flood risk, development of local land use ordinances and emergency plans, and evaluation of regional flood risk reduction projects. As this case study demonstrates, advanced analysis methods incorporating unsteady and uncertain hydrologic and hydraulic parameters can be readily performed using commonly available software with the framework of existing regulatory requirements. Future work in this area could include assessment of other potentially significant uncertain parameters on coastal floodplain variability and use of flood risk in development of infrastructure damage models.

6.3 Modeling of Water Infrastructure Reliability

In the water network impact analysis, the water system proved to be reliable under hurricane impact when studied in isolation. However, because the water network is dependent upon the electrical grid to provide operating power for water system pumps, it is necessary to consider the interdependencies between the power and water networks acting together to provide water to the community. To implement this analysis, a scenario-based, two-stage simulation is utilized to decouple system interdependencies, increase analysis flexibility and effectively reduce the computational complexity. The electrical grid and water network reliability realizations generated by this method are used as input to a hydraulic model to simulate the resulting water system pressure at consumption nodes throughout the network. Simulated system pressures are compared

against a regulatory minimum pressure criteria to determine if the water network is reliable or not. As this work demonstrates, survival of the electrical system network is the most important factor in determining the reliability of the water system.

This analysis considers the application of advanced stochastic and hydraulic analysis techniques to quantify system reliability given a highly dynamic hurricane impact event. According to this analysis, the impacted water system could meet minimum objective water pressures throughout the service area when studied in isolation. However, because the water network is also dependent upon the electrical grid to provide operating power for its system pumps, failure of the electrical grid to provide power at the pump station sites adversely impacts water system performance.

The reliability of the electrical grid was quantified using Monte Carlo analysis techniques driven by wind loading failure modes for each of five hurricane categories. Next, a Monte Carlo reliability model was implemented for the water system which considered survivability of water components driven by routine pipe failures related to pipe age, length, diameter and material. Finally, a third Monte Carlo analysis was conducted using a hydraulic model of the system in which water system components (i.e., pipes and pumps) were considered active or failed according to the reliability probabilities quantified in the first two steps. The combined results from this hydraulic analysis resulted in a probabilistic pressure distribution map of the impacted water system under each of the hurricane categories analyzed. This analysis suggests that the residual water system would meet minimum water pressure requirements under hurricane category 1, 2 and 3 landfall events. The results also suggests that the water system would

not meet minimum water pressure requirements under category 4 or 5 events, with that failure attributed to lack of electrical power to drive the water system pumps.

As this work demonstrates, survival of the electrical system network is critical to the reliability of the water system. This finding highlights the interdependence of the water and power networks and suggests that complete failure of one system can be largely attributed to vulnerabilities and failures in another. This level of quantitative information can assist engineers, planners and decision makers to adopt design and construction standards for base infrastructure systems that will withstand hurricane impact and can be the basis of a less vulnerable coastal community structure.

List of References

Adachi, T. and B.R. Ellingwood, 2008. Serviceability of earthquake-damaged water 27 systems: Effects of electrical power availability and power backup systems on system 28 vulnerability. *Reliability Engineering and System Safety*. 93(1): 78-88.

American Water Works Association (AWWA), 2011. AWWA D100-11, AWWA Standard for Welded Carbon Steel Tanks for Water Storage.

Anderson, J.B., 2007. The formation and future of the upper Texas coast, first edition. Texas A&M University Press, College Station, Texas.

Ang, W.K. and P.W. Jowitt, 2006. Solution for water distribution systems under 2 pressure-deficient conditions. *Journal of Water Resources Planning and Management* 3 132(3): 175-182. DOI 10.1061/(ASCE)0733-9496(2006)132:3(175).

Anthes, R.A, R.W. Corell, G. Holland, J.W. Hurrell, M.C. MacCracken, and K.E. Trenberth, 2006. Hurricanes and global warming – potential linkages and consequences. *American Meteorological Society*. 623-628.

Ataei, N., M. Stearns, and J. Padgett. 2010. Response Sensitivity for probabilistic damage assessment of coastal bridges under surge and wave loading. *Transportation Research Record*. 2202:93-101. DOI 10.3141/2202-12.

Bedient, P.B., A.W. Holder, J.F. Thompson and Z. Fang, 2007. Modeling of storm-water response under large tailwater conditions: Case study for the Texas Medical Center. *Journal of Hydrologic Engineering*. 12(3):256-266. DOI 10.1061/(ASCE)1084-0699(2007)12:3(256).

Bedient, P.B., W.C. Hubner and B.E. Vieux, 2008. Hydrology and floodplain analysis, fourth edition. Prentice Hall, Upper Saddle River, New Jersey.

Berardi, L., O. Giustolisi, Z. Kapelan, and D.A. Savic. 2008. Development of pipe deterioration models for water distribution systems using EPR. *Journal of Hydroinformatics*. 10(2):113-126. DOI 10.2166/hydro.2008.012.

Bird, E., 2008. Coastal geomorphology an introduction, second edition. John Wiley & Sons, Ltd., West Sussex, England.

Boxall, J.B., A. O'Hagan, S. Pooladsaz, A.J. Saul and D.M. Unwin, 2007. Proceedings of the Institution of Civil Engineers. *Water Management*. 160:73-82. DOI 10.1680/wama2007.160.2.73.

Brown, J.D., T. Spencer, and I. Moeller, 2007. Modeling storm surge flooding of an urban area with particular reference to modeling uncertainties: A case study of Canvey Island, United Kingdom. *Water Resources Research.* 43:W06402.

Buhl, J., J. Gautrais, R.V. Solé, P. Kuntz, S. Valverde, J.L. Deneubourg and G. Theraulaz, 18 2004. Efficiency and robustness in ant networks of galleries. *The European Physical* 19 *Journal B-Condensed Matter and Complex Systems.* 42(1): 123–129.

Byers, W.G., 2011. Railroad Damage from Two Hurricanes. *Natural Hazards Review.* 12(1):6-8. DOI 10.1061/(ASCE)NH.1527-6996.0000018.

Carr, R. S., D.C. Chapman, C.L. Howard and J.M. Biedenbach, 1996. Sediment quality triad assessment survey of the Galveston Bay, Texas system. *Ecotoxicology.* 5:341-364.

City of Houston (COH), 2011. Infrastructure Design Manual. Accessed on 22 January, 2012 at http://documents.publicworks.houstontx.gov/documents/design_manuals/idm.pdf.

Comfort, L.K., 2006. Cities at risk: Hurricane Katrina and the drowning of New Orleans. *Urban Affairs Review.* 41(4):501-516. DOI 10.1177/1078087405284881.

Crossett, K., T.J. Culliton and T.R. Goodspeed, 2004. Population trends along the coastal United States, 1980-2008. Silver Spring, Maryland: National Oceanic and Atmospheric Administration.

Crowell, M., S. Edelman, K. Coulton and S. McAfee, 2007. How many people live in coastal areas? *Journal of Coastal Research.* 23(5):iii-vi.

Crutitti P., V. Latora and M. Marchiori. 2004. A topological analysis of the Italian electric power grid. *Physica A.* 338:92-97.

Dawson, C., E.J. Kubatko, J.J. Westerind, C. Trahan, C. Mirabito, C. Michoski, and N. Panda, 2011. Discontinuous Galerkin methods for modeling hurricane storm surge. *Advances in Water Resources.* 34:1165-1176. DOI 10.1016/j.advwatres.2010.11.004.

Day, J.W., D.F. Boesch, E.J. Clairain, G.P. Kemp, S.B. Laska, W.J. Mitsch, D. Orth, H. Mashriqui, D.J. Reed, L. Shabman, C.A. Simenstad, B.J. Streever, R.R. Twilley, C.C. Watson, J.T. Wells, and D.F. Whigham, 2007. Restoration of the Mississippi delta: Lessons from Hurricanes Katrina and Rita. *Science.* 315:1679-1684.

Day, J.W., G.P. Kemp, D.J. Reed, D.R. Cahoon, R.M. Boumans, J.M. Suhayda and R. Gambrell, 2011. Vegetation death and rapid loss of surface elevation in two contrasting Mississippi delta salt marshes: The role of sedimentation, autocompaction and sea-level rise. *Ecological Engineering.* 37:229-240. DOI 10.1016/j.ecoleng.2010.11.021.

Der Kiureghian, A. and O. Ditlevsen. 2009. Aleatory or epistemic? Does it matter? *Structural Safety.* 31:105-112. DOI 10.1016/j.strusafe.2008.06.020.

Di Baldassarre, G., G. Schumann, P.D. Bates, J.E. Freer and K.J. Beven, 2010. Flood-plain mapping: a critical discussion of deterministic and probabilistic approaches. *Hydrologic Sciences Journal.* 55(3):364-376.

Dolan, G. and D.J. Wallace, 2012. Policy and management of hazards along the upper Texas coast. Oceans and Coastal Management. 59:77-82. DOI 10.1016/j.ocecoaman.2011.12.021.

Dueñas-Osorio, L. and S.M. Vemuru. 2009. Cascading failures in complex infrastructure systems. *Structural Safety.* 31:157-167.

East, J.W., et al., 2008: Monitoring inland storm surge and flooding from Hurricane Ike in Texas and Louisiana, September 2008: U.S. Geological Survey Open-File Report 2008–1365 [http://pubs.usgs.gov/of/2008/1365/].

Edmiston, H.L., S.A. Fahrny, M.S. Lamb, L.K. Levi, J.M. Wanat, J.S. Avant, K. Wren and N.C. Selly, 2008: Tropical storm and hurricane impacts on a Gulf Coast estuary: Apalachicola Bay, Florida. *Journal of Coastal Research.* 55:38-49.

Eng, J., 2003. Sample Size Estimation: How many individuals should be studied? *Radiology.* 227:309-313.

Epron, D., M.L. Toussaint and P.M. Badot, 1999. Effects of sodium chloride salinity on root growth and respiration in oak seedlings. *Annals of Forest Science.* 56(1):41-47. DOI 10.1051/forest:19990106.

Estrada, E. and D.J. Higham. 2010. Network properties revealed through matrix functions. *SIAM Review.* 52(4):696-714.

Evans-Cowley, J.S. and M.Z. Gough. 2008. Evaluating environmental protection in post-Hurricane Katrina plans in Mississippi. *Journal of Environmental Planning and Management.* 51(3):399-419. DOI 10.1080/09640560801979667.

Federal Emergency Management Agency (FEMA), 2003. Guidelines and specifications for flood hazard mapping partners. FEMAs's Flood Hazard Mapping Program, Washington, D.C.

Federal Emergency Management Agency (FEMA). 2008. Hazards U.S. Multi-Hazard (HAZUS-MH) Assessment Tool v1.3, www.fema.gov/plan/prevent/hazus/index.shtm.

Freeman, L.C. 1977. Set of measures of centrality based on betweenness. *Sociometry.* 37 40(1): 35-41. DOI 10.2307/3033543

Fujiwara, O. and T. Ganesharajah. 1993. Reliability assessment of water supply systems with storage and distribution networks. *Water Resources Research.* 29(8): 2917-2924.

Galveston County Drainage District No. 1 (GCDD1). 2007. Drainage criteria manual. Accessed online at http://galvestoncountydrainagedistrict1.us/criteria_manual.pdf.

Galveston County Drainage District No. 1 (GCDD1). 2008. Dickinson Bayou watershed floodplain delineation. Santa Fe, Texas.

Gierach, M.M. and B. Subrahmanyam, 2008. Biophysical responses of the upper ocean to major Gulf of Mexico hurricanes in 2005. *Journal of Geophysical Research.* 113:C04029.

Greater Houston Partnership (GHP), 2009. Resolution dated February 3, 2009.

Greening, H., P. Doering and C. Corbett, 2006. Hurricane impacts on coastal ecosystems. *Estuaries and Coasts.* 29(6A):877-879.

Groisman, P.Y., R.W. Knight, T.R. Karl, D.R. Easterling, B.M. Sun and J.H. Lawrimore, 2004. Contemporary changes of the hydrological cycle over the contiguous United States: trends derived from in situ observations. *Journal of Hydrometeorology.* 5(1):64-85. DOI 10.1175/1525-7541(2004).

Groisman, P.Y., R.W. Knight, D.R. Easterling, T.R. Karl, G.C. Hegerl and V. Razuvaev, 2005. Trends in intense precipitation in the climate record. *Journal of Climate.* 18(9):1326-1350. DOI 10.1175/JCLI3339.1.

Haddow, G.D. and J.A. Bullock, 2006. Introduction to emergency management, second edition. Elsevier Inc., Burlington, Massachusetts.

Haimes, Y.Y., 2004. Risk modeling, assessment, and management - second edition. John Wiley & Sons, Inc., Hoboken, New Jersey.

Hansen, B., 2007. Weathering the Storm: the Galveston Seawall and Grade Raising. *Civil Engineering.* 77(4):32-33.

Harris County Flood Control District (HCFCD), 2009. Hydrology and Hydraulics Guidance Manual. Accessed on 22 January 2012 at http://www.hcfcd.org/downloads/manuals/HCFCD_Hydrology-Hydraulics_Manual_12-2009.pdf

Harris County Homeland Security and Emergency Management (HCHSEM), 2011. Flood data document library, data archives for 2008. Accessed on 31 October 2011.

Hernandez-Fajardo, I. and L. Duenas-Osorio. 2011. Seqential propogation of seismic 40 fragility across interdependent lifeline systems. *Earthquake Spectra.* 27: 23-43.

Hine, D. and J.W. Hall, 2010. Information gap analysis of flood model uncertainties and regional frequency analysis. *Water Resources Research.* 46:W01514.

Howard, J. and I.A. Mendelssohn, 1999. Salinity as a constrain on growth of oligohaline marsh macrophytes. II. Salt pulses and recovery potential. *American Journal of Botany.* 86(6):795-806.

Intergovernmental Panel on Climate Change (IPCC) 2007: Climate Change 2007 Synthesis Report.

International Code Council (ICC), 2012. 2012 International Building Code.

Irish, J.L., D.T. Resio and D. Divoky, 2011. Statistical properties of hurricane surge along a coast. *Journal of Geophysical Research.* 116:C10007. DOI 10.1029/2010JC006626.

Kaiser, M.J., Y. Yunke, and J.C. Jablonowski, 2009. Modeling lost production from destroyed platforms in the 2004-2005 Gulf of Mexico hurricane season. *Energy.* 34: 1156-1171. DOI 10.1016/j.energy.2009.04.032.

Keim, B.D. and R.A. Muller, 2007. Spatiotemporal patterns and return periods of tropical storm and hurricane strikes from Texas to Maine. *Journal of Climate.* 20:3498-3509. DOI 10.1175/JCLI4187.1.

Keim, B.D. and R.A. Muller, 2009. Hurricanes of the Gulf of Mexico. Louisiana State University Press, Baton Rouge, Louisiana.

Kinney R., P. Crucitti, R. Albert, and V. Latora, 2005. Modeling cascading failures in the North American power grid. *The European Physical Journal B—Condensed Matter and Complex Systems.* 46(1):101-107.

Kolker, A.S., M.A. Allison and S. Hameed, 2011. An evaluation of subsidence rates and sea-level variability in the northern Gulf of Mexico. *Geophysical Research Letters.* 38:L214404. DOI 10.1029/2011GL049458.

Kousky, C. and H. Kunreuther, 2010. Improving flood insurance and flood-risk management: Insights from St. Louis, Missouri. *Natural Hazards Review.* 163-172.

Kousky, C., E.F.P. Luttmer, and R.J. Zeckhauser, 2006. Private investment and government protection. *Journal of Risk Uncertainty.* 33:73-100. DOI 10.1007/s11166-006-0172-y.

Koutsoyiannis, D., 1994. A stochastic disaggregation method for design storm and flood synthesis. *Journal of Hydrology.* 156:193-225.

Kunstmann, H. and M. Kastens, 2006. Direct propagation of probability density functions in hydrological equations. *Journal of Hydrology*. 325:82-95.

Kwasinski, A., W.W. Weaver, P.L. Chapman, and P.T. Krein, 2009. Telecommunications power plant damage assessment for Hurricane Katrina – site survey and follow-up results. *IEEE Systems Journal*. 3(3): 277-286. DOI 10.1109/JSYST.2009.2026783.

Li, M., L.J. Zhong, W.C. Boicourt, S.L. Zhang and D.L. Zhang, 2006. Hurricane-induced storm surges, currents and destratification in a semi-enclosed bay. *Geophysical Research Letters*. 33(2):L02604. DOI 10.1029/2005GL024992.

Linsley, R.K., M.A. Kohler, and J.L.H. Paulhus, 1982. Hydrology for engineers – third edition. McGraw-Hill Book Company, New York, New York.

Liu, S.C., C.B. Fu, C.J. Shiu, J.P. Chen and F.T. Wu, 2009. Temperature dependence of global precipitation extremes. *Geophysical Research Letters*. 36:L17702. DOI 10.1029/2009GL040218.

Liu, Y. and H.V. Gupta, 2007. Uncertainty in hydrologic modeling: Toward an integrated data assimilation framework. *Water Resources Research*. 43:W07401.

Luettich, R. and J. Westerink, 2006. ADCIRC: A (parallel) advanced circulation model for oceanic, coastal and estuarine waters. User's Manual, version 47.11. Accessed at http://adcirc.org/documentv47/ADCIRC_title_page.html.

Marcum, K.B., 2006: Use of saline and non-potable water in turfgrass industry: Constraints and developments. *Agricultural Water Management*. 80:132-146.

Maybauer M., M. Megne, G. Kafke, and D. Maybauer, 2009. Hurricane Ike and the University of Texas Medical Branch Hospital's evacuation. *Critical Care Medicine*. 37(12):A520-A520.

McBean, E., J. Penel, and K.L. Siu, 1984. Uncertainty analysis of a delineated floodplain. *Canadian Journal of Civil Engineering*. 11:387-395.

McMillan, H.K., and J. Brasington, 2008. End-to-end flood risk assessment: A coupled model cascade with uncertainty estimation. *Water Resources Research*. 44:W03419.

Melton, G., M. Gall, J.T. Mitchell and S.L. Cutter, 2010. Hurricane Katrina storm surge delineation: Implications for future storm surge forecasts and warnings. *Natural Hazards*. 54:519-536. DOI 10.1007/sl1069-009-9483-z.

Miller, L.M., R.J. Antonio, and A. Bonanno, 2011. Hazards of neoliberalism: delayed electric power restoration after Hurricane Ike. *British Journal of Sociology*. 62(3): 504-522. DOI 10.1111/j.1468-4446.2011.01376.x.

Miner, M.D., M.A. Kulp, D.M. Fitzgerald, and I.Y. Georgiou, 2009. Hurricane-associated ebb-tidal delta sediment dynamics. *Geology.* 37(9):851-854. DOI 10.1130/G25466A.1.

Mirck, J., T.A. Volk, 2010. Response of three shrub willow varieties (Salix spp.) to storm water treatments with different concentrations of salts. *Bioresource Technology.* 101:3484-3492.

Mousavi, M.E., J.L. Irish, A.E. Frey, F. Olivera and B.L. Edge, 2011. Global warming and hurricanes: The potential impact of hurricane intensification and sea level rise on coastal flooding. *Climatic Change.* 104(3):575-597. DOI 10.1007/s10584-009-9790-0.

Multi-Resolution Land Characteristics Consortium. National Land Cover Database. 2001, http://www.mrlc.gov/.

O'Gorman, P.A., T. Schneider, 2009. The physical basis for increases in precipitation extremes in simulations of 21st-century climate change. *PNAS.* 106:14773-14777.

Ouyang M. and L. Dueñas-Osorio, 2011. An approach to design interface topologies across interdependent urban infrastructure systems. *Reliability Engineering and System Safety.* 96(11):1462-1473. DOI 10.1016/j.ress.2011.06.002.

Palacios, E. and I.S. Racotta, 2007. Salinity stress test and its relation to future performance and differenc physiological responses in shrimp postlarvae. *Aquaculture.* 268:123-135.

Pappenberger, F., K. Beven, K. Frodsham, R. Romanowicz, and P. Matgen, 2007. Grasping the unavoidable subjectivity in calibration of flood inundation models: A vulnerability weighted approach. *Journal of Hydrology.* 333:275-287.

Pappenberger, F., P. Matgen, K.J. Beven, J.B. Henry, L. Pfister, and P. Fraiponte de, 2006. Influence of uncertain boundary conditions and model structure on flood inundation predictions. *Advances in Water Resources.* 29:1430-1449.

Pielke, R.A., C. Landsea, M. Mayfield, J. Laver and R. Pasch, 2005. Hurricanes and global warming. *Bulletin of the American Meteorological Society.* 86(11):1571-1575. DOI 10.1175/BAMS-86-11-1571.

Poirrier, M.A. and Z. Rodriguez del Rey, 2008. Acute disturbance of Lake Pontchartrain benthic communities by Hurricane Katrina. *Estuaries and Coasts.* 31:1221-1228.

Pompe, J.J. and J.R. Rinehart, 2008. Mitigating damage costs from hurricane strikes along the southeastern U.S. Coast: A role for insurance markets. *Ocean and Coastal Management.* 51(12):782-788.

Pryor, S.C., J.A. Howe and K.E. Kunkel, 2009. How spatially coherent and statistically robust are temporal changes in extreme precipitation in the contiguous USA? *International Journal of Climatology.* 29(1):31-45. DOI 10.1002/joc.1696.

Rajani, B. and S. Tesfamariam, 2007. Estimating time to failure of cast-iron water mains. *Water Management.* 160(2): 83-88. DOI 10.1680/wama.2007.160.2.83.

Raso, J., P. Malgrat and F. Castillo, 1995. Improvement in the selection of design storms for the new master drainage plan of Barcelona. *Water Science and Technology.* 32(1):217-224. DOI 10.1016/0273-1223(95)00558-5.

Reed, D.J., 2002. Sea-level rise and coastal marsh sustainability: Geological and ecological factors in the Mississippi delta plain. *Geomorphology.* 48:233-243.

Roth, R.E., 2009a. The impact of user expertise on geographic risk assessment under uncertain conditions. *Cartography and Geographic Information Science.* 36(1):29-43.

Roth, R.E., 2009b. A qualitative approach to understanding the role of geographic information uncertainty during decision making. *Cartography and Geographic Information Science.* 36(4):315-330.

Sampaio, L.A. and A. Bianchini, 2002. Salinity effects on osmoregulation and growth of the euryhaline flounder *Paralichthys orbignyanus. Journal of Experimental Marine Biology and Ecology.* 269:187-196.

Sirkin, A., 1995. Engineering overview of Hurricane-Andrew in South Florida. *Journal of Urban Planning and Development.* 121(1):1-10. DOI 10.1061/(ASCE)0733-9488(1995)121:1(1).

Smemoe, C.M., E.J. Nelson, A.K. Zundel, and A.W. Miller, 2007. Demonstrating floodplain uncertainty using flood probability maps. *Journal of the American Water Resources Association.* 43(2):359-371.

Smith, J.M., M.A. Cialone, T.V. Wamsley and T.O. McAlpin, 2010. Potential impact of sea level rise on coastal surges in southeast Louisiana. *Ocean Engineering.* 37:37-47. DOI 10.1016/j.oceaneng.2009.07.008.

Stehr, S.D., 2006. The political economy of urban disaster assistance. *Urban Affairs Review.* 41(4):492-500. DOI 10.1177/1078087405284887.

Syvitski, J.P.M., A.J. Kettner, I. Overeem, E.W.H. Hutton, M.T. Hannon, G.R. Brakenridge, J. Day, C. Vörösmarty, Y. Saito, L. Giosan and R.J. Nicholls, 2009. Sinking deltas due to human activities. *Nature Geoscience.* 2:681-686. DOI 10.1038/NGEO629.

Tanyimboh, T.T. and A.B. Templeman. 2010. Seamless pressure-deficient water
22 distribution system model. *Proceedings of the Institution of Civil Engineers-Water*
23 *Management*. 163(8): 389-396. DOI 10.1680/wama.900013.

Texas Administrative Code (TAC). Title 30, Part 1, Chapter 290, Subchapter D, "Rules and Regulations for Public Water Systems." Accessed at www.sos.state.tx.us/tac/index.shtml on 16 December, 2011.

Texas Commission on Environmental Quality (TCEQ). 2011. Response to request for information for permitted storage facilities along the Houston Ship Channel. Information was provided by the Emissions Assessment Section in April, 2011.

Thyer, M., B. Renard, D. Kavetski, G. Kuczera, S.W. Franks, and S. Srikanthan, 2009. Critical evaluation of parameter consistency and predictive uncertainty in hydrological modeling: A case study using Bayesian total error analysis. *Water Resources Research.* 45:W00B14.

Tilmant, J.T., R.W. Curry, R. Jones, A. Szmant, J.C. Zieman, M. Flora, M.B. Robblee, D. Smith, R.W. Snow, and H. Wanless, 1994. Hurricane Andrew's effect on marine resources. *BioScience.* 44(4):230-237. DOI 10.2307/1312227.

Trenberth, K.E., A. Dai, R.M. Rasmussen and D.B. Parsons, 2003. The changing character of precipitation. *Bulletin of the American Meteorological Society.* 84(9):1205-1217. DOI 10.1175/BAMS-84-9-1205.

Tolley, S.G., A.K. Volety and M. Savarese, 2005. Influence of salinity on the habitat use of oyster reefs in three southwest Florida estuaries. *Journal of Shellfish Research.* 24(1):127-137.

Tomasko, D.A., c. Anastasiou and C. Kovach, 2006. Dissolved oxygen dynamics in Charlotte Harbor and its contributing watershed, in response to Hurricanes Charley, Frances, and Jeanne – Impacts and recovery. *Estuaries and Coasts* 29(6A):932-938.

Turner, R.E., J.J. Baustian, E.M. Swenson and J.S. Spicer, 2006. Wetland sedimentation from Hurricanes Katrina and Rita. *Science* 314(5798):449-452. DOI 10.1126/science.112116.

U.S. Army Corps of Engineers (USACE), 2010a. HEC-RAS river analysis system: User's manual, version 4.1. USACE Hydrologic Engineering Center, Davis, California.

U.S. Army Corps of Engineers (USACE), 2010b. HEC-RAS river analysis system: Hydraulic reference manual, version 4.1. USACE Hydrologic Engineering Center, Davis, California.

U.S. Census Bureau. 2011. accessed 1-12-2012.
http://www.census.gov/newsroom/emergencies/additional/additional_information_on_coastal_areas.html

U.S. Environmental Protection Agency (USEPA), 2000. EPANET 2 Users Manual v2.0, www.epa.gov/nrmrl/wswrd/dw/epanet.html.

U.S. Department of Commerce (USDOC), 1992. SLOSH: sea, lake and overland surges from hurricanes. NOAA Technical Report NWS 48. National Weather Service, Silver Spring, Maryland.

U.S. Geological Survey (USGS), 2008. Monitoring inland storm surge and flooding from Hurricane Ike in Texas and Louisiana, September 2008. Open File Report 2008-1365. U.S. Geological Survey, Ruston, Virginia.

Wallace, D.J. and J.B. Anderson, 2010. Evidence of similar probability of intense hurricane strikes for the Gulf of Mexico over the late Holocene. *Geology*. 38:511-514. DOI 10.1130/G30729.1.

Wang, P. J.H. Kirby, J.D. Haber, M.H. Horwitz, P.O. Knorr and J.R. Krock, 2006. Morphological and sedimentological impacts of Hurricane Ivan and immediate poststorm beach recovery along the northwestern Florida barrier-island coasts. *Journal of Coastal Research.* 22(6):1382-1402. DOI 10.2112/05-0440.1.

Warnken, K.W. G.A. Gill, P.H. Santschi and L.L. Griffin, 2000. Benthic exchange of nutrients in Galveston Bay, Texas. *Estuaries.* 23(5):647-661. DOI 10.2307/1352891.

Waugh, W.L., 2006. The political costs of failure in the Katrina and Rita disasters. *Annals of the American Academy of Political and Social Science*. 604:10-25.
Werner, M.G.F., N.M. Hunter, and P.D. Bates, 2005. Identifiability of distributed floodplain roughness values in flood extent estimation. *Journal of Hydrology*. 314:139-157.

Winkler J., L. Dueñas-Osorio, R. Stein, and D. Subramanian, 2010. Performance assessment of topologically diverse power systems subjected to hurricane events. *Reliability Engineering and System Safety* 95(4):323-336.

Xu, C., I.C. Goulter, and K.S. Tickle, 2003. Assessing the capacity reliability of ageing water distribution systems. *Civil Engineering and Environmental Systems*. 20(2):119-133. DOI 10.1080/1028660021000051620.

Yazdani and Jeffrey, 2011. Complex network analysis of water distribution systems. *Chaos*. 21:016111. DOI 10.1063/1.3540339.

Zhang, J.Z., C.R. Delble, C.J. Fischer and L. Moore, 2009. Hurricane Katrina induced nutrient runoff from an agricultural area to coastal waters in Biscayne Bay, Florida. *Estuarine, Coastal and Shelf Science* 84(2):209-218. DOI 10.1016/j.ecss.2009.06.026.

Zhuge, H. and J. Zhang, 2010. Topological centrality and its e-science applications. *Journal of American Society for Information Science and Technology* 61(9):1824-1841.